Telemark University College
Faculty of technology
M.Sc. Programme

MASTER THESIS 2008

Candidate : Timothy Greer

Title :Modeling and Simulation of Post Combustion CO_2 Capturing

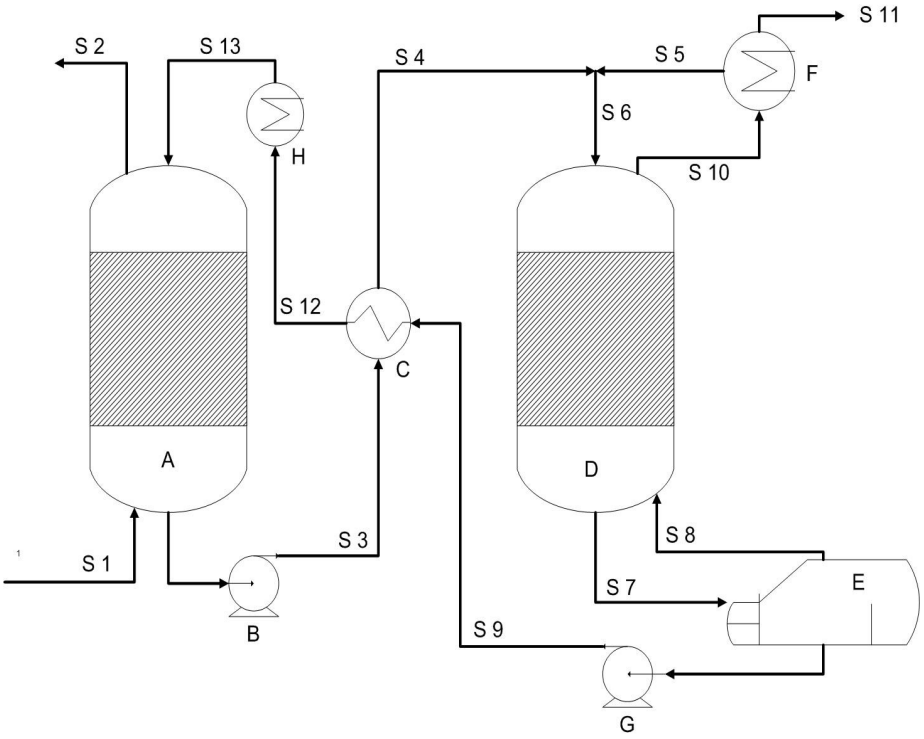

Faculty of Technology
Address: Kjolnes Ring 56, N-3914 Porsgrunn, Norway, tel: +47 35 57 50 00, fax: +47 35 55 75 47

Telemark University College

Faculty of Technology
M.Sc. Programme

WRITTEN REPORT MASTER THESIS, COURSE CODE FMH606

Student	**:Timothy Greer**
Thesis Title	**:** Modeling and Simulation of Post Combustion CO_2 Capturing
Signature	**:** . . . .
Number of pages	**::**166
Keywords	**:** . . . .
Supervisor	**: Bernt Lie**
sign.	: . . . .
2nd Supervisor	**:**
sign.	: . . . .
Sensor	**: John Arild Svendsen**
sign.	: . . . . . .
External partner : <name>	
Availability	**:** Open
Archive approval (supervisor signature)	: . . . . .
.**Date**	**:** . . . . .

Abstract:

A dynamic model for the chemical absorption of carbon dioxide in Monoethanolamine is developed and implemented. The model includes absorption tower, de-absorption tower, reboiler, condenser and rich/lean heat exchanger. The chemical reactions of MEA and CO_2 are included in the model and the vapour liquid equilibrium for CO_2 is described by henrys law. The concentrations of MEA, H_2O N_2 and O_2 in both phases are calculated with the Peng Robinson equation of state utilising the individual species fugacities. The model was solved as a PDE, for both absorption and de-absorption columns implementing the method of lines. The full model was simulated in Matlab and results where obtained that agree with other published values.

Telemark University College

Faculty of Technology

FMH606 Master Thesis

Title: Modeling and simulation of post combustion CO_2 capturing

Student: Timothy Greer

College supervisor: Bernt Lie, prof. dr.ing.

External partners:

Task description:

The following tasks should be carried out:

1. Give an overview of possible CO_2 capturing methods, with an emphasis on post combustion amine capture.
2. Based on previous work, develop a dynamic model of an absorption column for post combustion CO_2 capturing. The model should be validated through simulations.
3. Develop a dynamic model of the temperature swing de-absorption process. The model should be validated through simulations.
4. The models for the absorption and de-absorption are to be integrated, with the introduction of necessary additional models such as heat exchangers, pumps, etc.
5. Illustrate the use of the model through simulations.
6. Optional: study how to include amine decomposition in the model.
7. Optional: study possibilities for refining the model for other amine solutions.

Task background:

Global warming is among the main environmental problems today. According to UN's Intergovernmental Panel on Climate Change (IPCC), it is beyond doubt that climate gases caused by human activities (e.g. CO_2) contribute to this process. To develop efficient and environmental friendly capturing and deposition of CO_2 is thus of prime concern.

Telemark University College is currently involved in a project for the study of post combustion capturing of CO_2. In such a process, exhaust gas is run through an absorption column where CO_2 is transferred from the gas phase to a liquid phase consisting of amines dissolved in water. The liquid with captured CO_2 is next sent to a distillation column (”stripper”), where the mixture is heated such that CO_2 gas is separated out at the top of the distillation column, and the liquid (water + amines + fractions of CO_2) leaves at the bottom. The liquid is then recycled to the top of the absorption column, while the CO_2 is sent to a storage tank. The post combustion process thus consists of an absorption column and a stripper (distillation column), with some heat integration, some pumps, and some storage tanks.

To improve the CO_2 capturing, it is important to remove CO_2 from the liquid mixture in the stripper. This implies that the liquid needs to be heated up in the boiler of the stripper. At the same time, the amines start to decompose if they are heated too much. There is thus a balance in how the stripper can be operated.

It is thus of interest to develop dynamic models of the post combustion process. In this modeling phase, models of suitable complexity for the various units and mechanisms should be developed. Relevant mechanisms are those related to amine decomposition, as well as equilibrium relations in the distillation column, mass transfer in the absorption column, heat transfer in the heat exchangers, mass flow in the pumps, etc. A suitable balance between complexity and accuracy is sought.

It is also of interest to develop sensor systems to measure the concentration of CO_2 in the exhaust gas, and of amine concentration/amine decomposition in the liquid mixture.

Previous work:

Hansen, Dag-Kjetil (2004). *Dynamic modelling of an absorption tower for the removal of carbon dioxide from exhaust gas by means of Mono-ethanol-amine*. Telemark University College, Faculty of Technology. Thesis carried out at NTNU.

Practical information (where, how, available equipment etc.):

There is room for more than one thesis in this project. A thesis may be carried out at Telemark University College, but it may also be carried out e.g. at ISEL in Lisbon, Portugal, with co-supervisors from ISEL.

Formal acceptance by the student (with ultimate task description as stated above):

Student's signature and date:

Supervisor's signature and date:

If the above date is other than 14/1-05 it is administratively set to 14/1-05. Any later date is allowed only in special circumstances and shall be agreed upon specifically (written application is required).

Preface

When I meet the Rector at the ISEL during my exchange in Lisbon, Portugal, he asked me why I had chosen such a large and difficult task for my final year masters Thesis. The answer I gave was because I wanted a multi discipline topic which would require detailed understanding and also because I believe the engineering of CO_2 capture will gain more prominence in the foreseeable future. The project included aspects of many of the subjects that I have learnt over the last two years requiring me to dig out my old notes and refresh my memory numerous times. The task has been an interesting project which required me to research about many different aspects of engineering which has increased my understanding greatly. The skills I have acquired in this thesis will serve me well in the future.

I greatly appreciate the help and guidance of my supervisors Bernt Lie in Norway and , José Manuel Igreja and Joao Gomes, who provided direction when ever I asked. Two months of this thesis was undertaken at ISEL in Lisbon so I would like to thank the people who made this possible most notably Bernt and Jose Manuel. I would also like to thank Alamt Bedelbayev who working on a similar project was a great sounding board and helped a lot in every aspect of the modeling process and also Lars Erik Øi who provided direction when asked. My last thank you is to my poor computer which over the lat 4 months has done many hours of simulations and has been the work horse of my project.

Table of Contents

Nomenclature

Symbols

A	Area	(m^2)
C	Concentration	(mol/m^3)
C	Coefficient	
C_p	Heat capacity at constant pressure	(J/mol K)
D	Diameter	(m)
D	Diffusivity	(m^2/s)
E	Energy	(J)
E	Enhancement factor	
H	Enthalpy	(J)
H	Height	(m)
H	Henrys Constant	(Pa m^3/mol)
Ha	Hatta number	
I	Ionic strength	
J	Colburn factor	
K	Equilibrium Constant	
K	Kinetic energy	(J)
MW	Molecular weight	(g/mol)
Q	Heat transfer	(J)
P	Pressure	(Pa)
P	Power	(W)
Po	Potential energy	(J)
Pr	Prandtl number	
R	Universal gas constant	(J/mol K)
Re	Reynolds number	
Sc	Schmitt number	
St	Stanton number	

T	Temperature	(K)
U	Internal energy	(J)
U	Overall heat transfer coefficient	(J/m^2 K s)
V	Volume	(m^3)
W	Work	(J)
Z	Compressibility	
a	Specific surface area	(m^2/m^3)
f	Fugacity	(Pa)
g	Gravitational constant	(m/s^2)
h	Liquid hold up	
h	von Krevelen factor	
h	Convective heat transfer	(J/m^2 K s)
k	Reaction rate coefficient	(m^3/mol s).
k	Binary interaction parameter	
k	Thermal Conductivity	(J/s m K)
kd	Mass transfer coefficient	(m/s)
m	Mass	(g)
n	Mol	(mol)
q	Heat transfer	(J)
r	Reaction rate	(mol/m^3s)
t	Time	(s)
u	Velocity	(m/s)
x	mol fraction for liquid phase	
y	Mol fraction for vapour phase	
z	Height above datum	(m)
z	Ion valence	

ϕ	Fugacity coefficient	
α	CO_2 loading	
ε	packing void fraction	
μ	Viscosity	(kg/m s)
ρ	Density	(kg/m^3)
γ	Activity co-efficient	
ψ	Arbitrary function or variable	

Subscripts, superscripts and accents

$\Delta\psi$	Change of quantity	ψ_i	Species variable
$\dot{\psi}$	Flow of variable	ψ_{in}	Inlet conditions
Ψ''	per specific area	Ψ_j	Reaction variable
Ψ^*	Interface	ψ^l	Liquid phase
$\hat{\boldsymbol{\psi}}$	Specific in a mixture	Ψ^{lv}	liquid –vapour
$\delta\psi$	Incremental change	Ψ_{lm}	Log mean
$\tilde{\boldsymbol{\psi}}$	Mol Specific	Ψ_m	Mass
Ψ^{alt}	Alternative	Ψ_{mix}	Mixture
Ψ_{amb}	Ambient	ψ_{out}	Outlet conditions
Ψ^B	Bulk phase	Ψ_r	Reduced
Ψ_C	Cross sectional	Ψ_{rich}	Rich loading
Ψ_C	Critical	Ψ_R	Reverse
Ψ_{diff}	Diffusion	Ψ_{Re}	Reaction
Ψ_f	Forward	Ψ^{salt}	Salting out
Ψ_f	Friction	ψ_T	Interface area
Ψ_{gen}	Generation	ψ_T	Total
Ψ_h	Liquid hold up constant	$\Psi^{Unreact}$	Un reacting system
Ψ_h	Heat	ψ^v	Vapour phase
		ψ_w	Wetted

1 Introduction

1.1 Background

Carbon is present in the atmosphere, water and earth in various forms and chemical compounds. It is a building block for life on earth being an essential element in many items such as biomass, petroleum compounds, mineral deposits and the atmosphere. Over many millions of years the carbon dioxide in the atmosphere has been sub quested by plants and some of this eventually ends up in the form of petroleum and coal under the earth's surface. In this form the Carbon is relatively inert and has been stable for millions of years. In the last century mankind has utilized extensively this energy that is stored in this carbon by burning fossil fuels to provide energy. An estimated 90% of the world's energy is derived from fossil fuels in the form of Coal, Natural gas and crude oil (IPCC 2007). The products of liberating this fossil fuel energy are principally carbon dioxide and water. The effect of carbon dioxide on the environment and in particular the gases role in the enhanced greenhouse effect and the effect on the earth's climate, sea levels and sustainability has been a topic of increasing research.

The atmosphere presently contains an estimated CO_2 content of about 385 ppmv (Wikipedia/greenhouse). Before the start of the industrial revolution the atmospheric level is estimated to have been about 35% lower (Wikipedia/greenhouse). This value has been steady rising as humans have released the stored Carbon from beneath the earth's surface and removing biomass by burning forests while clearing land. Carbon dioxide is known as a greenhouse gas as CO_2 in the atmosphere traps energy that is being radiated from the earth's surface. The Earth receives energy from the sun mostly in the wavelength 400-2000nm (Tidel and Weir 2006) but radiates the excess energy back to the universe at a wavelength of about 8-50µm refer to figure 1a.

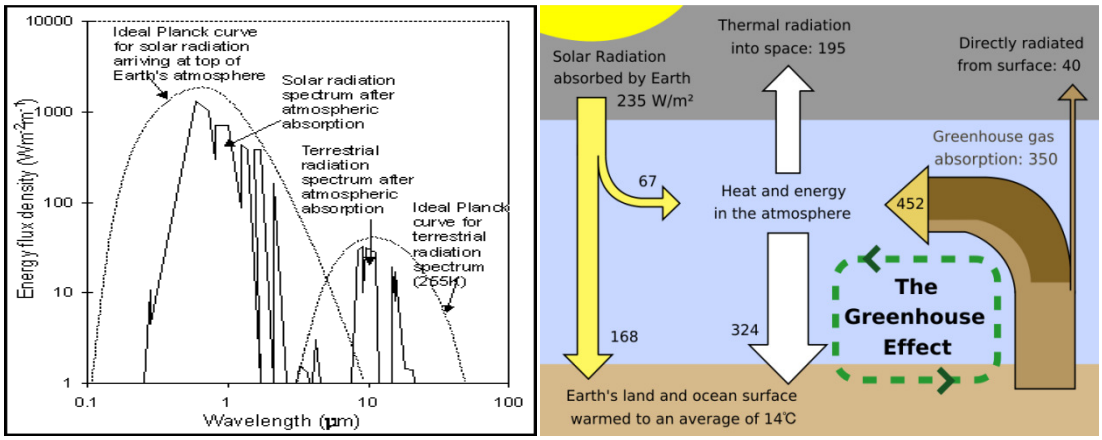

Figure 1a: Wavelength of radiation from the sun and terrestrial sources (Carleton) and figure 1b the green house effect (Wikipedia/greenhouse).

Carbon dioxide is a compound which absorbs this longer wavelength terrestrial radiation, capturing the flow of energy out. Figure 1b illustrates how the greenhouse effect operates in practice. This captured energy increases the temperature of the atmosphere and is required for life on earth otherwise the average atmospheric temperature would be 33^{o}C less (Wikipedia/greenhouse). The enhanced greenhouse effect is the effect of the extra carbon dioxide (and other gases) that have been released by humans and its effect on temperature. The IPCC estimated to have added 0.75°C to the earth's average atmospheric temperature in the previous century (Wikipedia/greenhouse).

The Carbon cycle is a complex system with many interactions as the carbon can be stored in many "carbon sinks" such as the ocean, mineral form ($CaC0_3$ etc) and biomass. There is many feed back loops which regulate the Carbon concentration in each sink but in general can be generalized as having a long feedback time e.g. the ocean is estimated to take several hundred years to move carbon in the upper layers to ocean depths via currents and biomass (Royal Science 2005). Mankind's influence on the carbon cycle is a topic of ongoing research but is generally accepted by the IPCC that carbon dioxide released by humans from fossil fuels is most likely to be effecting the earths climate as "*Warming of the climate system is unequivocal, as is now evident from observations of increases in global average air and ocean temperatures, widespread melting of snow and ice and rising global average sea level" (*IPCC 2007)

The rate of increase is estimated to at approximately 1.5ppmv per year which corresponds to a temperature increase e of between 4-8 degrees in the next century (IPCC 2007). The amount

of increase is probably not as critical as to the speed of release as essentially the Carbon that has been sequestrated over millions of years is released in a few hundred greatly affecting the feedback systems of planet earth.

Most countries have accepted that global warming is an important issue and the reduction of CO_2 emissions into the atmosphere is a growing concern which must be addressed. The Kyoto treaty requires developed countries to reduce their green house gas emissions to 5.2% below 1990 levels by 2012 (Wallace 2000). The use of fossil fuels and therefore energy is closely related to the prosperity of a country as energy is required in all aspects of the economy. Developed countries have a higher per capita consumption of energy than developing countries and have released the majority of the fossil fuel generated carbon dioxide in the last century and this has essentially propelled these countries to their higher standard of living. The application of quotas and limits then becomes a hotly contested geopolitical debate as should the quotas be applied to every country which is a burden on the less developed countries creating an unlevel playing field in the world economy or should the quotas apply mostly to the developed countries tilting the global economy playing field in the other direction. The importance of the debate is further increased by the substantial cost of reducing the carbon emissions with an estimated 30-80% increase in cost for the energy when current carbon capture technology is employed (Greenfacts 2005). Therfore it is imperative the most economical solution is applied. Presently carbon capture technology is applied on very limited scale and is mostly for gas purification, where the carbon dioxide is removed from a gas stream to purify the gas stream and is not for carbon dioxide sequestration. The majority of carbon dioxide from these removal processes is released back into the atmosphere with very little captured for long term storage.

1.2 Carbon Capture and Storage.

In 2000, 23.5 gigatonnes of CO_2 was released from manmade sources with approximately 60% released from point sources (>0.1megatonne) such as fossil fuel power stations, industrial process (cement, metal processing etc) and oil and gas extraction (IPCC 2005). The majority of CO_2 is present at a concentration of less than 15% by volume often as low as 3%, figure 1.2 displays the summary of point source emitters from 2000. It is uneconomical to compress and store the complete gas stream as the gas may have to be compressed up to 100 bar pressure for storage. If the complete gas stream is compressed the amount of energy required to

compress the gas will produce more emissions than what would be captured. Therefore it is imperative that the CO_2 is concentrated to a value of greater than 90% to reduce the transport and storage costs.

Process	Number of sources	Emissions ($MtCO_2$ yr^{-1})
Fossil fuels		
Power	4,942	10,539
Cement production	1,175	932
Refineries	638	798
Iron and steel industry	269	646
Petrochemical industry	470	379
Oil and gas processing	N/A	50
Other sources	90	33
Biomass		
Bioethanol and bioenergy	303	91
Total	**7,887**	**13,466**

Figure 1.2: Point source emissions (>0.1Mt CO_2) for 2000 (IPCC 2005)

The IPCC has recommended that the capture of CO_2 from point sources is an area for major focus as technology exists for it to be feasible to remove CO_2 from concentrated point sources. In general the more concentrated the CO_2 stream the easier it is to capture. The three choices of technology for removing CO_2 from point sources are post combustion, pre combustion and oxy fuel. Note the three technologies relate to the combustion of fossil fuels, for other point source emitters such as industrial processes the post combustion technologies are applicable. An overview is shown in figure 1.3.

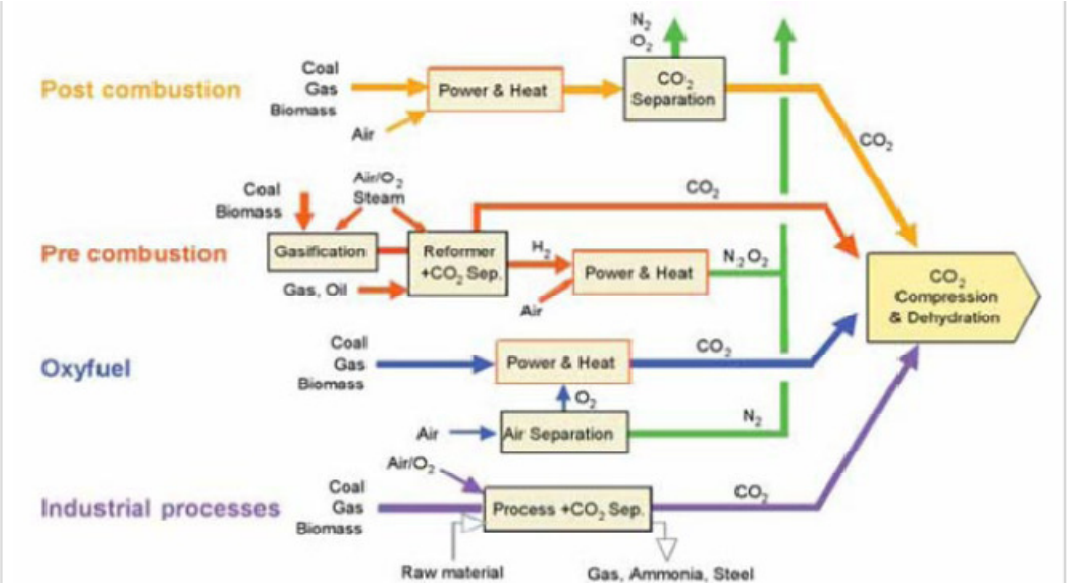

Figure 1.3: Overview of carbon capture processes (IPCC 2005)

1.2.1 Pre Combustion

In pre combustion the fossil fuel is reacted first with air/oxygen to form carbon monoxide and then with steam in a reactor to form the products of carbon dioxide and hydrogen gas. The process is known as the water shift reaction and is used industrially for the production of ammonia.

$$CO + H_20 \rightarrow CO_2 + H_2$$

The carbon dioxide is in a relatively concentrated form (40-50%) and can be separated from the hydrogen. The hydrogen can then be used as a fuel or as an energy carrier. The process is used industrially but the use of hydrogen as a fuel is not well spread. The products from the fuel and air reaction are Carbon dioxide and the inert gases within the air (such as nitrogen) and this is required to be removed from the CO. The development of equipment such as fuel cells and turbines to convert the hydrogen into useful energy is still not ready for wide spread implementation. The development of pre combustion removal of CO_2 is technically feasible but is still not ready for full-scale use.

1.2.2 Oxyfuel

Another option for removal of CO_2 from fossil fuel products is to combust the fossil fuels in pure oxygen where the products of combustion are H_2O and CO_2. This method involves both pre and post combustion as the water must be separated from the CO_2 which is a simply procedure but the pre combustion process of purifying the O_2 is more complicated and expensive and is presently more expensive than the post combustion capture of CO_2 from an air/ fuel mixture (Wallace 2000).

1.2.3 Post Combustion

The removal of carbon dioxide from post combustion is characterized by the removal of carbon dioxide from a gas stream which contains other gases and components. Gases from a natural gas fired power station have concentrations of CO_2 between 3-8% per volume and emissions from a coal fired power station have CO_2 concentrations between 12-15% per volume (Charkravarti et al 2001). The other components in the gas streams are typically water, nitrogen and oxygen. When up to 95% of the gas stream is not CO_2 it is not feasible to store all the gas in a storage system such as an under ground reservoir or ocean therefore the CO_2 must be purified. With large volumes of gas to be treated often the capital cost of the equipment is

large with corresponding large operating costs. The main technologies that can be applied to post combustion carbon dioxide treatment are:

- Membrane separation
- Low temperature distillation
- Physical Adsorption
- Chemical absorption
- Physical absorption
- Chemical absorption.

Membrane Separation

A membrane is a semi impregnable barrier which allows selected species to pass through while restricting others. It is possible to select membranes that allow the CO_2, N_2 and O_2 to be separated. The use of membranes is some what restricted by the low partial pressure of the CO_2 in the gas stream which is the driving force. This can be over come by increasing the pressure of the gas stream to be cleaned but this in turn requires energy to pressurize and the majority of the energy is used in compressing the nitrogen and oxygen. Chemicals on the back side of the membrane to absorb the CO_2 as it passes through the membrane have been shown by Hoff (2003) to be a feasible alternative. Membrane technology is advancing rapidly with increasing efficiency as new membranes are developed but membrane life and poisoning are still major issues.

Low Temperature Distillation

Low temperature distillation is used in industry to produce pure CO_2 by cooling and/or pressurizing the gases until the CO_2 becomes liquid. This process is not commercially possible for the large amount of gas required to be cooled/compressed.

Physical Adsorption

The adsorption of carbon dioxide is when the molecules of CO_2 accumulated on the surface of a solid or a liquid (Wikipedia/adsorption). This process is dependent on the partial pressure of the CO_2 as the driving force and requires the gas stream to be compressed to increase the partial pressure. Activated carbon and zeolite have been studied by of Muñoz et al (2006) but this is still in development stage and is not deemed feasible until higher temperature compounds are developed.

Chemical Adsorption

The capture and storage of Carbon dioxide on minerals such as Calcium oxide (CaO) and Magnesium oxide (MgO) has long been an area of research as the two products of the reactions $CaCO_3$ and $MgCO_3$ are stable inert compound that can "store" the captured CO_2 indefinitely. The products could be disposed of relatively easily and could also be utilized as building materials (Green facts 2005). The amount of mineral oxide is a major draw back as CaO has a mol weight of 56g/mol and the product $CaCO_3$ has a mol weight of 100 g/mol. This translate that 1 kg of CO_2 (at 44g/mol) produces 2.25 kg of product so for a typical 400 MW gas fired power station producing 1 million tonnes of CO_2 per year requires 1.25 million tonnes of calcium oxide and 2.25 million tonnes of product to be disposed of. It is not suitable for CO_2 captured from a cement factory as cement processes utilizes $CaCO_3$ as the feed stock and the liberated CO_2 is the plant emissions.

Physical Absorption

The process of absorption is when particles diffuse into the bulk of a liquid or solid and are captured. This is different from adsorption which occurs on the surface of the liquid or solid (Wikipedia/absorption). The process is driven by the partial pressure of the CO_2 in the gas and is not very effective for the post combustion gases at atmospheric pressure. For higher efficiency, larger partial pressures are required but this involves compressing the gas stream which is usually uneconomical. The process of absorption of CO_2 into water is mostly physical absorption and is limited by the solubility of CO_2 in water which at 25°C is 0.09 m^3/m^3 (CO_2/water). This is henrys law which relates the concentration of a species in a liquid to the partial pressure of that species.

Chemical Absorption

In chemical absorption the CO_2 reacts within the liquid to reduce the concentration of the CO_2 in the liquid and maintain the driving force. This is the most common form of CO_2 capture process. Most reactions can be considered reversible depending on the temperature of the system. In temperature swing absorption the rich liquid is removed and the temperature is increased to reverse the reaction. The most common process is to use amine as the chemical solvent which reacts quickly with the CO_2 keeping the driving forces higher. The most common amine in use is Monoethanolamine which is a primary amine but other amines are also currently in use and are increasing in popularity. The absorption of CO_2 in sea water is also a

semi-chemical absorption process as the CO_2 react with both water and OH^- ions to form bicarbonate. The equations for the reaction with water is;

$$CO_2 + 2H_20 \Leftrightarrow HCO_3^- + H_3^+O \ and \ CO_2 + OH^- \Leftrightarrow HCO_3^-$$

The reaction with CO_2 and H_2O is relatively slow but the reaction with OH^- ions is a lot faster. Sea water has a higher concentration of OH^- ions than fresh water which is why the absorption of CO_2 in sea water is greater than that of fresh water.

1.3 Amines

Amines are the most widely used chemical absorbents presently in use. Amine is a chemical compound based on ammonia molecule NH_3. When various functional groups replace the H atoms then various amines can be formulated with a typical substitution being $HOCH_2CH_2$ which when substituted with one of the H bonds produces Monoethanolamine (MEA). Various other alkanolamines can be constructed by adding other functional groups (Solbraa 2003). The amines can be classed into three types primary, secondary and tertiary. The amines can react with CO_2 by three mechanisms, base catalyst hydration, zwittertion and termolecular. The review by Vaidya and Kenig (2007) provides a good summary of the reaction mechanisms for amines with carbon dioxide

1.3.1 Base Catalyst Hydration

The base catalyst hydration involves the formation of bicarbonate and is quite slow as the CO_2 first forms carbonic acid with water before reacting with the amine (Svendsen and Silvia 2007) . The reaction rate for H_2O to form the intermediate carbonic acid is increased by the presence of amine but is still slower than the other mechanisms.

$$H_2O + CO_2 + Am \rightarrow HCO_3^- + AmH^+$$

The advantage of this pathway is one mole of CO_2 reacts with one mole of amine. All amines can react in this pathway and it is the only possible way for tertiary amines. .

1.3.2 Zwittertion

The formation of an intermediate compound called a zwittertion as proposed by Danckwerts, is generally accepted as a mechanism for CO_2 to react with amine.

$$CO_2 + Am \rightarrow AmH^+COO^-$$

The zwittertion complex then reacts with another base molecule which can be either H_2O, OH^- or another amine. The second reaction which is the deportation of the zwittertion happens very quickly as requires the transfer of a proton and can be considered instantaneous (Aboudheir et al 2003). Typically the base is another amine so the overall reaction is 2 mols of amine consumed for each mol of CO_2.

$$Am + AmH^+COO^- \rightarrow AmH^+ + AmCOO^-$$

For some amines such as AMP the second reaction is not instantaneous and the reverse reaction of the zwitterion must be allowed for (Vaidya and Kenig 2007)

1.3.3 Termolecular

The termolecular mechanism as introduce by Crooks and Donnellan, has not been widely accepted as a reaction pathway but is still used to explain the reaction of CO_2 and amine. The Termolecular reaction is for the amine CO_2 and another base to react simultaneously and produce the products of the $AmCOO^-$ and BH^+, where the B is typically another amine (Vaidya and Kenig 2007). The termolecular mechanism has the same products and reactants as the zwittertion but is a third order reaction.

1.4 Monoethanolamine

This study utilizes Monoethanolamine (MEA) as the amine used in the chemical absorption process. MEA is the most common amine currently used in industrial applications. This is mainly due to the fast reaction rate with CO_2 and the higher saturation pressure which minimizes evaporation losses (Kohl 1995). The disadvantage of MEA is the high heat of reaction which is required to reverse the reaction with CO_2 and the fact that 2 moles of MEA are required to be reacted with one mol of CO_2 for removal. MEA also is very corrosive and can not be used at high concentrations. Typically the working concentration is recommended at 15% by weight but some applications use up to 30% by weight concentration with the addition of corrosion inhibitors (Kohl 1995) . The advantage of using a higher concentration of MEA is that less energy is required to heat the solution in the de absorption process. When the concentration is 15% then excess energy is consumed heating the other 85% of the solution (water) up to the stripper temperature of 120°C. It can clearly be seen that the greater the concentration of MEA then the less energy consumed in the de-absorption process but this is traded off against the increased corrosiveness of the solution.

1.5 Packed Tower Scrubber

The advantage of using Amine as the chemical absorption is that the absorbed CO_2 solution of carbamate protanated amine and bicarbonate can be heated and the reaction reversed to release the CO_2 and regenerate the amine solution. The rate of reaction for absorption is fast and generally happens in the first few μm of the liquid film boundary layer (Perry and Green 1999). The rate of diffusion of the gas into the liquid is the rate limiting value therefore the surface area has to be maximized to allow for the maximum amount of diffusion and therefore the maximum removal of CO_2.

A packed tower is a cylindrical tower which is filled with packing which has a high surface area per volume. The packing can be either random or structured. Random is generally cheaper and with a greater pressure drop and less surface area per m^3. The structured packing has a higher specific surface area and less pressure drop but is typically more expensive. The packing can be made of plastic, steel or ceramic and there are many varieties supplied by different suppliers. Two types of random packing (Pallring and Dinpac) and a structured packing (melpack 250Y) are shown in figure 1.4 (a,b and c).

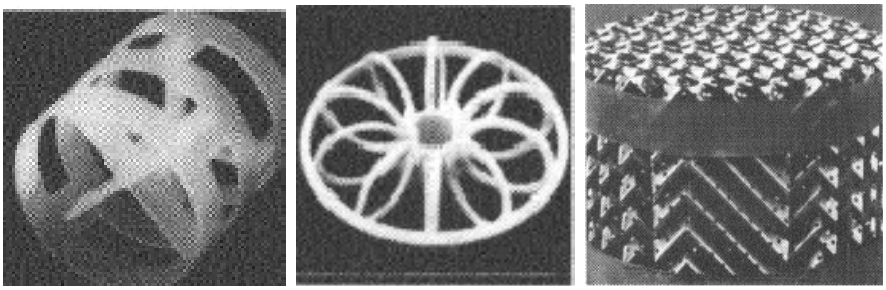

Figure 1.4:Pallring packing, Dinpac and Melpack 250Y structured packing. (Billet 1995)

Each packing piece has certain values which are used in the process selection. They are

- a = specific surface area (m^2/m^3)
- ε = void fraction (the ratio of material to free volume)
- N= Number of packing pieces per m^3. (random packing)
- C=Constant(s)used in calculation of hydrodynamic properties

The formulas for calculating the performance of the packing typically are correlated to the characteristic values listed above therefore the performance of each packing can be evaluated and compared by substituting the corresponding values into the process selection equations.

1.6 Process Description

A typical schematic of the absorption process is shown in figure 1.5. The main components of the system are;

A. The absorption tower
B. The rich amine pump
C. The rich/ lean amine heat exchanger
D. The de-absorption tower (Stripper)
E. The de-absorption reboiler
F. The de-absorption condenser
G. The lean amine pump
H. The lean amine heat exchanger

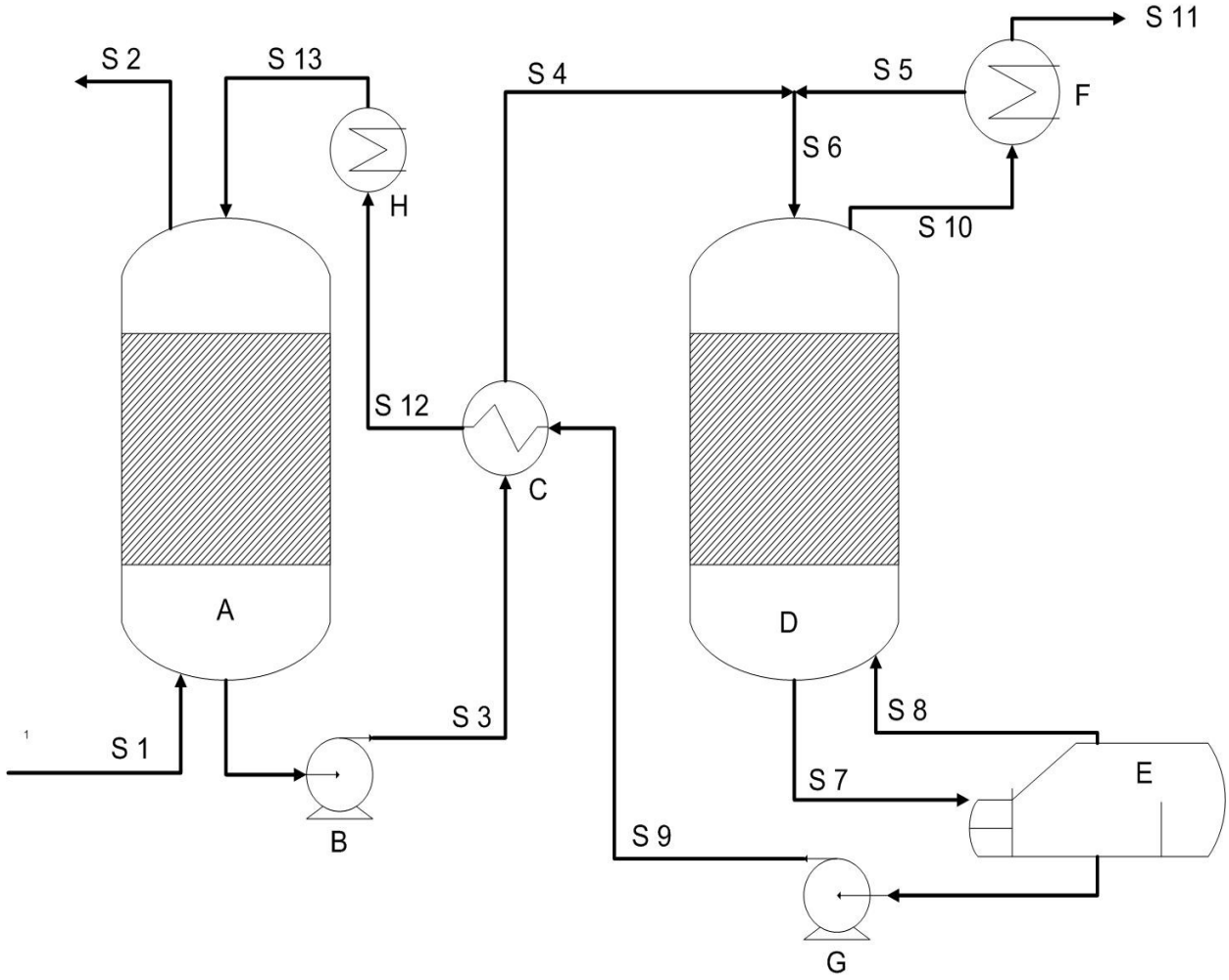

Figure 1.6:Prcocess flow diagram of CO2 removal plant with Monoethanolamine.

A: The absorption tower is a large cylindrical tower that is filled with the packing. The inlet gas enters at the bottom and flows up trough the tower while the lean liquid mixture enters at the top and flows down over the packing. The liquid velocity is typically in the range of 0.001-0.01 m/s (Billet 1995) with a minimum value required to wet the packing and a maximum value required so as not to disrupt the gas flow and increase the pressure drop. The gas flow is typically between 1-4 m/s (Billet 1995) and is a balance between minimizing the pressure drop (decreasing velocity) and increased process throughput and smaller tower diameter (increasing velocity).

B: The rich amine pump pumps the liquid from the bottom of the absorption tower to the rich/lean heat exchanger and to the top of the stripping tower. The liquid from the bottom of the absorber is called the rich mixture as it contains the highest concentration of CO_2. The pump will control the recycle rate of the system and the pump has a reservoir at the bottom of the absorption tower.

C: The rich/lean heat exchanger transfer heat from the lean mixture to the rich mixture. The typical temperature of the rich solution is 45-50°C from the absorption tower and this is heated to 105-110°C in the heat exchanger. The lean mixture from the stripper can be up to 120°C and this is cooled by the rich solution. The flow rates of the rich and lean mixture are typically the same when the system is in steady state.

D: The de-absorption tower (stripper) is a cylindrical tower filled with packing like the absorption tower. The purpose of the stripper is to heat the mixture to 110-120°C to reverse the chemical reactions and decrease the solubility of the CO_2 in the solution. The heating of the liquid in the tower is achieved by boiling water in the reboiler to 120°C and this steam flows up through the tower. The volume flow rate of the steam is less than the gas in the absorption tower so the stripper tower typically has a smaller diameter. A flow rate for the steam of maximum 2 m/s is recommended by Kohl (1995). The rich liquid flows down over the packing and the increased temperature of the solution reduces the solubility of the CO_2 and reverse the chemical reactions resulting in the CO_2 being released back into the gas stream.

E: The reboiler is located at the bottom of the de-absorption tower and provides the stripping gas for the stripper. The reboiler is typically heated by steam at 3 bar (130°C) and evapourates some of the lean liquid solution for the stripping gas.

F: The gas stream at the top of the stripper is cooled in a condenser to condense the water vapour and dehydrate the CO_2 gas stream. The gas stream can be concentrated up to greater than 90% when the majority of the water is condensed. The condensed water is added back into the top of the tower.

H: The lean amine pump transfers the lean amine solution from the stripper to the lean/rich heat exchanger and on to the top of the absorption tower. The lean mixture temperature out of the lean/rich heat exchanger is typically 55-60°C and is cooled in a second heat exchanger to less than 40 °C.

2. Model Development

2.1 Absorption Tower Model Development

The model of the absorption tower is developed by taking a small slice of the tower as shown in figure 2.1. The bottom of the packing is defined as z=0 and the top as z=H where H is the height of the packing. The components in the gas phase are CO_2, MEA, H_2O,N_2, and O_2 while the species modeled in the liquid phase are CO_2, MEA, H_2O,N_2, O_2 $MEAH^+$, $MEACOO^-$, HCO_3^-, OH^- and H_3O^+.

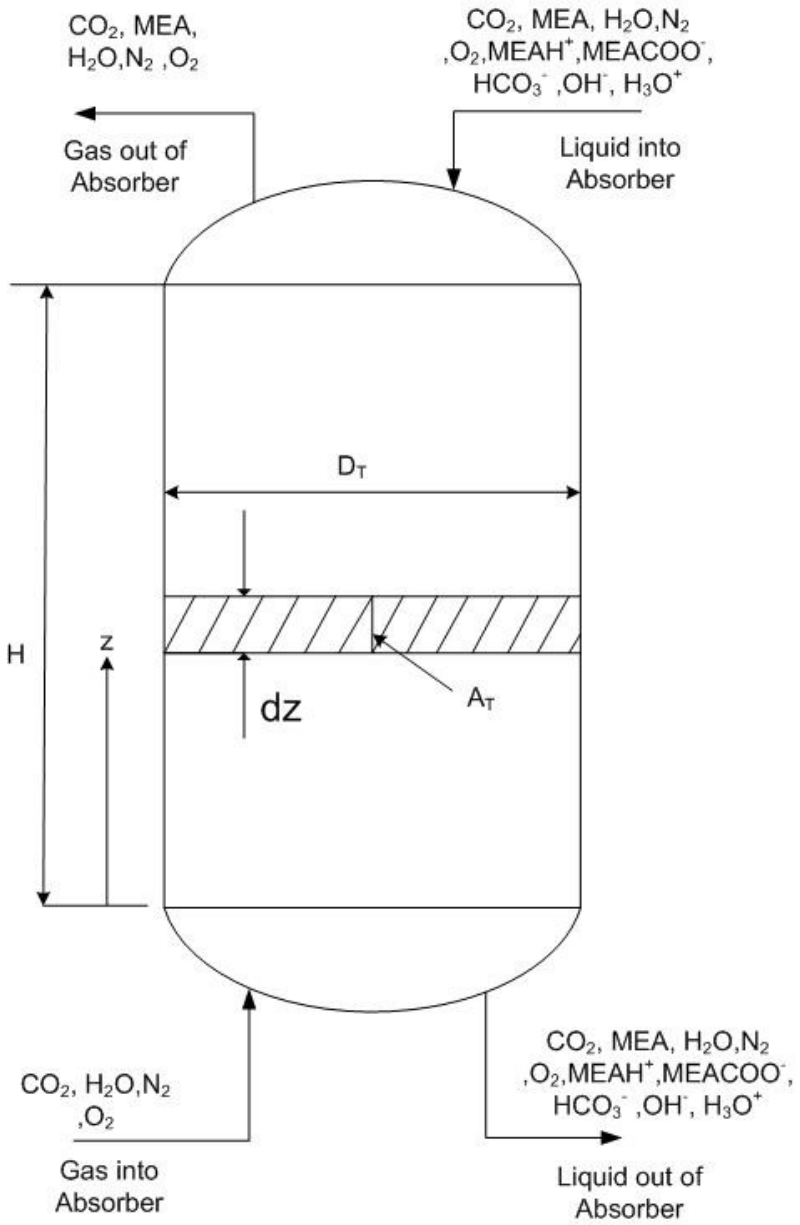

Figure 2.1: Control volume for development of the model

2.1.1 Mol Balance for each Species (Liquid Phase)

Taking a small slice of the absorption tower Δz and calculating the mol balance for the liquid phase in general form;

$$\frac{dn}{dt} = \dot{n}_{in} - \dot{n}_{out} - \dot{n}_{diff} + \dot{n}_{gen} \quad \text{(Eq 2.1)}$$

Where

$\frac{dn}{dt}$ = Rate of accumulation of mols within the control volume $\left(\frac{mol}{s}\right)$

$\dot{n}_{in}$= Mol flow into the control volume by convection $\left(\frac{mol}{s}\right)$

$\dot{n}_{out}$= Mol flow out of the control volume by convection $\left(\frac{mol}{s}\right)$

$\dot{n}_{diff}$= Mol flow out of the control volume by diffusion $\left(\frac{mol}{s}\right)$

Note: the diffusion flow is defined as flow from liquid to vapour phase and the molecular diffusion of the fluid from the inlet to the outlet of the control volume is assumed to be a lot less than the convective flow so is neglected.

$\dot{n}_{gen}$= Mol generation value $\left(\frac{mol}{s}\right)$

The mol flows can be reproduced in the form of concentration by making the following substations;

$$n = cV, \qquad \dot{n}_{in} = c_z \dot{V} \;\; \dot{n}_{out} = c_{z+\Delta z} \dot{V}, \qquad \dot{n}_{diff} = \dot{n}^{"}_{diff} A_T, \qquad \dot{n}_{gen} = R_{gen} V$$

$$\dot{V} = Volumetric\ flow\ rate\ of\ liquid = -uA_c \ \left(\frac{m^3}{s}\right)$$

Note: Volumetric flow rate is negative as liquid flow is from top to bottom in the column.

c_i = Concentration of species within control volume $\left(\frac{mol}{m^3}\right)$

A_T = Area of transfer for diffusion (m) , $\dot{n}^{"}_{diff}$= diffusion mol flux $\left(\frac{mol}{m^2 s}\right)$ u = Velocity of fluid $\left(\frac{m}{s}\right)$,

A_C = Cross sectional area of absorption column (m), V = Volume of control volume = Δz A_C (m^3)

a_w= bed specific area $\left(\frac{m^2}{m^3}\right)$ which can be rewritten $a_w = \frac{A_T}{V}$

$$\frac{dn}{dt} = \dot{n}_{in} - \dot{n}_{out} - \dot{n}_{diff} + \dot{n}_{gen}$$

$$\frac{\partial(cV)}{\partial t} = c_z \dot{V} - c_{z+\Delta z} \dot{V} - \dot{n}''_{diff} a_w V + R_{gen} V$$

$$V \frac{\partial c}{\partial t} = -uA_c \ (c_z - c_{z+\Delta z}) - \dot{n}''_{diff} a_w V + R_{gen} V$$

$$(\Delta z A_c) \frac{\partial c}{\partial t} = uA_c \ (c_{z+\Delta z} - c_z \ ) - \underbrace{\dot{n}''_{diff} a_w}_{\dot{n}_d} \Delta z A_c + R_{gen} \Delta z A_c$$

Dividing by $\Delta z A_c$ and letting Δz tend to zero results in the partial differential equation for the liquid phase. The subscript i is added to the equation to denote that the mol balance is for each species. The species that are present in the liquid phase are shown in table 2.1 with the information if it has a diffusion term, generation term or both.

$$\frac{dc_i^l}{dt} = u \frac{dc_i^l}{dz} - \dot{n}_{i,d} + R_{i,gen} \quad \text{(Eq 2.2)}$$

The derivation for the gas phase is the same method except the Volume flow rate is positive, the diffusion mol flow is positive and there is no generation term. The vapour phase has the general formula of equation 2.3;

$$\frac{dc_i^v}{dt} = -u \frac{dc_i^v}{dz} + \dot{n}_{i,d} \quad \text{(Eq 2.3)}$$

For each species the diffusion mol flow ($\dot{n}_d$) is the same so what leaves the liquid phase enters the vapour phase.

Table 2.1:Terms for each species in Concentration model

Species	Gas phase	Liquid phase	Generation term	Diffusion term
CO_2	Yes	Yes	Yes	Yes
MEA	Yes	Yes	Yes	Yes
H_20	Yes	Yes	No	Yes
N_2	Yes	Yes	No	Yes
O_2	Yes	Yes	No	Yes
$MEAH^+$	No	Yes	Yes	No
$MEACOO^-$	No	Yes	Yes	No
HCO_3^-	No	Yes	Yes	No
OH^-	No	Yes	Yes	No
H_3O^+	No	Yes	Yes	No

2.1.2 Vapour Liquid Equilibrium Model Development

Equation of State

The development of a vapour equilibrium model is an integral part in the development of the dynamic model of the system as it is required to evaluate the diffusion mol flow. For vapour-liquid equilibrium the fugacity of the liquid is equal to the fugacity of the vapour for each phase. Typically an Equation of state is used to calculate the fugacity of the vapour phase. The fugacity of the liquid can be either calculated with an equation of state or with activity co-efficient. The model in this work was developed with an equation of state for the fugacity of the liquid and vapour phases for each component. The Peng Robinson equation of state was used which has the standard form of equation 2.4 (Smith 2005).

$$Z = \frac{V}{V-b} - \frac{aV}{RT(V^2+2bV-b^2)} \quad \text{(Eq 2.4)}$$

Where $Z = \frac{PV}{RT}$

V= Molar Volume $\left(\frac{m^3}{mol}\right)$

P= Pressure (Pa)

R= Gas constant (J/mol*K)

T= Temperature (K)

a= $0.45724\frac{R^2T_c^2}{P_c}\alpha$

b= $0.0778\frac{RT_c}{P_c}$

$\alpha =$ $\left(1+\kappa(1-\sqrt{T_R})\right)^2$ ..

$\kappa =$ $0.37464 + 1.54226\omega - 0.26992\omega^2$

T_c= Critical Temperature (K)

P_c= Critical Pressure (Pa) .

ω= $\left[-log\left(\frac{P^{Sat}}{P_c}\right)_{T_R=0.7}\right] - 1$ Acentric factor

T_r= $\frac{T}{T_c}$ Reduced Temperature

This can be rearranged into a cubic equation and solved. The largest root is typically the compressibility factor for the vapour phase while the smallest root is typically the compressibility factor for the liquid phase. The form of the cubic equation is equation 2.5 which can be solved to find the three roots for which the equation equals zero.

$$Z^3 + \beta Z^2 + \gamma Z + \delta = 0 \quad \text{(Eq 2.5)}$$

Where $\beta = B - 1$

$$\gamma = A - 3B^2 - 2B$$

$$\delta = B^3 + B^2 - AB$$

$$A = \frac{aP}{R^2T^2}$$

$$B = \frac{bP}{RT}$$

Mixing Rules

For multi component systems mixing rules can be applied to determine values for A and B. The van der Waals mixing equations (Elliot and Lira 1998) are

$$A^l_{mix} = \frac{a^l_{mix}P}{R^2T^2} \; and \; A^v_{mix} = \frac{a^v_{mix}P}{R^2T^2}$$

$$B^l_{mix} = \frac{b^l_{mix}P}{RT} and \; B^v_{mix} = \frac{b^v_{mix}P}{RT}$$

Where: $b^l_{mix} = \sum_i^N x_i b_i \quad and \quad b^v_{mix} = \sum_i^N y_i b_i$

$$a^l_{mix} = \sum_i^N \sum_j^N x_i x_j \sqrt{a_i a_j} \left(1 - k_{ij}\right)$$

$$a^v_{mix} = \sum_i^N \sum_j^N y_i y_j \sqrt{a_i a_j} \left(1 - k_{ij}\right)$$

k_{ij}=binary interaction parameter

y_i= mol fraction of component i in gas phase

x_i= mol fraction of component i in liquid phase

Note: The mol fraction in the gas phase is $y_i = \frac{n_i^v}{n_T^v}$ and $c_i^v \equiv \frac{n_i^v}{V^v}$

Therefore the mol fraction of the gas can be evaluated as a function of the component concentration in the vapour phase. The mol fraction in the liquid phase takes the same form.

This can be expressed in equation form $y_i = \frac{c_i^l}{c_T^l}$ $x_i = \frac{c_i^l}{c_T^l}$

Where c_i^v= Concentration of component in vapour phase $(\frac{mol}{m^3})$

c_i^l= Concentration of component in liquid phase $(\frac{mol}{m^3})$

c_T^v= Sum of component concentrations vapour phase $(\frac{mol}{m^3})$

c_T^l= Sum of component concentrations liquid phase $(\frac{mol}{m^3})$

The compressibility factor Z for the vapour phase is computed by solving the Peng Robinson equation for the largest root using the vapour A and B coefficients. Likewise the compressibility factor Z is the smallest root of the equation of state with the liquid co-efficient for A and B.

Fugacity

The fugacity coefficient of each component in each phase can be calculated by solving equation 2.6 (Elliot and Lira).

$$ln\ \varphi_i = \frac{1}{RT}\int_V^\infty \left[\left(\frac{\partial P}{\partial N_i}\right)_{T,V,N_j} - \frac{RT}{V}\right] dV - RTln\ Z \quad \text{(Eq 2.6)}$$

For the Peng Robinson equation of state this integration yields for the liquid phase (Elliot and Lira 1998) .

$$ln\varphi_i^L = \frac{B_i^l}{B_{mix}^l}(Z^l - 1) - \ln\left(Z^l - B_{mix}^l\right) - \frac{A_{mix}^l}{2\sqrt{2}B_{mix}^l}\left(\frac{2\sum x_i A_i^l}{A_{mix}^l} - \frac{B_i^l}{B_{mix}^l}\right) ln\left(\frac{Z^l + (1+\sqrt{2})B_{mix}^l}{Z^l + (1-\sqrt{2})B_{mix}^l}\right) \quad \text{(Eq 2.7)}$$

In this formula $A_i^l$and B_i^l are the A and B co-efficient for the pure component while A_{mix}^l and B_{mix}^l are the mixture coefficients.

Similarly the Vapour phase fugacity for each component in the mixture has the same form except that it is evaluated with A and B co-efficient for vapour phase and the x liquid mol fraction is replaced with y gas mol fraction.

Vapour Liquid Equilibrium

It is assumed at the interface of vapour and liquid that there are equilibrium conditions. This requires that the Gibbs free energy is at a minimum and the chemical potential of the vapour and liquid are equal. Fugacity is used to evaluate the equilibrium conditions and it can be shown for each component i in the mixture that:

$$\hat{f}_i^V = \hat{f}_i^V$$

Where $\hat{f}_i^V = y_i \varphi_i^V P$ Vapour fugacity of component in mixture

$\hat{f}_i^L = x_i \varphi_i^L P$ Liquid fugacity of component in mixture

Equating the two expressions and eliminating P

$$y_i \varphi_i^V = x_i \varphi_i^L$$

Defining the vapour-liquid equilibrium in terms of K values where

$$K_i = \frac{\varphi_i^L}{\varphi_i^V}$$

This results in the simplified expression in equation 2.8 for the vapour liquid equilibrium

$$y_i = K_i x_i \quad \text{(Eq 2.8)}$$

The value K_i for each component can be computed from the equation of state.

2.1.3 Vapour Phase Equilibrium for MEA System

We are wishing to model 5 components in the liquid-gas equilibrium system. The five components are water, MEA, nitrogen, carbon dioxide and oxygen. Figure 2.2 is of the concentration profile in the bulk, film and interface.

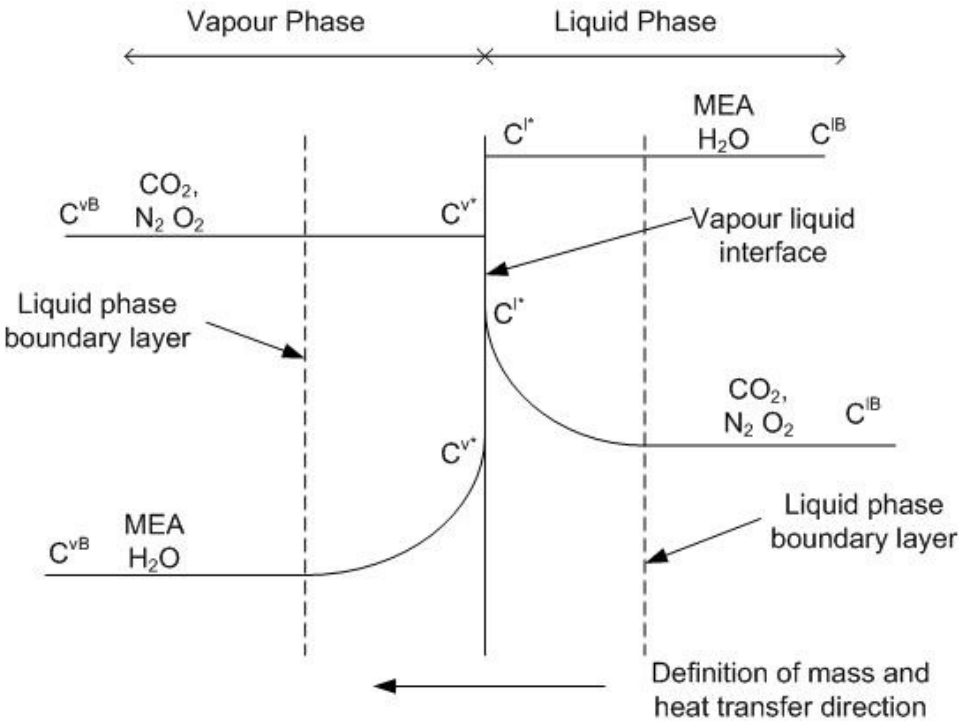

Figure 2.2: Concentration gradients of two film theory for vapour liquid system.

For water and MEA an assumption that can be made is that in the liquid phase the concentration at the interface is the same as the bulk layer of the fluid. This is a reasonable assumption as the liquid is mostly composed of water and MEA and as diffusion takes place form a low concentration to a high concentration then if the liquid film is mostly composed of MEA and water then there is assumed a negligible concentration gradient of the water and MEA in the liquid film. Therefore it is assumed the only resistance to mol transfer for water and MEA is in the vapour phase.

In the gas phase the resistance to mol transfer for O_2, CO_2 and N_2 is considerably less than the resistance to transfer in the liquid phase. This is because the liquid phase is pre-dominantly water and MEA and therefore there is a large concentration gradient for O_2, N_2 and CO_2 in the liquid film. The liquid resistance for O_2, N_2 and CO_2 is in the order of 1000 times greater in the liquid phase than in the vapour phase where there is more space between the particles hence diffusion proceeds much quicker. For this reason the resistance in the vapour phase is assumed to be negligible and bulk vapour phase concentration is assumed to be the same as the interface concentration for O_2, and N_2. The CO_2 is affected by the enhancement factor as discussed in section 2.1.8 which reduces the resistance in the liquid phase by a factor of about

100. Therefore for CO_2 the liquid resistance is include as it comprises up to 15% of the resistance.

To calculate the liquid-vapour equilibrium from the fugacity co-efficient and utilize the relationship $y_i = K_i x_i$, the x and y mol fractions must be evaluated at the vapour liquid interface. From the assumptions listed above the unknown and known interface concentrations are. Note :* is the interface concentration and without is the bulk phase concentration.

$$c_{CO_2}^{v*} = c_{CO_2}^{v}$$

$$c_{CO_2}^{l*} = Unkown$$

$$c_{MEA}^{v*} = Unkown$$

$$c_{MEA}^{l*} = c_{MEA}^{l}$$

$$c_{H_2O}^{v*} = Unkown$$

$$c_{H_2O}^{l*} = c_{H_2O}^{l}$$

$$c_{N_2}^{v*} = c_{N_2}^{v}$$

$$c_{N_2}^{l*} = Unkown$$

$$c_{O_2}^{v*} = c_{O_2}^{v}$$

$$c_{O_2}^{l*} = Unkown$$

The general form of the mol fraction is $x_i \; or \; y_i = \frac{c_i}{c_{N_2} + c_{CO_2} + c_{O_2} + c_{MEA} + c_{H_2O}}$

A reasonable approximation that can be made is that for the components in the vapour phase which have the same bulk and interface concentration also have the same vapour mol fraction at the interface i.e. $y_{CO_2}^{v*} \approx y_{CO_2}^{v}, \quad y_{O_2}^{v*} \approx y_{O_2}^{v} \; and \; y_{N_2}^{v*} \approx y_{N_2}^{v}$

This is a reasonable assumption as the majority of the components in the vapour phase are O_2, N_2 and CO_2, hence the mol fractions between the bulk vapour and interface are not effected greatly by the change in vapour concentration of MEA and H_20 in the bulk and interface.

Likewise in the liquid phase $x^{l*}_{H_2O} \approx x^{l}_{H_2O}$, $x^{l*}_{MEA} \approx x^{l}_{MEA}$

This is also a reasonable approximation also the bulk of the concentration of the liquid is water and MEA and is not effected greatly by the change in liquid concentrations of the O_2, N_2 and CO_2. This is essentially applying a one film theory for all components with the components water and MEA having a vapour film while the remaining components O_2, N_2 and CO_2.having a liquid film.

2.1.4 Solving for Unknown Mol Fractions at the VL Interface

The unknown mol fractions ($x^{l*}_{CO_2}$, $x^{l*}_{O_2}$, $x^{l*}_{N_2}, y^{v*}_{H_2O}$ and y^{v*}_{MEA}) can be solved by successive approximation by iterating on the fugacity ratio K_i. A constraint of the system is that the mol fractions sum to 1 for both the liquid and the vapour phases. This allows one of the unknowns to be eliminated. Water is chosen to be eliminated from the liquid phase and nitrogen from the vapour phase.

$$x^{l}_{H_2O} = 1 - x^{l*}_{CO_2} - x^{l*}_{O_2} - x^{l*}_{N_2} - x^{l}_{MEA} \quad \text{and} \quad y^{v}_{N_2} = 1 - y^{v}_{CO_2} - y^{v}_{O_2} - y^{v*}_{H_2O} - y^{v*}_{MEA}$$

Rewriting the unknowns in terms of the known values

$$x^{l*}_{CO_2} = \frac{y^{v}_{CO_2}}{K_{CO_2}(x,y)}$$

$$y^{v*}_{MEA} = K_{MEA}(x,y) * x^{l}_{MEA}$$

$$y^{v*}_{H_2O} = K_{H_2O}(x,y) * x^{l}_{H_2O}$$

$$x^{l*}_{O_2} = \frac{y^{v}_{O_2}}{K_{O_2}(x,y)}$$

$$y^{v}_{N_2} = 1 - y^{v}_{CO_2} - y^{v}_{O_2} - y^{v*}_{H_2O} - y^{v*}_{MEA}$$

$$x^{l*}_{N_2} = \frac{y^{v}_{N_2}}{K_{N_2}(x,y)}$$

$$x^{l}_{H_2O} = 1 - x^{l*}_{CO_2} - x^{l*}_{O_2} - x^{l*}_{N_2} - x^{l}_{MEA}$$

Initial guesses for the unknowns ($x^{l*}_{CO_2}$, $x^{l*}_{O_2}$, $x^{l*}_{N_2}$, $y^{v*}_{H_2O}$ and y^{v*}_{MEA}) at the interface can be approximated by the mol fractions of the component in the bulk phase for a first iteration and

the fugacities and K_i calculated. The unknowns are then updated by the above formulas and reiterated until the values do not change. This is essentially solving four non-linear equations simultaneously and the output is the mol fractions at the interface for the gas and liquid phases. This is included as a sub routine called NLPE.m within the code and is attached in appendix D.

2.1.5 Solving for Concentrations at the Interface

Knowing the mol fractions of each component at the interface allows the concentration of each component at the interface to be calculated by solving the linear equations.

$$c_{CO_2}^{l*} = x_{CO_2}^{*} c_T^{l*}$$

$$c_{MEA}^{v*} = y_{MEA}^{*} c_T^{v*}$$

$$c_{H_2O}^{v*} = y_{H_2O}^{*} c_T^{v*}$$

$$c_{N_2}^{l*} = x_{N_2}^{*} c_T^{l*}$$

$$c_{O_2}^{l*} = x_{O_2}^{*} c_T^{l*}$$

Expanding out the first term for CO_2:

$$c_{CO_2}^{l*} = x_{CO_2}^{*}(c_{CO_2}^{l*} + c_{MEA}^{l} + c_{H_2O}^{l} + c_{N_2}^{l*} + c_{O_2}^{l*})$$

$$c_{CO_2}^{l*}(1 - x_{CO_2}^{*}) - x_{CO_2}^{*} c_{N_2}^{l*} - x_{CO_2}^{*} c_{O_2}^{l*} = x_{CO_2}^{*}(c_{MEA}^{l} + c_{H_2O}^{l})$$

Likewise for the other components

$$c_{MEA}^{v*}(1 - y_{MEA}^{*}) - y_{MEA}^{*} c_{H_2O}^{v*} = y_{MEA}^{*}(c_{N_2}^{v} + c_{CO_2}^{v} + c_{O_2}^{v})$$

$$c_{H_2O}^{v*}(1 - y_{H_2O}^{*}) - y_{H_2O}^{*} c_{MEA}^{v*} = y_{H_2O}^{*}(c_{N_2}^{v} + c_{CO_2}^{v} + c_{O_2}^{v})$$

$$c_{N_2}^{l*}(1 - x_{N_2}^{*}) - x_{N_2}^{*} c_{CO_2}^{l*} - x_{N_2}^{*} c_{O_2}^{l*} = x_{N_2}^{*}(c_{MEA}^{l} + c_{H_2O}^{l})$$

$$c_{O_2}^{l*}(1 - x_{O_2}^{*}) - x_{O_2}^{*} c_{N_2}^{l*} - x_{O_2}^{*} c_{CO_2}^{l*} = x_{O_2}^{*}(c_{MEA}^{l} + c_{H_2O}^{l})$$

In matrix form this is:

$$\overbrace{\begin{bmatrix} 1-x^*_{CO_2} & 0 & 0 & -x^*_{CO_2} & -x^*_{CO_2} \\ 0 & 1-y^*_{MEA} & -y^*_{MEA} & 0 & 0 \\ 0 & -y^*_{H_2O} & 1-y^*_{H_2O} & 0 & 0 \\ -x^*_{N_2} & 0 & 0 & 1-x^*_{N_2} & -x^*_{N_2} \\ -x^*_{O_2} & 0 & 0 & -x^*_{O_2} & 1-x^*_{O_2} \end{bmatrix}}^{A} * \overbrace{\begin{bmatrix} C^{l*}_{CO_2} \\ C^{v*}_{MEA} \\ C^{v*}_{H_2O} \\ C^{l*}_{N_2} \\ C^{l*}_{O_2} \end{bmatrix}}^{C} = \overbrace{\begin{bmatrix} x^*_{CO_2}(C^l_{MEA}+C^l_{H_20}) \\ y^*_{MEA}(C^v_{CO_2}+C^v_{O_2}+C^v_{N_2}) \\ y^*_{H_2O}(C^v_{CO_2}+C^v_{O_2}+C^v_{N_2}) \\ x^*_{N_2}(C^l_{MEA}+C^l_{H_20}) \\ x^*_{O_2}(C^l_{MEA}+C^l_{H_20}) \end{bmatrix}}^{B}$$

This can be solved within Matlab by $C = A^{-1}B$ to provide the interface concentrations.

An alternative method using fugacity as the driving force is developed in appendix A.

2.1.6 Mol Flow Due to Diffusion.

The general equation for the mass transfer is given in equations 2.9 for the vapour phase and 2.10 for the liquid phase. Note the liquid mol flow has a negative value because the mol flow is defined as flow from liquid to gas so is leaving the liquid phase and adding to vapour phase.

$$\dot{n}^v_{d,i} = kd^v_i(C^{*v}_i - C^v_i)a_w \quad \text{(Eq 2.9)}$$

$$\dot{n}^l_{d,i} = -kd^l_i(C^{*l}_i - C^l_i)a_w \quad \text{(Eq 2.10)}$$

Where $\dot{n}^v_{d,i}$ = diffusion mol flow rate of component in vapour phase $\left(\frac{mol}{sm^3}\right)$

$\dot{n}^l_{d,i}$ =diffusion mol flow rate of component in liquid phase. $\left(\frac{mol}{sm^3}\right)$

kd^v_i = Transfer coefficient for component in vapour. $\left(\frac{m}{s}\right)$

kd^l_i = Transfer coefficient for component in liquid. $\left(\frac{m}{s}\right)$

C^*_i = Species interface concentration. $\left(\frac{mol}{m^3}\right)$

C_i = Species bulk concentration. $\left(\frac{mol}{m^3}\right)$

a_w = Actual wetted hydraulic specific transfer area $\left(\frac{m^2}{m^3}\right)$

2.1.7 Mass Transfer Coefficient

Billet and Schultes (1999) provides an empirical formula for the mass transfer coefficients for each component. The liquid transfer coefficient for the O_2, N_2 and CO_2 is:

$$kd_i^l = C_l \left(\frac{\rho^l g}{\mu^l}\right)^{1/6} \left(\frac{a_t D_i^l}{4\epsilon}\right)^{1/2} \left(\frac{u^l}{a_t}\right)^{1/3} \quad \text{(Eq 2.11)}$$

And for the vapour transfer coefficient for MEA and water is:

$$kd_i^v = C_v \frac{a_t D_i^v}{(4\varepsilon^2 - 4\varepsilon h_T)^{1/2}} \left(\frac{\rho^v u^v}{a_t \mu^v}\right)^{3/4} \left(\frac{\mu^v}{\rho^v D_i^v}\right)^{1/3} \quad \text{(Eq 2.12)}$$

Where

C_l= packing constant for liquid

ρ^l= density of liquid $\left(\frac{kg}{m^3}\right)$

g= Gravity constant $\left(\frac{m}{s^2}\right)$

μ^l= dynamic viscosity of liquid $\left(\frac{kg}{m\ s}\right)$

a_T= bed specific area $\left(\frac{m^2}{m^3}\right)$

D_i^l= Diffusion coefficient of component in liquid $\left(\frac{m^2}{s}\right)$

ε= Packing void fraction

u^l= Liquid velocity $\left(\frac{m}{s}\right)$

ρ^v= density of vapour $\left(\frac{kg}{m^3}\right)$

μ^v= dynamic viscosity of vapour $\left(\frac{kg}{m\ s}\right)$

a_T= bed specific area $\left(\frac{m^2}{m^3}\right)$

D_i^v= Diffusion coefficient of component in vapour $\left(\frac{m^2}{s}\right)$

u^v= Vapour velocity $\left(\frac{m}{s}\right)$

h_T= liquid hold up per bed volume (-)

Where h_T is given by the equation (Billet and Schultes 1999):

$$h_T = \left(\frac{12u^l\, a_T^2\ \ \mu^l}{g\rho^l}\right)^{1/3} \left(\frac{a_w}{a_T}\right)^{2/3} \quad \text{(Eq 2.13)}$$

And $$\frac{a_w}{a_T} = C_h \left(\frac{\rho^l u^l}{a_T \mu^l}\right)^{0.15} \left(\frac{a_T (u^l)^2}{g}\right)^{0.1} \quad \text{when } Re^l < 5 \quad \text{(Eq 2.14)}$$

. $$\therefore \frac{a_w}{a_T} = 0.85 C_h \left(\frac{\rho^l u^l}{a_T \mu^l}\right)^{0.25} \left(\frac{a_T (u^l)^2}{g}\right)^{0.1} \quad \text{when } Re^l > 5 \quad \text{(Eq 2.15)}$$

$$Re^l = \frac{\rho^l u^l}{a_T \mu^l}$$

Where C_h= Packing Constant for liquid holdup

The values of a_T, ε, C_l ,C_h and C_v are properties of the packing material.

2.1.8 Enhancement Factor

The resistance to mol transfer of the carbon dioxide into the liquid phase is dominated by the resistance in the liquid film as it takes time for the CO_2 molecules to diffuse into the bulk fluid. Since the reactions with MEA and CO_2 happen very quickly in the first part of the film, the CO_2 does not have to diffuse all the way from the interface to the bulk of the fluid. This is represented by an enhancement factor which accounts for the continual removal of CO_2 by the MEA from the liquid film. Figure 2.3 is a plot of the Hatta number verse the enhancement factor for a pseudo first order reaction and also for second order reactions. The Hatta number is defined in Perry and Green (1999) as

$$HA = \frac{maximum\ connversion\ in\ the\ film}{maximum\ diffuisional\ transport\ through\ the\ film}$$

when the Hatta number is greater than 1 all of the diffusing species (CO_2) is reacted in the film (but not necessarily consumed depending on the equilibrium constants). The reactions of MEA and CO_2 typically react quickly a within the film and the ratio of the MEA concentration and

MEA diffusivity (c_{BL} D_B) is typically at least 1000 times greater than the concentration of CO_2 and diffusivity of CO_2.($c_{AL}D_A$) .so the enhancement factor can be taken as the Hatta number.

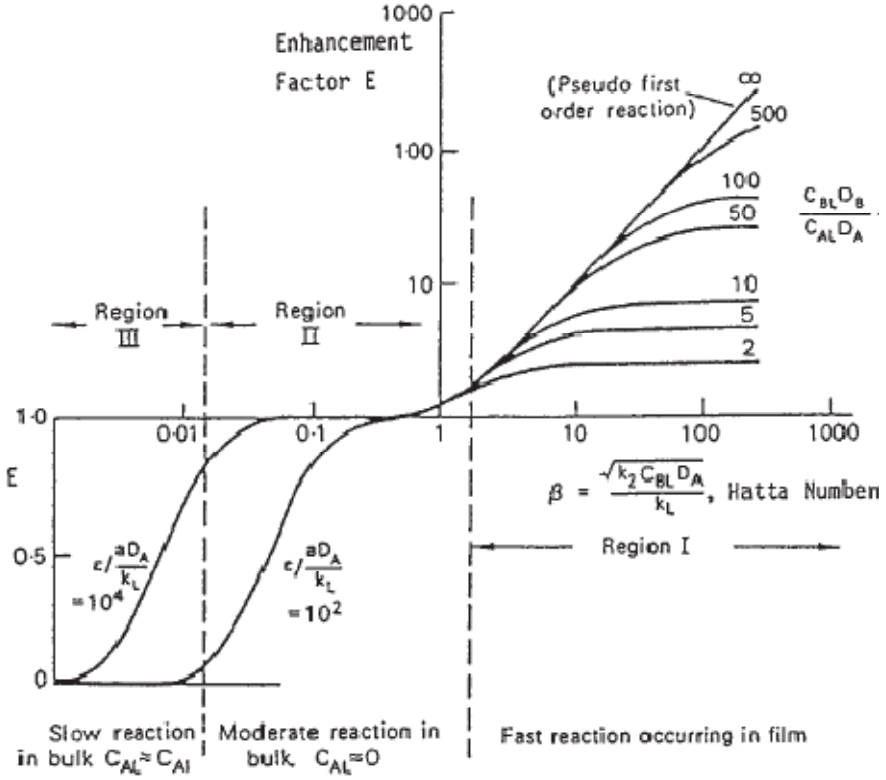

Figure 2.3: Hatta number and enhancement number from Perry and Green (1999).

The Hatta number is a function of the MEA concentration, MEA reaction rate, CO_2 diffusivity, CO_2 concentration and CO_2 reaction rate (reaction 3). Hoff (2003) recommends that when the Hatta number is greater than 2 then Ha = E. The Hatta number and the enhancement factor is given by:

$$Ha = \frac{\sqrt{D_{CO_2}^{l,unreact}\left(k_{1f}\, C_{MEA}^{l} + k_{3f}\, C_{CO_2}^{l}\right)}}{k d_{CO_2}^{l}} = E$$

*note: Refer to section 2.1.10 on chemical reactions for definition of reaction rate values k_{1f} and k_{3f}

The reaction rate of k_{3f} and concentration of CO_2 are included as recommended by Versteeg et al (2006); to allow for the enhancement factor when the MEA is all consumed and reaction 3 is the dominant CO_2 removal reaction. For the typical case the concentration of CO_2 is close to

zero and the enhancement factor is predominantly a function of the rate of reaction for reaction 1 and the concentration of free MEA.

Inserting the enhancement factor into the equation 2.10 for the rate of mol diffusion for CO_2 leads to the modified equation 2.16:

$$\dot{n}^l_{d,CO_2} = -kd^l_{CO_2} E\left(C^{*l}_{CO_2} - C^l_{CO_2}\right)a_w \quad \text{(Eq 2.16)}$$

The enhancement factor is multiplied by the CO_2 transfer coefficient in the liquid phase to allow for the reactions taking place in the liquid film layer. This method assumes the resistance in the liquid phase is ignored where in practice this can be 15% of the value. Therefore henrys law for CO_2 is used to model the diffusion of CO_2.

2.1.9 Henrys Law for CO_2

Henrys law relates the concentration of a component in the liquid to an equivalent interface pressure. Henrys law takes the form

$$P^*_i = H_i c^{l*}_i \; or \; P^*_i = H^{alt}_i x^*_i$$

Where H_i= Henrys law in units of $\frac{Pa\, m^3}{Mol}$

H_i^{alt}= Henrys law in units of Pa

The relationship between the two forms of the henrys law coefficient is:

$$H_i = \frac{H^{alt}_i}{c^l_T}$$

Assuming a two film model with no accumulation and steady state the mol flux component entering the vapour phase film is equal to the mol flux of the leaving the liquid film. In equation form this is

$$\dot{n}^l_{d,i} = -Ekd^l_i a_w (C^{l*}_i - C^l_i) = \dot{n}^v_{d,i} = kd^v_i a_w (C^{v*}_i - C^v_i)$$

Rearranging the equations to eliminate the interface values.

$$\dot{n}^l_{d,i} = -Ekd^l_i a_w (C^{l*}_i - C^l_i) \qquad \dot{n}^v_{d,i} = \frac{kd^v_i a_w}{RT^v Z^v}(P^{v*}_i - P^v_i)$$

$$C_i^{l*} = C_i^l - \frac{\dot{n}_{d,i}^l}{Ekd_i^l a_w} \qquad P_i^{v*} = P_i^v + \frac{\dot{n}_{d,i}^v RT^v Z^v}{kd_i^v a_w}$$

$$C_i^{l*} = C_i^l - \frac{\dot{n}_{d,i}^l}{Ekd_i^l a_w} \qquad H_i C_i^{l*} = P_i^v + \frac{\dot{n}_{d,i}^v RT^v Z^v}{kd_i^v a_w}$$

$$\Rightarrow \qquad H_i\left(C_i^l - \frac{\dot{n}_{d,i}^l}{Ekd_i^l a_w}\right) = P_i^v + \frac{\dot{n}_{d,i}^v RT^v Z^v}{kd_i^v a_w}$$

$$\Rightarrow \qquad H_i C_i^l - P_i^v = \frac{\dot{n}_{d,i}^v RT^v Z^v}{kd_i^v a_w} + \frac{H_i \dot{n}_{d,i}^l}{Ekd_i^l a_w}$$

$$\Rightarrow \quad \dot{n}_{d,i}^l = \dot{n}_{d,i}^v = \left(\frac{1}{\frac{H_i}{Ekd_i^l a_w} + \frac{RT^v Z^v}{kd_i^v a_w}}\right)\left(H_i C_i^l - P_i^v\right)$$

This can be simplified to equation 2.17:

$\dot{n}_{d,CO_2}^l = -kd_{CO_2}^H a_w\left(P_{CO_2}^v - H_{CO_2} C_{CO_2}^l\right)$ (eq 2.17)

Where

$$kd_{CO_2}^H = \frac{1}{\frac{H_i}{Ekd_i^l} + \frac{RT^v Z^v}{kd_i^v}}$$

Henry Law Coefficients

The henrys law coefficient for CO_2 in water and MEA are form Liu et al 1999.

$$H_{H_2O}^{alt} = exp\left(170.7126 - \frac{8477.771}{T^l} - 21.95743 lnT^l + 0.005781 T^l\right) \ (Pa)$$

$$H_{MEA}^{alt} = exp\left(89.452 - \frac{2934.6}{T^l} - 11.592 lnT^l + 0.01644 T^l\right) \ (Pa)$$

The mixing rule for henrys law for CO_2 in an amine solution is given from Reid et al (1987)

$$H_{mixture}^{alt} = x_{H_2O} H_{H_2O}^{alt} + x_{MEA} H_{MEA}^{alt}$$

The ionic strength of the liquid affects the solubility of the CO_2 in the liquid. The value of henrys constant can be correlated for the ionic effect of the solution by the van Krevelen and Hoftijzer.

$$log_{10}\left(\frac{H_i^{salt}}{H_i}\right) = h_{vk} I$$

Where H_i^{salt} = adjusted henrys constant $\frac{Pa\ m^3}{Mol}$

$h_{vk} = \sum h_{vk,i}$ = Factor from ion in solution $\frac{l}{mol}$

I = Ionic strength of mixture $\frac{mol}{l}$

The ionic strength is converted to mol/ l for the van Krevelen formula.

$$I = \frac{1/2 \sum c_i^i z_i^2}{1000}$$

Where z_i =Valence of ion

The valance of each ionic species and van Krevelen co-efficient are listed in table 2.2 and are taken from Hoff (2003) .

Table 2.2: van Krevelen constants used in this work

Species	$h_{vk,i}$	z_i
CO_2	-0.019	0
RNH_3^+	0.055	1
$RNHCOO^- +$	0.043	-1
HCO_3^-	0.073	-1

The contribution of the H_3^+0 , HO^- are not included as the concentrations of these ions are low.

2.1.10 Reactions

General

For a general reaction of the form, where capital letters denote concentrations and small letters denote stoichmetric coefficients.

$$aA \quad + bB \underset{k_{jf},k_{jr},K_{j1}}{\Longleftrightarrow} cC + dD$$

Where j denotes the reaction number

k_{jf} = Forward reaction rate

k_{jr} = Reverse reaction rate

K_1 = Equilibrium constant = $\left(\frac{k_{jf}}{k_{jr}}\right)$

Theoretically the equilibrium is defined in terms of reactivity of the various species present in the reaction, The reactivity of a species is related to the concentration of the species by the activity coefficient of the species. (Smith 2005).

$$K_1 \equiv \frac{\{C\}^c\{D\}^d}{\{A\}^a\{B\}^b}$$

$$\{i\} \equiv \gamma_i[i]$$

Where

$\{i\}$ = Reactivity of the species $\frac{mol}{m^3}$

$[i]$= Concentration of the species $\frac{mol}{m^3}$

γ_i= Activity coefficient of the species

When $\gamma_i$the solute is at unity then is at infinite dilution and is a typical reference state (except for water). As the activity coefficients deviates from unity the effects of the ions in the solution become relevant. The Debye-Huckel method to calculate the activity coefficient of a species is a function of the ionic strength of the mixture and the ion valance. In the general case this is:

$$log\gamma_i = \frac{-0.51z_i^2\sqrt{I}}{1+\sqrt{I}}$$

With the Debye-Hukel formula all ions with the same valance have the same activity coefficient (strictly speaking the γ_i is also a function of the ions atomic radius but this is usually not accounted for (chembuddy)). This result often allows simplifications to be applied to the MEA-CO_2 system as some of the activity coefficients can be cancelled in the calculation of the equilibrium concentration.

Many papers and researchers investigate the correct form of the equilibrium constants and correlate experimental data to activity coefficients. The well known and used Kent Eisenberg model has all activity coefficients set to unity and the equilibrium constants fitted to saturation pressure experimental data (Kohl 1995). The model of Deshmukh and Mather applies the Debye-Huckel theory to fit activity coefficients to the equilibrium constants. This was later modified by Li and Mather to use the Pitzer method to regress the activity coefficients (Kohl 1995). Liu et al (1999) developed a set of new equilibrium constants for the MEA-CO_2 system regressed to include the activity coefficients and these constants where used in this work. We assume at equilibrium that the forward reaction rate is equal to the backward reaction rate

Therefore at equilibrium.

$$r_{jf} = k_{jf}[A]^a[B]^b = r_{jr} = k_{jr}[C]^c[D]^d$$

$$\frac{k_{jf}}{k_{jr}} = \frac{[C]^c[D]^d}{[A]^a[B]^b} = K$$

Vaidya and Kenig (2007) and Svendsen and da Silvia (2007) provide a summary of the reactions that can take place in amine systems and the various pathways that have been proposed. It is noted that there is not overall agreement within all the researchers of the exact mechanisms in action.

Reaction 1 Overall reaction rate of MEA and Carbon dioxide

$$CO_2 + 2RNH_2 \underset{k_{1f},k_{1r},K_1}{\Longleftrightarrow} RNHCOO^- + RNH_3^+$$

There is debate among authors of the exact mechanisms in play in the formation of the carbamate and protanated MEA but there is general agreement on the products and the reactants of the general equation. The forward reaction is initially between a CO_2 and MEA

molecule forming an intermediate compound which then further reacts with another MEA molecule. The second step happens much faster than the first step hence the first step is rate limiting and of second order. For the loading rate of CO_2 to MEA of less than 0.5 this is the overall equation. For a 30% MEA solution the concentration of MEA is approximately 5000 mol/m^3 the operating CO_2 loading is typically between 0.2-0.45 so reaction 1 is the dominant reaction. Aboudheir et al (2003) reviews literature for values of the forward rate and observes a varied spread and a strong function of temperature. Jamal et al (2006) recommended the following forward rate

$$k_{1f} = 3.95x10^{10} exp\left(-\frac{6864}{T^l}\right)\left(\frac{m^3}{mol\ s}\right)$$

$$r_{1f} = k_{1f}[RNH_2][CO_2]\left(\frac{mol}{m^3\ s}\right)$$

The equilibrium constant is evaluated as a combination of three other equilibrium constants. This can be done because at equilibrium all concentrations are steady therefore the equilibrium concentrations can be interchanged:

$$K_1 = \frac{K_2}{K_5 K_6} = \frac{[HCO_3^-]_e[H_3^+O]_e}{[H_20]_e^2[CO_2]_e}\frac{[RNCOO^-]_e}{[HCO_3^-]_e[RNH_2]_e}\frac{[RNH_3^+]_e}{[RNH_2]_e[H_3^+O]_e} = \frac{[RNHOO^-]_e[RNH_3^+]_e}{[RNH_2]_e^2[CO_2]_e}$$

Therefore the reverse reaction rate is:

$$r_{1r} = \frac{k_{1f}}{K_1}[RNHOO^-]\,[RNH_3^+] \qquad \left(\frac{mol}{m^3\ s}\right)$$

Reaction 2 Hydrolyze of CO_2 with Water

This reaction is slow and can generally be ignored (Versteeg & van Swaaij 1984) but the equilibrium K_2 is used in determining the equilibrium value for K_1 and K_3.

$$CO_2 + 2H_20 \underset{k_{2f},k_{2r},K_2}{\Longleftrightarrow} HCO_3^- + H_3^+O$$

The forward reaction is given by Pinsent (1956) for 298K and is a first order reaction with CO_2. Temperature dependence of the forward rate is not included because the rate is small and the contribution insignificant.

$$k_{2f} = 0.024 \left(\frac{1}{s}\right)$$

$$r_{2f} = k_{2f}[CO_2] \left(\frac{mol}{m^3\ s}\right)$$

The equilibrium constant is given by Liu et al (1999).

$$K_2 = \frac{[HCO_3^-]_e[H_3^+O]_e}{[H_20]_e^2[CO_2]_e} = exp\left(231.465 - \frac{12092.1}{T^l} - 36.7816 \ln(T^l)\right) 1x10^6$$

The reverse reaction rate is:

$$r_{2r} = \frac{k_{2f}}{K_2}[HCO_3^-]\,[H_3^+O] \qquad \left(\frac{mol}{m^3\ s}\right)$$

Reaction 3 Bicarbonate Formation

$$CO_2 + OH^- \underset{k_{3f},k_{3r},K_3}{\Longleftrightarrow} HCO_3^-$$

The forward rate for the formation of bicarbonate is significantly fast but the overall rate is usually quite small due to the low concentration of OH^- ions. At loadings of CO_2 /MEA above 0.5 this becomes the dominant reaction for CO_2 removal. The forward rate is from Freguia and Rochelle (2003).

$$k_{3f} = \frac{exp\left(31.396 - \frac{6658}{T^l}\right)}{1000} \left(\frac{m^3}{mol\ s}\right)$$

$$r_{3f} = k_{3f}[OH^-][CO_2] \left(\frac{mol}{m^3\ s}\right)$$

The equilibrium constant is evaluated as a combination of the equilibrium constants from reactions K_2 and K_4:

$$K_3 = \frac{K_2}{K_4} = \frac{[HCO_3^-]_e[H_3^+O]_e}{[H_20]_e^2[CO_2]_e} \frac{[H_20]_e^2}{[OH^-]_e[H_3^+O]_e} = \frac{[HCO_3^-]_e}{[OH^-]_e\,[CO_2]_e}$$

The reverse reaction rate is:

$$r_{3r} = \frac{k_{3f}}{K_3}[HCO_3^-] \qquad \left(\frac{mol}{m^3\ s}\right)$$

Reaction 4 Disassociation of Water

$$2H_2O \underset{k_{4f},k_{4r},K_4}{\Longleftrightarrow} H_3^+O + OH^-$$

This reaction has a forward rate which is quite slow and due to the small number of the equilibrium constant (typically 1x10^{-12}) the backwards rate is fast and considered instantaneous therefore temperature dependence of the forward rate is not included The value for the dissociation rate is taken from Tanaka (2002).

$$k_{4f} = 2x10^{-5}\left(\frac{1}{s}\right)$$

The forward reaction rate is

$$r_{4f} = k_{4f}\ \left(\frac{1}{s}\right)$$

And the equilibrium constant from Liu et al (1999).

$$K_4 = [OH^-][H_3^+O] = 1x10^6 exp\left(132.899 - \frac{13445}{T^l} - 22.4773 \ln\left(T^l\right)\right)$$

The reverse reaction rate is:

$$r_{4r} = \frac{k_{4f}}{K_4}[OH^-]\ [H_3^+O] \qquad \left(\frac{mol}{m^3\ s}\right)$$

Reaction 5 Dissociation of Protanated MEA

This reaction occurs quickly and is considered instantaneous and at equilibrium.

$$RNH_3^+ + H_20 \underset{k_{5f},k_{5r},K_5}{\Longleftrightarrow} RNH_2 + H_3^+O$$

The forward reaction rate is given a low value of 1e-1 as this was found to make the reaction proceed quickly to equilibrium.

$$k_{5f} = 1x10^{-1} \qquad \left(\frac{1}{s}\right)$$

$$r_{5f} = k_{5f}[RNH_3^+] \qquad \left(\frac{mol}{m^3\ s}\right)$$

The equilibrium constant is taken from Lou et al (1999) and is a modification of the Li and Mather (1999) to fit the activity coefficients to experimental data.

$$K_5 = \frac{[RNH_2]_e[H_3^+O]_e}{[RNH_3^+]_e} = 1x10^6 exp\left(0.79960 - \frac{8094.81}{T^l} - 0.007484(T^l)\right)$$

The corresponding reverse reaction rate is shown below.

$$r_{5r} = \frac{k_{4f}}{K_5}[RNH_2]\,[H_3^+O] \qquad \left(\frac{mol}{m^3\,s}\right)$$

Reaction 6 MEA Carbonate Revision

$$H_2O + RNHCOO^- \underset{k_{6f},k_{6r},K_6}{\Longleftrightarrow} HCO_3^- + RNH_2$$

This reaction is also assumed to proceed instantaneously and also be in equilibrium therefore by having a small forward rate the reverse rate is high and the reaction quickly proceeds to equilibrium.

$$k_{6f} = 1x10^{-1} \qquad \left(\frac{1}{s}\right)$$

$$r_{6f} = k_{6f}[RNCOO^-] \qquad \left(\frac{mol}{m^3\,s}\right)$$

The equilibrium constant is also taken from Liu et al (1999) and is also a modified version of the Li Mather constants. The constant had to be multiplied by 2x10^5 to fit the plot to literature.

$$K_6 = \frac{[HCO_3^-]_e[RNH_2]_e}{[RNCOO^-]_e} = \frac{1x10^6}{5} exp\left(1.282562 - \frac{3456.179}{T^l}\right)$$

$$r_{6r} = \frac{k_{6f}}{K_6}[RNH_2]\,[HCO_3^-] \qquad \left(\frac{mol}{m^3\,s}\right)$$

2.1.11 Energy Balance Liquid

Energy balance for the liquid phase:.

$$\frac{dE}{dt} = \dot{E}_z - \dot{E}_{z+\Delta z} - \dot{Q} + \dot{W} - \dot{D}$$

Where

$\frac{dE}{dt}$ = Change in energy of the control volume wrt time $\left(\frac{J}{s}\right)$

$\dot{E}_z$ = Energy transported into contol volume via mol flow at z $\left(\frac{J}{s}\right)$

$\dot{E}_{z+\Delta z}$ = Energy transported out of control volume via mol flow at z+Δz $\left(\frac{J}{s}\right)$

$\dot{Q}$ = Heat transfer at control volume boundaries $\left(\frac{J}{s}\right)$

$\dot{W}$ = Work transfer at control volume boundaries. $\left(\frac{J}{s}\right)$

$\dot{D}$ = Energy of vapour leaving control volume as a vapour due to diffusion $\left(\frac{J}{s}\right)$

Taking the energy terms and defining the values in terms of there individual components.

$$E = K + U + Po$$

$$\dot{E}_z = \dot{K}_z + \dot{U}_z + \dot{P}o_z$$

$$\dot{E}_{z+\Delta z} = \dot{K}_{z+\Delta z} + \dot{U}_{z+\Delta z} + \dot{P}o_{z+\Delta z}$$

$$\dot{W} = \dot{W}_F + P_z\dot{V} - P_{z+\Delta z}\dot{V}$$

$$H = U + PV$$

$$\dot{H} = \dot{U} + P\dot{V}$$

Where K= Kinetic energy of control volume (J)

U= Internal energy of control volume (J)

Po= Potential energy of control Volume (J)

$\dot{K}$= Kinetic energy entering /exciting control volume with mol flow $\left(\frac{J}{s}\right)$

$\dot{P}o$= Potential energy entering /exciting control volume with mol flow $\left(\frac{J}{s}\right)$

$\dot{U}$= Internal energy entering /exciting control volume with mol flow $\left(\frac{J}{s}\right)$

$\dot{W}_F$= Friction work $\left(\frac{J}{s}\right)$

PV= pressure work by external pressure on control volume $\left(\frac{J}{s}\right)$

P$\dot{V}$=Pressure work by external pressure on control volume (inlet/outlet) $\left(\frac{J}{s}\right)$

P=Pressure (Pa)

H= Enthalpy of control volume $\left(\frac{J}{s}\right)$

$\dot{H}$=Enthalpy entering/exiting control volume with mol flow $\left(\frac{J}{s}\right)$

Simplifying the equations by making some assumptions

1. The potential and kinetic energy of the control volume are a lot less than the internal energy hence K and P $\ll$ U $\Rightarrow$ E≈U
2. The potential and kinetic energy of the fluid entering and exiting the control volume is a lot less than the corresponding internal energy of the mol flow.

$$\dot{K}_z \; and \; \dot{P}o_z \ll \dot{U}_z \Rightarrow \; \dot{E}_z \approx \dot{U}_z$$

$$\dot{K}_{z+\Delta z} \; and \; \dot{P}o_{z+\Delta z} \ll \dot{U}_{z+\Delta z} \Rightarrow \; \dot{E}_{z+\Delta z} \approx \dot{U}_{z+\Delta z}$$

3. The friction work is assumed to be approximately zero $\dot{W}_F = 0$
4. The control volume is assumed to have fixed volume $\Rightarrow$PV=0
5. The volume flow rate is constant as the liquid is incompressible.

   Therefore the energy balance simplifies to:

$$\frac{d(U)}{dt} = \dot{U}_z - \dot{U}_{z+\Delta z} - \dot{Q} + P_z\dot{V} + P_{z+\Delta z}\dot{V} - \dot{D}$$

$$\frac{d(H^l)}{dt} = \left(\dot{H} - P\dot{V}\right)_z - \left(\dot{H} - P\dot{V}\right)_{z+\Delta z} - \dot{Q} + P_z\dot{V} - P_{z+\Delta z}\dot{V} - \dot{D}$$

$$\frac{d(H)}{dt} = (\dot{H})_z - (\dot{H})_{z+\Delta z} - \dot{Q} - \dot{D}$$

Where the enthalpies are defined as the sum of the component enthalpies for the control volume and also the entry and exit enthalpies.

$$H = H_{CO_2} + H_{MEA} + H_{H_2O} + H_{N_2} + H_{O_2} + H_{MEAH^+} + H_{MEACOO^-} + H_{OH^-} + H_{H_3O^+} + H_{HCO_3^-}$$

$$= \sum_{i \in X} H_i$$

Similarly for the inlet and outlet enthalpies.

$$\dot{H}_z = \sum_{i \in X} \dot{H}_{z,i}$$

$$\dot{H}_{z+\Delta z} = \sum_{i \in X} \dot{H}_{z+\Delta z,i}$$

The enthalpy can be expressed as a product of the mol/ mol flow and the specific molar enthalpy.

$$H_i = n_i \widetilde{H}_i \; and \; \dot{H}_i = \dot{n}_i \widetilde{H}_i$$

Where $\widetilde{H}_i$ is the molar specific enthalpy for each species $\left(\frac{J}{mol}\right)$

$\dot{n}_i$ = Mol flow of each species $\left(\frac{mol}{s}\right)$

Inserting back into the energy balance

$$\frac{d(H)}{dt} = (\dot{H})_z - (\dot{H})_{z+\Delta z} - \dot{Q} - \dot{D}$$

$$\frac{d\sum_{i \in X} n_i \widetilde{H}_i}{dt} = \left(\sum_{i \in X} \dot{n}_i \widetilde{H}_i\right)_z - \left(\sum_{i \in X} \dot{n}_i \widetilde{H}_i\right)_{z+\Delta z} - \dot{Q} - \dot{D}$$

$$\sum_{i \in X} \left(n_i \frac{d\widetilde{H}_i}{dt} + \widetilde{H}_i \frac{dn}{dt}\right) = \left(\sum_{i \in X} \dot{n}_i \widetilde{H}_i\right)_z - \left(\sum_{i \in X} \dot{n}_i \widetilde{H}_i\right)_{z+\Delta z} - \dot{Q} - \dot{D}$$

Inserting the expression for change in mol flow from the mol balance.

$$\frac{dn}{dt} = \dot{n}_z - \dot{n}_{z+\Delta z} - \dot{n}_{diff} + \dot{n}_{gen}$$

$$\sum_{i\in X}\left(n_i\frac{d\widetilde{H}_i}{dt}+\widetilde{H}_i(\dot{n}_z-\dot{n}_{z+\Delta z}-\dot{n}_{diff}+\dot{n}_{gen})_i\right)$$

$$=\left(\sum_{i\in X}\dot{n}_i\widetilde{H}_i\right)_z-\left(\sum_{i\in X}\dot{n}_i\widetilde{H}_i\right)_{z+\Delta z}-\dot{Q}-\dot{D}$$

$$\sum_{i\in X}\left(n_i\frac{d\widetilde{H}_i}{dt}\right)=\left(\sum_{i\in X}\dot{n}_i\widetilde{H}_i\right)_z-\left(\sum_{i\in X}\dot{n}_i\widetilde{H}_i\right)_{z+\Delta z}-\dot{Q}-\dot{D}-\sum_{i\in X}\left(\widetilde{H}_i(\dot{n}_z-\dot{n}_{z+\Delta z}-\dot{n}_{diff}+\dot{n}_{gen})_i\right)$$

$$\sum_{i\in X}\left(n_i\frac{d\widetilde{H}_i}{dt}\right)=\sum_{i\in X}\dot{n}_{i,z}(\widetilde{H}_{i,z}-\widetilde{H}_i)-\sum_{i\in X}\dot{n}_{i,z+\Delta z}(\widetilde{H}_{i,z+\Delta z}-\widetilde{H}_i)-\sum_{i\in X}\dot{n}_{gen,i}\widetilde{H}_i+\sum_{i\in X}\dot{n}_{diff,i}\widetilde{H}_i-\dot{Q}-\dot{D}$$

We can make the assumption that the control volume is well mixed and the enthalpy of the fluid exiting the control volume is the same as the enthalpy within the system boundaries which allows us to eliminate the exit enthalpy term.

$$\sum_{i\in X}\left(n_i\frac{d\widetilde{H}_i}{dt}\right)=\sum_{i\in X}\dot{n}_{i,z}\left(\widetilde{H}_{i,z}-\widetilde{H}_i\right)^l-\sum_{i\in X}\dot{n}_{gen,i}\widetilde{H}_i^l+\sum_{i\in X}\dot{n}_{diff,i}\widetilde{H}_i^l-\dot{Q}-\dot{D}$$

The system has a low constant pressure and this is mostly constant so a reasonable assumption is that the enthalpy is a function of temperature only therefore;

$$d\widetilde{H}_i=\frac{\partial\widetilde{H}_i}{\partial T^l}dT^l+\frac{\partial\widetilde{H}_i}{\partial P}dP$$

$$d\widetilde{H}_i\approx\left|\frac{\partial\widetilde{H}_i}{\partial T^l}dT^l\right|_P$$

And the specific heat capacity for the species is defined as:

$$\tilde{C}p_i^l\equiv\frac{\partial\widetilde{H}_i}{\partial T^l}$$

For a constant pressure The expression from $d\widetilde{H}_i$ can be integrated wrt to Temperature:

$$\int_{\widetilde{H}_i}^{\widetilde{H}_{i,z}}d\widetilde{H}_i\;=\;\widetilde{H}_{i,z}-\widetilde{H}_i=\int_{T_i^l}^{T_{z,i}^l}\tilde{C}p_i^l dT^l=\tilde{C}p_i^l\left[T_{z,i}^l-T_i^l\right]$$

Where $\widetilde{H}_{i,z}$= spectfic molar enthalpy of each species entering control volume $\left(\frac{J}{mol}\right)$

$\widetilde{H}_i$= spectfic molar enthalpy of each species inside control volume $\left(\frac{J}{mol}\right)$

$T_{z,i}^{l}$= Temperature of species entering control volume (K)

T^{l}= Temperature of liquid inside control volume (K)

$\tilde{C}p_{i}^{l}$= Specific molar heat capacity of species $\left(\frac{J}{mol\ K}\right)$

Heat from Species Generation

The term for the temperature change due to the rate of generation is the sum of the heat of reaction for each reaction. For the derivation the reader is referred to Lie (2005).

$$\sum_{i\in X}\left(\dot{n}_{gen,i}\widetilde{H}_{i}^{l}\right)=V\sum_{j\in X}\dot{R}_{j,rate}(\Delta H_{j})=V\left[\dot{R}_{j,rate}\right]\left[\Delta H_{j}\right]$$

Where

$\dot{R}_{j,rate}$ = Rate of reaction for each reaction $\left(\frac{mol}{m^{3}s}\right)$

ΔH_{j}= Enthalpy of reaction per mol CO_2. $\left(\frac{J}{mol}\right)$

$\left[\dot{R}_{j,rate}\right]\left[\Delta H_{j}\right]$=terms in vector form where $\dot{R}_{j,rate}$ is a 1x6 row vector and ΔH_{j} is a 6x1 column vector

V = Volume of control volume (m^3)

Heat of Reaction Alternative

The heat amount from the reactions was found to be difficult to solve because at the start of the simulations the fast reaction rates resulted in large rate of generations for some species as the states moved to chemical equilibrium. Unless the start values where very close to the equilibrium values then the model would take a long time to solve. An alternative method was to fit a polynomial function (equations 2.18 and 2.19) to the data in figure 2.4 from Kohl (1995).

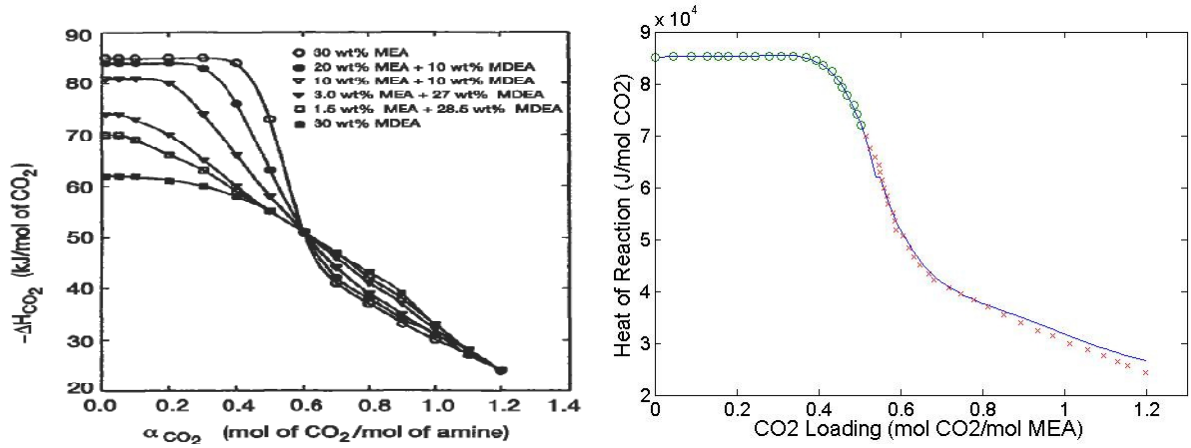

Figure 2.4: Heat of reaction for CO_2 and MEA from Kohl (2005) on left and fitted polynomial function on right

The polynomial has the form

$$\Delta H_{Re} = (-2.80(\alpha)^5 + 1.65(\alpha)^4 - 0.17(\alpha)^3 - 0.045(\alpha)^2 + 0.0084(\alpha)^1 + 0.085)x10^6 \text{ eq 2.18}$$

For α < 0.55 and for α> 0.55:

$$\Delta H_{Re} = (-0.13(\alpha)^5 + 0.64(\alpha)^4 - 1.28(\alpha)^3 + 1.28(\alpha)^2 - 0.63(\alpha)^1 + 0.13)x10^7 \text{ eq 2.19}$$

Where α= CO_2 loading (mol $(CO_2)_{Total}$ /mol MEA_{Total})

It is noted that $(CO_2)_{Total}$ is the sum of the CO_2, $MEACOO^-$ and HCO_3^- concentrations and that MEA_{Total} is the sum of the MEA, $MEAH^+$ and $MEACOO^-$ concentrations. Using the assumption that the concentration of CO_2 in the liquid phase is low and that any absorbed CO_2 will react with the MEA. The simplification is made that the heat from the reactions is the diffusion mol flow of CO_2 multiplied by the heat of reaction from the poly nominal function. The heat of reaction for 30% MEA is the only available data so this was used in the model. The equation is

$$\sum_{i \in X} \left(\dot{n}_{gen,i} \tilde{H}_i^l \right) = V \dot{n}_{CO_2} \Delta H_{RE} \qquad \left(\frac{\mathrm{m^3 J}}{\mathrm{s}} \right)$$

Heat Transfer

The heat transfer term $\dot{Q}$is the heat that is transferred at the control volume boundaries to the surroundings and to the vapour phase. The heat transfer flux is the heat transfer per specific area and is a function of the temperature difference and the resistance to heat transfer. The overall resistance to heat transfer is denoted U and is a resistance to convective and conductive

heat transfer. U can be calculated by the same analogy that was used to find the mol transfer rate. The heat flux for transfer from the liquid to the gas is equal for both phases and the driving force is the temperature difference between the interface temperature and the bulk fluid temperatures. The heat flux equation is known as Newton's law of cooling (Dewitt and Incropera 2005) and for transfer from liquid to gas being defined as positive the equations are:.

$$\dot{q}^{"} = h^{v}\left(T^{i} - T^{v}\right) = h^{l}\left(T^{l} - T^{i}\right) \text{ (Eq 2.20)}$$

$$T^{i} = \frac{\dot{q}^{"}}{h^{v}} + T^{v} \Rightarrow \dot{q}^{"} = h^{l}\left(T^{l} - \left(\frac{\dot{q}^{"}}{h^{v}} + T^{v}\right)\right)$$

$$\frac{\dot{q}^{"}}{h^{l}} + \frac{\dot{q}^{"}}{h^{v}} = (T^{l} - T^{v})$$

$$\dot{q}^{"} = \frac{1}{\underbrace{\left(\frac{1}{h^{l}} + \frac{1}{h^{v}}\right)}_{U_{lv}}}(T^{l} - T^{v})$$

$$\dot{q}^{"}{}_{lv} = U_{lv}(T^{l} - T^{v}) \ and \ \dot{Q}_{lv} = U_{lv}A_{T}(T^{l} - T^{v}) \text{ (Eq 2.21)}$$

Where

$\dot{q}^{"}{}_{lv}$ = Heat flux from liquid to vapour $\frac{J}{m^2\ s}$

h^{v} = Convective heat transfer coefficient for the vapour phase $\frac{J}{m^2\ K\ s}$

h^{l} = Convective heat transfer coefficient for the liquid phase $\frac{J}{m^2\ K\ s}$

T^{i} = Temperature at interface of liquid and vapour. (K)

U_{lv} = Overall Convective heat transfer coefficient for the liquid phase $\frac{J}{m^2\ K\ s}$

A_{T} = Area of transfer between liquid and vapour (m^2)

The formula for the heat transfer from the liquid to the ambient temperature has the same form but with different coefficients it is shown in equation 2.22. The Overall heat transfer coefficient $U_{l,amb}$ is a function of the thermal conduction in the absorption tower wall which is

typically insulated therefore has a low value. The heat transfer out of the system is small compared to the other energy values and can typically be neglected.

$$\dot{q}^{"}_{amb} = U_{amb}(T^{l} - T^{amb}) \ and \ \dot{Q}_{amb} = U_{amb}A_{w}(T^{l} - T^{amb}) \quad \text{(Eq 2.22)}$$

Where

$\dot{q}^{"}_{amb}$ = Heat flux from liquid to ambient $\left(\frac{J}{m^2\ s}\right)$

T^{amb} = Ambient temperature of surroundings ouside tthe tower. (K)

U_{amb} = Overall Convective heat transfer coefficient, liquid phase heat loss to ambient $\left(\frac{J}{m^2\ K\ s}\right)$

A_w = Area of transfer between liquid and the wall tower (m^2)

Heat Energy from Phase Change

The term $\dot{D}$ is the energy associated with the vapour leaving the control CV. The formula for the phase change term is:

$$\dot{D} = \sum_{i \in X} \dot{n}_{diff,i}\widetilde{H}_i^{v}$$

$\widetilde{H}_i^{V}$ = specific molar enthalpy of each species in vapour phase $\left(\frac{J}{mol}\right)$

Inserting the value for $\dot{D}$ into the energy balance allows for the enthalpy of the change associated with diffusion to be written in the form of the latent heat of vapourization. The latent heat of vapourization is the difference between the enthalpy of vapour and liquid for each species.

$$\Delta\widetilde{H}_i^{vl} = \widetilde{H}_i^{v} - \widetilde{H}_i^{v}$$

Total Energy Balance for Liquid

Therefore the energy balance for the liquid bulk is:

$$\sum_{i \in X}\left(n_i \frac{d\widetilde{H}_i}{dt}\right) = \sum_{i \in X}\dot{n}_{i,z}\left(\widetilde{H}_{i,z} - \widetilde{H}_i\right)^{l} - \sum_{i \in X}\dot{n}_{gen,i}\widetilde{H}_i^{l} + \sum_{i \in X}\dot{n}_{diff,i}\widetilde{H}_i^{l} - \sum_{i \in X}\dot{n}_{diff}\widetilde{H}_i^{v} - \dot{Q}_{lv} - \dot{Q}_{amb}$$

$$\frac{dT^{l}}{dt}\sum_{i \in X} n_i \tilde{C}p_i^{l} = \sum_{i \in X}\dot{n}_{i,z}\,\tilde{C}p_i^{l}\left(T_{z,i}^{l} - T^{l}\right) - \sum_{i \in X}\dot{n}_{i,diff}\Delta\widetilde{H}_i^{vl} - V\left[\dot{R}_{j,rate}\right]\left[\Delta H_j\right] - \dot{Q}_{lv} - \dot{Q}_{amb}$$

Where

$$\dot{Q}_{amb} = U_{amb} A_w (T^l - T^{amb})$$
$$\dot{Q}_{lv} = U_{lv} A_T (T^l - T^v)$$

Introducing the expressions

$$n_i = C_i^l V \ , \ \dot{n}_{i,z} = C_{i,z}^l \dot{V} \ , \ \ \dot{n}_{diff} = \dot{n}_{diff}^{"} A_T,$$

$$\dot{V} = u A_C \, , V = A_C \Delta z, \ \ A_T = V a_w, \qquad A_w = \pi D_{twr} \Delta z \ and \ T^l = T_{z+\Delta z}^l$$

We reintroduce $T^l = T_{z+\Delta z}^l$ as the assumption is the control volume is well mixed and homogenous.

This leads to the expression:

$$\frac{dT^l}{dt} \sum_{i \in X} C_i^l A_C \Delta z \tilde{C} p_i^l$$
$$= \sum_{i \in X} C_{i,z}^l u A_C \ \tilde{C} p_i^l \left[T_{z,i}^l - T_{z+\Delta z}^l\right] - \sum_{i \in X} \dot{n}_{diff}^{"} A_C \Delta z a_w \Delta \tilde{H}_i^{vl} - A_C \Delta z \left[\dot{R}_{j,rate}\right]\left[\Delta H_j\right]$$
$$- U_{amb} \pi D \Delta z (T^l - T^{amb}) - U_{lv} a_w A_C \Delta z (T^l - T^v)$$

Dividing by $A_C \Delta z$

$$\frac{dT^l}{dt} \sum_{i \in X} C_i^l \tilde{C} p_i^l$$
$$= u \sum_{i \in X} C_{i,z}^l \tilde{C} p_i^l \frac{\left[T_{z,i}^l - T_{z+\Delta z}^l\right]}{\Delta z} - \sum_{i \in X} \underbrace{\dot{n}_{diff}^{"} a_w}_{\dot{n}_d} \Delta \tilde{H}_i^{vl} - \left[\dot{R}_{j,rate}\right]\left[\Delta H_j\right] - \underbrace{\frac{U_{amb} \pi D}{A_C}}_{U_{T,amb}} (T^l - T^{amb})$$
$$- \underbrace{U_{lv} a_w}_{U_{T,lv}} (T^l - T^v)$$

In the limit when $\Delta z \to 0$ we can see that $C_{i,z}^l = C_i^l \ \Rightarrow \sum_{i \in X} C_i^l \tilde{C} p_i^l \approx \sum_{i \in X} C_{i,z}^l \tilde{C} p_i^l$ also we introduce $U_{T,amb}$ and $U_{T,lv}$ for the overall heat transfer coefficients and write the diffusion in the form of two vectors $[\dot{n}_d]^T$ and $\left[\Delta \tilde{H}_i^{vl}\right]$ where both are 6x1 vectors. The summation of the spies concentrations multiplied by the specific molar heat capacity of each component can also be written in matrix from.

$$\sum_{i \in X} C_i^l \tilde{C}p_i^l = \left[C_i^l\right]^T \left[\tilde{C}p_i^l\right]$$

The change in liquid temperature in the Control volume is:

$$\frac{dT^l}{dt} = -u\frac{\partial T^l}{\partial z} - \frac{[\dot{n}_d]^T\left[\Delta\tilde{H}_i^{vl}\right]}{\left[C_i^l\right]^T[\tilde{C}p_i^l]} - \frac{[\dot{R}_{j,rate}][\Delta H_j]}{\left[C_i^l\right]^T[\tilde{C}p_i^l]} - \frac{U_{T,amb}(T^l - T^{amb})}{\left[C_i^l\right]^T[\tilde{C}p_i^l]} - \frac{U_{T,lv}(T^l - T^v)}{\left[C_i^l\right]^T[\tilde{C}p_i^l]} \quad \text{(Eq 2.23)}$$

The energy balance with the alternative heat of reaction term and the heat transfer to ambient emitted is:

$$\frac{dT^l}{dt} = -u\frac{\partial T^l}{\partial z} - \frac{[\dot{n}_d]^T\left[\Delta\tilde{H}_i^{vl}\right]}{\left[C_i^l\right]^T[\tilde{C}p_i^l]} - \frac{\dot{n}_{CO_2}\Delta H_{RE}}{\left[C_i^l\right]^T[\tilde{C}p_i^l]} - \frac{U_{T,lv}(T^l - T^v)}{\left[C_i^l\right]^T[\tilde{C}p_i^l]} \quad \text{(Eq 2.24)}$$

The velocity is assigned a negative value within the model to denote that the flow of liquid is from the top of the column down. The heat of vapourization is only included for MEA and H_2O as theses are the only species which contribute and the other values for $\Delta\tilde{H}_i^{vl}$ are set to zero.

2.1.12 Energy Balance for the Vapour Phase.

The energy balance for the vapour phase follows the same form as the liquid phase except that the generation terms are absent and the diffusion and heat flows between the gas and liquid phase are equal but opposite to the terms in the liquid energy balance.

$$\frac{dE}{dt} = \dot{E}_z - \dot{E}_{z+\Delta z} + \dot{Q} + \dot{W} + \dot{D}$$

Introducing the same assumptions as per the liquid phase with regard to simplifying the energy flow terms and neglecting kinetic and potential energy.

$$E = K + U + Po$$

$$\dot{E}_z = \dot{K}_z + \dot{U}_z + \dot{P}o_z$$

$$\dot{E}_{z+\Delta z} = \dot{K}_{z+\Delta z} + \dot{U}_{z+\Delta z} + \dot{P}o_{z+\Delta z}$$

$$\dot{W} = \dot{W}_F + P_z\dot{V} - P_{z+\Delta z}\dot{V}$$

$$H = U + PV$$

$$\dot{H} = \dot{U} + P\dot{V}$$

1. K and P ≪ U ⇒ E≈U

$$\dot{K}_z \; and \; \dot{P}o_z \ll \dot{U}_z \Rightarrow \; \dot{E}_z \approx \dot{U}_z$$

$$\dot{K}_{z+\Delta z} \; and \; \dot{P}o_{z+\Delta z} \ll \dot{U}_{z+\Delta z} \Rightarrow \; \dot{E}_{z+\Delta z} \approx \dot{U}_{z+\Delta z}$$

2. The friction work is assumed to be approximately zero $\dot{W}_F = 0$
3. The control volume is assumed to have fixed volume ⇒ $\frac{d(PV)}{dt}$=0
4. The volume flow rate is assumed to be constant. This is a simplified assumption but for low pressure we find that the vapour velocity changes very little so can be assumed to be constant.

   Therefore the energy balance simplifies to:

$$\frac{d(U)}{dt} = \dot{U}_z - \dot{U}_{z+\Delta z} + \dot{Q} + P_z\dot{V} + P_{z+\Delta z}\dot{V} + \dot{D}$$

$$\frac{d(H^v)}{dt} = \left(\dot{H} - P\dot{V}\right)_z - \left(\dot{H} - P\dot{V}\right)_{z+\Delta z} + \dot{Q} + P_z\dot{V} - P_{z+\Delta z}\dot{V} + \dot{D}$$

$$\frac{d(H^v)}{dt} = \left(\dot{H}\right)_z - \left(\dot{H}\right)_{z+\Delta z} + \dot{Q} + \dot{D}$$

Where the enthalpies are defined as the sum of the component enthalpies for the control volume and also the entry and exit enthalpies.

$$H^v = H_{CO_2} + H_{MEA} + H_{H_2O} + H_{N_2} + H_{O_2} = \left(\sum_{i \in X} H_i\right)$$

Similarly for the inlet and outlet enthalpies.

$$\dot{H}_z = \left(\sum_{i \in X} \dot{H}_{z,i}\right)^v$$

$$\dot{H}_{z+\Delta z} = \left(\sum_{i \in X} \dot{H}_{z+\Delta z,i}\right)^v$$

$$H_i^v = n_i \widetilde{H}_i^v \; and \; \dot{H}_i^v = \dot{n}_i \widetilde{H}_i^v$$

Therefore:

$$\frac{d\sum_{i \in X} n_i H_i^v}{dt} = \left(\sum_{i \in X} \dot{n}_i H_i^v\right)_z - \left(\sum_{i \in X} \dot{n}_i H_i^v\right)_{z+\Delta z} + \dot{Q} + \dot{D}$$

$$\sum_{i\in X}\left(n_i\frac{dH_i^v}{dt}+H_i^v\frac{dn}{dt}\right)=\left(\sum_{i\in X}\dot{n}_iH_i^v\right)_z-\left(\sum_{i\in X}\dot{n}_iH_i^v\right)_{z+\Delta z}+\dot{Q}+\dot{D}$$

Inserting the expression for change in mol flow from the mol balance and not including diffusion term.

$$\frac{dn}{dt}=\dot{n}_z-\dot{n}_{z+\Delta z}+\dot{n}_{diff}$$

$$\sum_{i\in X}\left(n_i\frac{dH_i^v}{dt}+H_i^v(\dot{n}_z-\dot{n}_{z+\Delta z}+\dot{n}_{diff})_i\right)=\left(\sum_{i\in X}\dot{n}_iH_i^v\right)_z-\left(\sum_{i\in X}\dot{n}_iH_i^v\right)_{z+\Delta z}+\dot{Q}+\dot{D}$$

$$\sum_{i\in X}\left(n_i\frac{dH_i^v}{dt}\right)=\left(\sum_{i\in X}\dot{n}_iH_i^v\right)_z-\left(\sum_{i\in X}\dot{n}_iH_i^v\right)_{z+\Delta z}+\dot{Q}+\dot{D}-\sum_{i\in X}\left(\widetilde{H}_i(\dot{n}_z-\dot{n}_{z+\Delta z}+\dot{n}_{diff})_i\right)$$

$$\sum_{i\in X}\left(n_i\frac{dH_i^v}{dt}\right)=\sum_{i\in X}\dot{n}_{i,z}\left(\widetilde{H}_{i,z}^v-H_i^v\right)-\sum_{i\in X}\dot{n}_{i,z+\Delta z}\left(\widetilde{H}_{i,z+\Delta z}^v-H_i^v\right)-\sum_{i\in X}\dot{n}_{diff,i}H_i^v+\dot{Q}+\dot{D}$$

As with the liquid energy balance we can make the assumption that the control volume is well mixed and the enthalpy of the fluid exiting the control volume is the same as the enthalpy within the system boundaries which allows us to eliminate the exit enthalpy term.

$$\sum_{i\in X}\left(n_i\frac{dH_i^v}{dt}\right)=\sum_{i\in X}\dot{n}_{i,z}\left(\widetilde{H}_{i,z}^v-H_i^v\right)-\sum_{i\in X}\dot{n}_{diff,i}H_i^v+\dot{Q}+\dot{D}$$

As the system pressure is low we can apply the same notation and relationship between cp and the enthalpy as per the liquid energy balance.

$$\int_{H_i^v}^{\widetilde{H}_{i,z}^v}d\widetilde{H}_i\;=\;\widetilde{H}_{i,z}^v-H_i^v=\int_{T_i^v}^{T_{z,i}^v}\tilde{C}p_i^v\,dT^v=\tilde{C}p_i^v\left(T_{z,i}^v-T_i^v\right)$$

Where $T_{z,i}^l$= Temperature of species entering control volume (K)

T^l= Temperature of liquid inside control volume (K)

$\tilde{C}p_i^l$= Specific molar heat capacity of species $\left(\frac{J}{mol\,K}\right)$

Heat Transfer

The heat transfer to the surroundings takes the same form as the liquid heat transfer but the value of U is different as the vapour properties effect the heat transfer. The heat transfer is defined as being into the system for the vapour control volume. The heat transfer from the liquid to the vapour is the same as the term derived in the liquid energy balance.

$$\dot{Q}^v_{amb} = U^v_{amb} A_w (T^l - T^{amb})$$
$$\dot{Q}_{lv} = U_{lv} A_T (T^l - T^v)$$

Heat Energy from Phase Change

The term $\dot{D}$ is the energy associated with the liquid which condenses within the control volume and joins the liquid phase. The formula for the energy added from the diffusion of liquid into the vapour is:

$$\dot{D} = \sum_{i \in X} \dot{n}_{diff} \widetilde{H}^l_i$$

$\widetilde{H}^l_i$= spectfic molar enthalpy of each species in liquid phase $\left(\frac{J}{mol}\right)$

Substituting the value for $\dot{D}$ into the energy balance allows us to introduce the latent heat of vapourization for the change between liquid and vapour for each species.

$$\Delta \widetilde{H}^{vl}_i = \widetilde{H}^v_i - \widetilde{H}^l_i$$

Vapour Energy Balance

Therefore the energy balance for the vapour bulk is:

$$\sum_{i \in X} \left(n_i \frac{dH^v_i}{dt} \right) = \sum_{i \in X} \dot{n}_{i,z} \left(\widetilde{H}^v_{i,z} - H^v_i \right) - \sum_{i \in X} \dot{n}_{diff,i} H^v_i + \sum_{i \in X} \dot{n}_{diff} \widetilde{H}^l_i + \dot{Q}_{lv} + \dot{Q}^v_{amb}$$

$$\frac{dT^v}{dt} \sum_{i \in X} n_i \tilde{C}p^v_i = \sum_{i \in X} \dot{n}_{i,z} \tilde{C}p^v_i \left(T^v_{z,i} - T^v \right) - \sum_{i \in X} \dot{n}_{i,diff} \Delta \widetilde{H}^{vl}_i + \dot{Q}_{lv} + \dot{Q}^v_{amb}$$

Introducing the expressions

$$n_i = C^v_i V \ , \ \dot{n}_{i,z} = C^v_{i,z} \dot{V} \ , \ \ \dot{n}_{diff} = \dot{n}^{"}_{diff} A_T,$$

$$\dot{V} = u A_C \ , V = A_C \Delta z, \ \ A_T = V a_w, \qquad A_w = \pi D_{twr} \Delta z \ and \ T^v = T^v_{z+\Delta z}$$

This leads to the expression:

$$\frac{dT^v}{dt}\sum_{i\in X} C_i^v A_C \Delta z \tilde{C}p_i^v$$
$$= \sum_{i\in X} C_{i,z}^v u A_C \ \tilde{C}p_i^v\left[T_{z,i}^v - T_{z+\Delta z}^v\right] - \sum_{i\in X} \dot{n}_{diff}^{"} A_C \Delta z a_w \Delta\tilde{H}_i^{vl} + U_{amb}\pi D\Delta z(T^v - T^{amb})$$
$$+ U_{lv} a_w A_C \Delta z (T^l - T^v)$$

Dividing by $A_C\Delta z$

$$\frac{dT^v}{dt}\sum_{i\in X} C_i^v \tilde{C}p_i^v$$
$$= u\sum_{i\in X} C_{i,z}^v \tilde{C}p_i^v \frac{\left[T_{z,i}^v - T_{z+\Delta z}^v\right]}{\Delta z} - \sum_{i\in X} \underbrace{\dot{n}_{diff}^{"} a_w}_{\dot{n}_d} \Delta\tilde{H}_i^{vl} + \underbrace{\frac{U_{amb}\pi D}{A_C}}_{U_{T,amb}^v}(T^v - T^{amb}) + \underbrace{U_{lv}a_w}_{U_{T,lv}}(T^l - T^v)$$

In the limit as $\Delta z \to 0$ The we can see that $C_{i,z}^v = C_i^v \ \Rightarrow \sum_{i\in X} C_i^v \tilde{C}p_i^v \approx \sum_{i\in X} C_{i,z}^v \tilde{C}p_i^v$ also we introduce $U_{T,amb}^v$ and $U_{T,lv}$ for the overall heat transfer coefficients and write the diffusion in the form of two vectors $[\dot{n}_d]^T$ and $\left[\Delta\tilde{H}_i^{vl}\right]$ where both are 6x1 vectors. The summation of the species concentrations multiplied by the specific molar heat capacity of each component can also be written in matrix from.

$$\sum_{i\in X} C_i^v \tilde{C}p_i^v = [C_i^v]^T\left[\tilde{C}p_i^v\right]$$

The change in liquid temperature in the Control volume ignoring the heat transfer to ambient:

$$\frac{dT^v}{dt} = -u\frac{\partial T^v}{\partial z} - \frac{[\dot{n}_d]^T\left[\Delta\tilde{H}_i^{vl}\right]}{[C_i^v]^T[\tilde{C}p_i^v]} + \frac{U_{T,lv}(T^l - T^v)}{[C_i^v]^T[\tilde{C}p_i^v]} \quad \text{(Eq 2.25)}$$

2.1.13 Heat Transfer Coefficient

The heat transfer between the liquid and vapour is controlled by the resistance to heat transfer in the vapour phase. The Chilton Coburn analogy (Dewitt and Incropera 2002) can be applied to approximate the heat transfer coefficient with the mass transfer coefficient. The Chilton Coburn analogy is abased on the assumption that the boundary layer profiles for the heat and

mass transfers are the same. The mass transfer diffusion formula and heat transfer formula have the same form i.e.

$$\dot{n}''_{d,i} = kd_i^v(C_i^{*v} - C_i^v)$$

$$\dot{q}''_{lv} = U_{lv}(T^l - T^v)$$

Where we can make the assumption that the resistance to heat transfer is in the vapour phase and the value for $h^l$is much greater than h^v

$$U_{lv} = \frac{1}{\left(\frac{1}{h^l} + \frac{1}{h^v}\right)} \Rightarrow U_{lv} = h^v$$

In the Chilton Colburn analogy the dimensionless heat transfer coefficient Colburn factor (j_H), is equal to the dimensionless mass transfer coefficient Colburn factor (j_m). The Colburn factors are a function of the Stanton, Prandtl, Schmidt and Stanton mass transfer coefficient.

$$j_H = St(Pr)^{2/3} \quad \text{(Eq 2.26)}$$

$$j_M = St_m(Sc)^{2/3} \quad \text{(Eq 2.27)}$$

Where:

j_H= Colburn factor for heat transfer

St= Stanton number which is modified nusselt number $St = \frac{h^v}{\rho V Cp} \left(\frac{1}{m^2 s}\right)$

Pr=Prandtl number which is given by $Pr = \frac{Cp\mu}{k}$

j_M= Colburn factor for mass transfer

St_m= Mass transfer Stanton number $St_m = \frac{kd}{V}\left(\frac{1}{m^2 s}\right)$

Sc=Schmidt number which is given by $Sc = \frac{\mu}{D\rho}$

V= Volume of gas in Control volume (m^3)

k= thermal conductivity of the vapour phase $\left(\frac{J}{msK}\right)$

The viscosity (μ), mass transfer coefficient (kd), density (ρ) and diffusivity (D) are as previously defined. The heat capacity (Cp_{mass}) is corrected to the units of J/Kg K by multiplying by the sum of the gas concentrations and dividing by the gas density.

$$j_H = St(Pr)^{2/3} = j_M = St_m(Sc)^{2/3}$$

$$\frac{h^v}{\rho V Cp_{mass}}\left(\frac{Cp_{mass}\,\mu}{k}\right)^{2/3} = \frac{kd}{V}\left(\frac{\mu}{D\,\rho}\right)^{2/3}$$

$$h^v = \frac{kd\;\rho\;V\;Cp_{mass}}{V}\left(\frac{\mu\;\;k}{D\;Cp_{mass}\;\rho\mu}\right)^{2/3}$$

$$h^v = kd(\rho\;Cp_{mass})^{1/3}\left(\frac{k}{D}\right)^{2/3} \quad \text{(Eq 2.28)}$$

The mixture diffusivity, specific heat capacity, density and thermal conductivity for the vapour phase are used in the calculation of the overall mass transfer coefficient and the corresponding heat transfer coefficient. The mixture properties are evaluated by calculating the properties of the 5 individual components in the vapour phase and combing by mol fraction to find an overall value. The density of the vapour is calculated by multiplying the concentration for each species with the corresponding molecular weight and summing the values.

2.2 Fluid Properties

The properties of the liquid and vapour phases are important for the accuracy of the model. Most of the fluid properties vary as a function of temperature therefore great effort was expended to find fluid property formulas as a function of temperature.

2.2.1 Molecular Weight

The molecular weight of the 10 species is listed in table 2.3

Table 2.3: Mol weight of species used in this model (g/mol)

CO_2	MEA	H_2O	N_2	O_2	$MEAH^+$	$MEACOO^-$	HCO_3^-	OH^-	H_3O^+
44	61	18	28	32	62	105	61	17	19

2.2.2 Density

The density of the fluid is calculated by multiplying the concentration for each species with the corresponding molecular weight and summing the values. The density is divided by 1000 to convert into kg/m^3.

$$\rho^v = \frac{\sum_{i \in X} C_i^v MW_i}{1000} \qquad and \qquad \rho^l = \frac{\sum_{i \in X} C_i^l MW_i}{1000}$$

2.2.3 Heat Capacity

Heat Capacity of Vapour

The heat capacity of the vapour (Cp^v) of each species is calculated as a function of temperature and is given by a polynomial function taken from Reid et al (1999). The heat capacity is for an ideal gas which is a reasonable approximation for the low pressures that the absorption process operates at. The coefficients of the polynomial function are different for each species and only the molecules in the vapour phase require a Cp^v value. The function has the form as shown in equation 2.29 and has units $\frac{J}{molK}$

$$Cp_i^v = C_1 + C_2 T^v + C_3 (T^v)^2 + C_4 (T^v)^3 \qquad (Eq\ 2.29)$$

The co efficient used in the model for the vapour Cp^v are listed in table 2.4

Table 2.4:vapour phase Cp co-efficients (Reid et al 1987)

Species	C_1	C_2	C_3	C_4
CO_2	19.1	7.342×10^{-2}	-5.602×10^{-5}	1.715×10^{-8}
MEA	9.311	3.009×10^{-1}	-1.818×10^{-4}	4.656×10^{-8}
H_2O	32.2	1.924×10^{-3}	1.055×10^{-5}	-3.596×10^{-9}
N_2	31.15	-1.357×10^{-2}	2.68×10^{-5}	-1.168×10^{-8}
O_2	28.11	-3.68×10^{-6}	1.746×10^{-5}	-1.065×10^{-8}

Heat Capacity of Liquid

The heat capacity of the liquid phase is also developed as a function of a polynomial function. The co-efficient for water are taken from the NIST web book and the co-efficient of MEA are calculated from correlated data from Jolicouer et al (1993). The heat capacity of CO_2 and HCO_3- OH and H_3O^+ are taken as the same as H_2O while the heat capacities of MEAH+ and MEACOO- are taken as the same as pure MEA. The polynomial is shown in equation 2.30 and has units $\frac{J}{molK}$. and the coefficients in table 2.5.

$$Cp_i^l = Co_1 + Co_2 \frac{T^l}{1000} + Co_3 \left(\frac{T^l}{1000}\right)^2 + Co_4 \left(\frac{T^l}{1000}\right)^3 + \frac{Co_5}{\left(\frac{T^l}{1000}\right)^2} \qquad (Eq\ 2.30)$$

Table 2.5: Liquid phase Cp co-efficients.

Species	Co_1	Co_2	Co_3	Co_4	Co_5
MEA	520.3	2749	5313	0	0
H_2O	-203.6060	1523.290	3196.413	2474.455	3.855326

The data for the MEA from Jolicouer et al (1993), is for a temperature range 25-40 °C so maybe incorrect at elevated temperatures.

2.2.4 Viscosity

Liquid Viscosity

The viscosity of the amine solution as a function of temperature can be estimated by the equations;

$$\mu_{am}^{l} = \frac{exp\left(-3.9356+\frac{1010.8}{T^{l}-151.17}\right)}{1000} \qquad \left(\frac{Ns}{m^2}\right) \text{ (Hansen 2004)}$$

$$\mu_{H_2O}^{l} = 2.414x10^{-5}x10^{\left(\frac{247.8}{T^{l}-140}\right)} \qquad \left(\frac{Ns}{m^2}\right) \text{ (Wikipedia/viscosity)}$$

The viscosity of the amine mixture is affected by the presence of CO_2 in the mixture, a correlation between the viscosity of the mixture as a function of water, CO_2 and amine is given by (Hansen 2004):

$$\mu_{mix+CO_2}^{l} = 1.2\mu_{mix}^{l} r$$

Where $$r = 1 + 0.8031\frac{x_{CO_2}}{x_{MEA}} + 0.35786\left(\frac{x_{CO_2}}{x_{MEA}}\right)^2$$

$$\mu_{mix}^{l} = exp\left(x_{H_20}\log\left(\mu_{H_20}^{l}\right) + x_{MEA}\log\left(\mu_{MEA}^{l}\right) + x_{MEA}\,x_{H_20}\,\mathrm{G}\right)$$

$$G = 372.1 - 3.11T^{l} + 8.8092x10^{-3}(T^{l})^2 - 8.3457x10^{-6}(T^{l})^3$$

Vapour Viscosity

Data from Perry and Green (1999) was used to fit a linear relationship for viscosity of CO_2, O_2, N_2 and H_2O as a function of temperature in the vapour phase. MEA was not calculated as it was considered not to contribute significantly to the overall gas viscosity. The individual gas viscosities were evaluated and the overall gas viscosity is a combination of the molecular

fraction and component gas viscosity. The individual formulas are shown below with also the mixing function which has a log mixing rule method. The raw data is included in appendix B.

$$\mu^v_{CO_2} = 4.35x10^{-8}T^v + 1.93x10^{-6}$$

$$\mu^v_{H_2O} = 4.44x10^{-8}T^v - 4.61x10^{-6}$$

$$\mu^v_{N_2} = 3.97x10^{-8}T^v + 6.03x10^{-6}$$

$$\mu^v_{O_2} = 4.84x10^{-8}T^v + 6.13x10^{-6}$$

$$\mu^v = exp(ln(\mu^v_{CO_2})y^v_{CO_2} + ln(\mu^v_{H_2O})y^v_{H_2O} + ln(\mu^v_{N_2})y^v_{N_2} + ln(\mu^v_{O_2})y^v_{O_2})$$

Where μ^v is the vapour viscosity $\left(\frac{Ns}{m^2}\right)$, μ^v_i is the vapour viscosity of the component $\left(\frac{Ns}{m^2}\right)$ and y^v_i is the molecular fraction of the component in the vapour phase

2.2.5 Diffusivity

Gas Diffusivity

The diffusivity of the in the gas phase is given by the Fuller equation which a modified version of the Chapman Enskog equation (Reid et al 1987).

$$D^v_i = \frac{0.00143\ (T^v)^{1.75}\sqrt{2}\left[\frac{1}{M_{mix}} + \frac{1}{M_i}\right]^{1/2}}{P\left[\sqrt[3]{(\sum V_{mix})} + \sqrt[3]{(\sum V_i)}\right]^2}$$

Where M_{mix}= Molecular weight of vapour

M_i= Molecular weight of component

V_{mix}= Structural volume of vapour components

V_i= Structural volume of component

From Reid (1777) values of M_{mix}, M_i,V_{mix} and V_i can be obtained and are used to calculate the diffusivity vapour phase. The general equation is of the form of equation 3.31 and the coefficient for each species is shown in table 2.6.

$$D^v_i = \frac{C_D(T^v)^{1.75}}{P} \text{ (Eq 2.31)}$$

Table 2.6: Diffusivity vapour constant from Reid et al (1987)

Species	C_D
CO_2	$8.65x10^{-5}$
MEA	$5.33\ x10^{-5}$
H_2O	$1.2\ x10^{-4}$
N_2	$9.5\ x10^{-5}$
O_2	$1.16\ x10^{-4}$

The diffusivity of the mixture is calculated as the total of the product of the gas molecular fraction multiplied by the component vapour diffusivity.

$$D_{mix}^{v} = \sum_{i \in X} D_i^v y_i$$

Liquid Diffusivity

For CO_2 diffusing into water the equation takes the form shown in equation 2.32.(Versteeg et al 1988).

$$D_{CO_2}^{l} = 2.35x10^{-6} exp\left(\frac{-2119}{T^l}\right) \text{ (Eq 2.32)}$$

Because The CO_2 reacts with the amine solution it is difficult to measure the diffusivity of CO_2 in the amine water mixture. The N_20 analogy (Al-ghawas et al 1989) relates the N_20 diffusivity to the CO_2 diffusivity in an amine solution by the formula:

$$\left(\frac{D_{CO_2}^{l}}{D_{N_2O}^{l}}\right)_{mix+CO_2} = \left(\frac{D_{CO_2}^{l}}{D_{N_2O}^{l}}\right)_{water}$$

Versteeg and Van Swaaij (1988) developed the expression for the diffusivity of N_20 in amine solution by modifying the Stokes Einstein equation which a function of the dynamic viscosity of the mixture. This equation takes the form:

$$\left(D_{N_2O}^{l}(\mu^l)^{\gamma}\right)_{mix+CO_2} = \left(D_{N_2O}^{l}(\mu^l)^{\gamma}\right)_{water}$$

Combining the two equations results in equation 2.33 for the diffusivity of CO_2 in amine solution for an un-reacting system:

$$D_{CO_2}^{l,unreact} = \frac{\left(D_{CO_2}^{l}(\mu^l)^{\gamma}\right)_{water}}{(\mu^l)^{\gamma}{}_{mix+CO_2}} \quad \text{(Eq 2.33)}$$

Macerias et al (2007) estimated a value for γ of 0.51 for MEA-water solution while Versteeg and Swaail (1988) estimated a value of 0.6 and Freguia and Rochelle (2003) use 0.545. The value of Macerias is used in this work.

2.2.6 Thermal Conductivity

The thermal conductivity of CO_2 H_2O and N_2 taken from Dewitt and Incropera (2002). A linear relationship with respect to temperature was plotted from the correlated data. The presence of MEA was neglected as the concentration is low and O_2 is modeled with the same function as nitrogen as the values were very similar. The equation (Eq 2.34) is shown below and the co efficient are listed in table 2.7

$$k_i^v = C_{k1}T^v + C_{k2}$$

Table 2.7: Fitted constants for thermal conductivity used in this model from Dewitt and Incropera (2002)

Species	CO_2	H_2O	N_2/O_2
C_{k1}	0.076	0.069	0.075
C_{k2}	-6.337	4.84	-3.9

The mixture thermal conductivity value k_{mix} is calculated by summing the product of the vapour molecular fraction and the respected component thermal conductivity. The sum is k_{mix} value is divided by 1000 to produce the units $\frac{W}{mK}$.

$$k_{mix}^v = \sum_{i \in X} k_i^v y_i$$

2.3 De-Absorption Tower

The stripper process flow diagram is shown in figure 2.5. Essentially the loaded rich amine enters the stripper at the top of the tower and flows down over the packing. A percentage of the lean mixture water from the bottom of the tower is evaporated into steam. This steam is the stripping gas providing heat to increase the temperature of the rich mixture which in turn reverses the chemical reactions and reduces the solubility of CO_2 in the liquid phase. As the stripping gas flows up the tower in a countercurrent direction to the liquid the concentration of CO_2 in the gas increases.

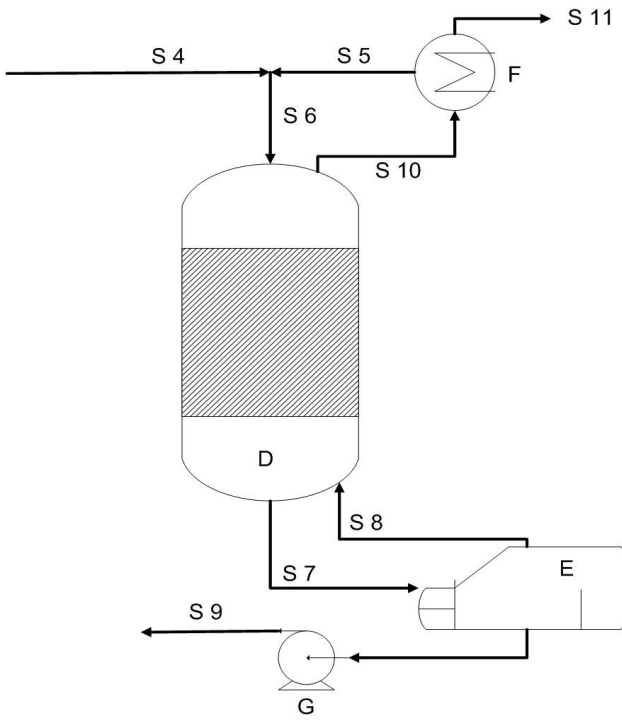

Figure 2.5: Process flow diagram of de-absorption process.

A condenser (F) at the top of the tower cools the outlet vapour from the tower condensing the steam and MEA in the vapour phase resulting in a concentrated CO_2 outlet gas stream. The model for the de absorption process is the same as the model for the absorption process within the tower. The reboiler and the condenser provide the inlet boundary conditions for the stripping process. The diameter of the stripping tower is smaller than the absorption tower as the volume of gas that passes up through the tower is less than the absorption process. The condensed H_2O and MEA are retuned to the top of the tower which somewhat dilutes the rich mixture and increases the liquid flow rate in the tower. The de-absorption process typically

operates at a pressure of 2 bar and the pressure of the system dictates the temperature. At the higher elevated temperatures the reactions precede faster than the absorption column. The controlling the factor is the equilibrium constants which dictate the amount of aqueous CO_2 is release from the bound CO_2 in the $MEACOO^-$ and HCO_3^- ions.

2.4 Reboiler

The liquid from the stripper (S7) enters the reboiler where it is heated by steam. A certain percentage of the liquid flow is boiled into vapour. Figure 2.6 illustrates this process.

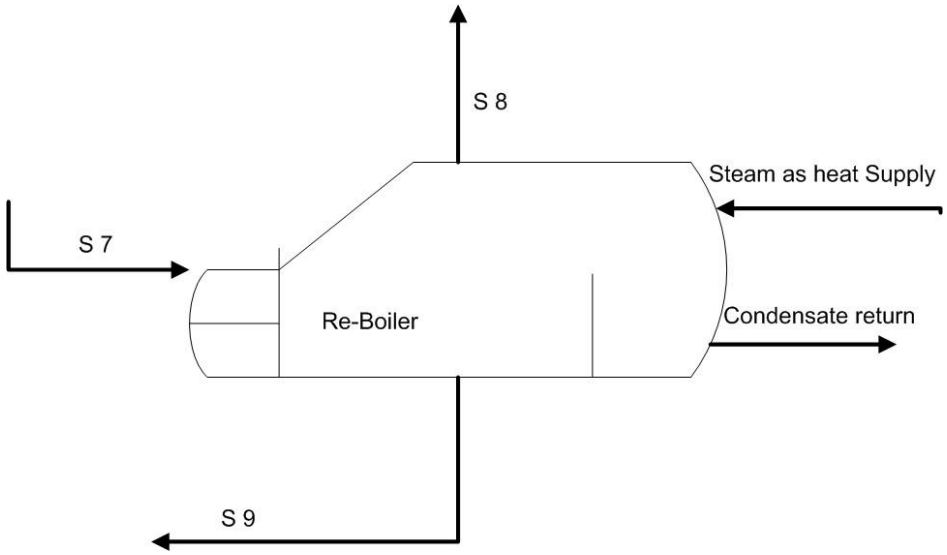

Figure 2.6: Reboiler schematic

A flash calculation is preformed at the pressure and temperature of the reboiler to calculate the mol fraction in the vapour and liquid phases. This is done with the Peng Robinson equation of state and the procedure is taken from Elliot and Lira (1999) . The majority of the vapour is H_2O because MEA has a low vapour pressure so does not tend to vaporize, the ions in the solution can not boil and the other concentrations of CO_2 N_2 and O_2 coming from the reboiler are minimal. The mol flow of each species is calculated from the liquid flow in the stripper and the concentration at the stripper outlet (i.e. the mol flow of each species in stream S 7). The flash calculation has an output of the liquid to feed ratio so therefore knowing the mol flow of S7 allows the mol flow of S9 and S8 to be calculated. From the flash calculation the mol fraction of each phase are known so the mol flow of each species can be calculated and then the concentration of each species which is the mol flow rate divided by the volume flow rate. The liquid flow rate from the stripper (S7) is assumed to be the volume flow rate of the liquid

entering the stripper (S6) the model. The flow rate of S9 is calculated from the EOS using the mol fractions of the liquid as inputs, a flow diagram in figure 2.7 shows the sequence of calculations for the reboiler and the output values

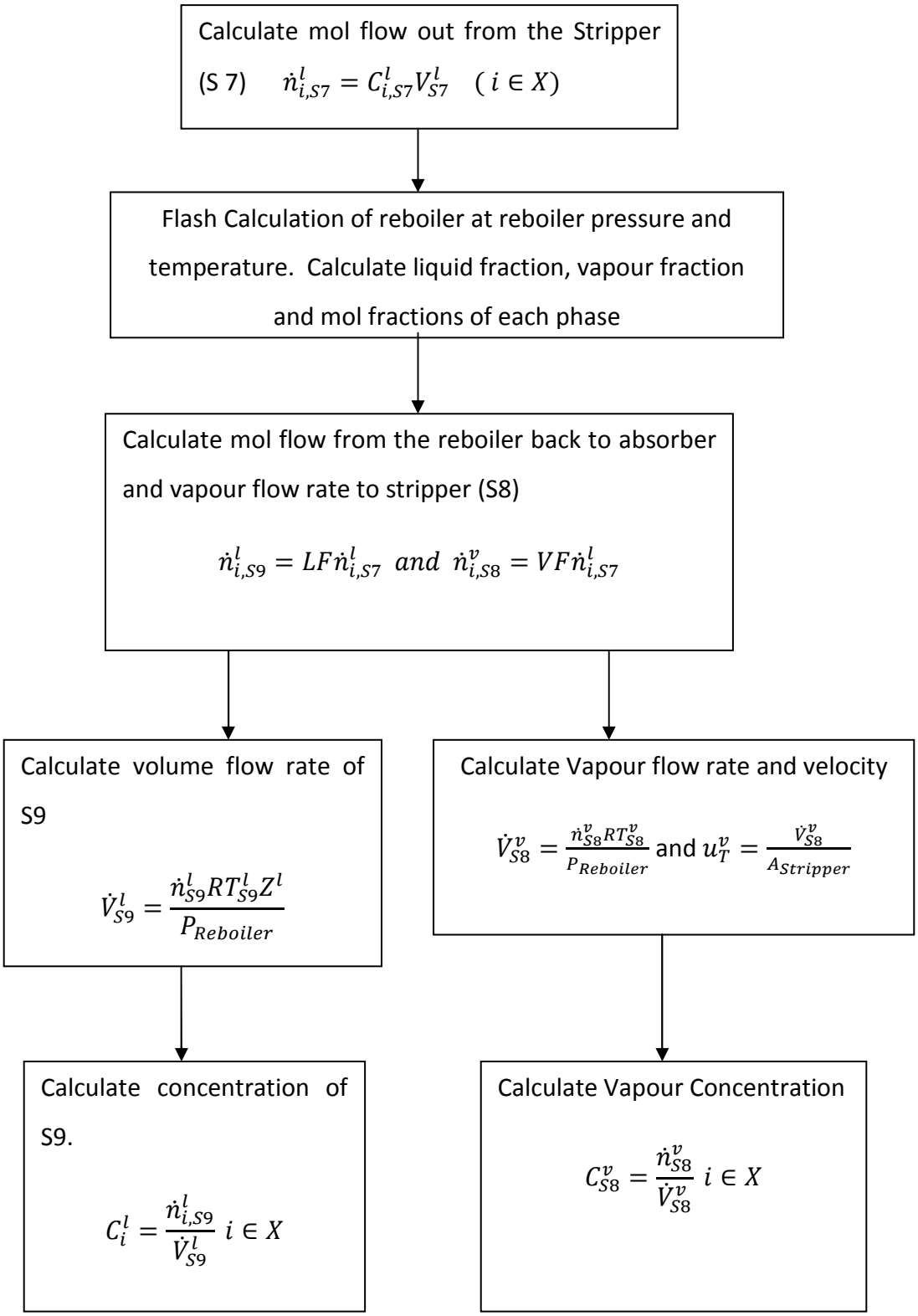

Figure 2.7: Flow diagram of Reboiler sequence of calculations

The heat consumption within the Reboiler is the major heat use of heat in the process. The heat energy is consumed in two parts

1. Heat consumed raising temperature of liquid from outlet temperature of stripper to reboiler temperature
2. Heat consumed vaporizing the vapour flow.

The formula for the energy required for the raising the liquid temperature is:

$$\dot{Q}_{1,RB} = \dot{n}_{S7}^{l} Cp_i^l (T_{S8}^l - T_{S7}^l)$$

Like wise the energy required to vapourize the steam is:

$$\dot{Q}_{2,RB} = \sum_{i=H_2O,MEA} \dot{n}_{i,S8}^{l} \Delta H_i^{lv}$$

The total energy is the sum of the two values ie. $\dot{Q}_{RB} = \dot{Q}_{1,RB} + \dot{Q}_{2,RB}$

2.5 Condenser

The condenser and the top of the tower cools the outlet vapour form the stripper condensing a percentage of the MEA and H_2O. The condensed liquid is recombined with the inlet flow from the absorption tower and is the inlet conditions into the stripper. This is in not how the system is constructed in practice as usually the feed from the de-absorber is not into the top of the tower but usually a few meters down the tower, typically 10% of the height from the top (Kohl 1995). The assumption that the flows are mixed before entering the column is primarily done to make the modeling simpler otherwise the PDE would have to be modified to have a side stream input. A simplified process flow diagram of the condenser is shown in figure 2.8.

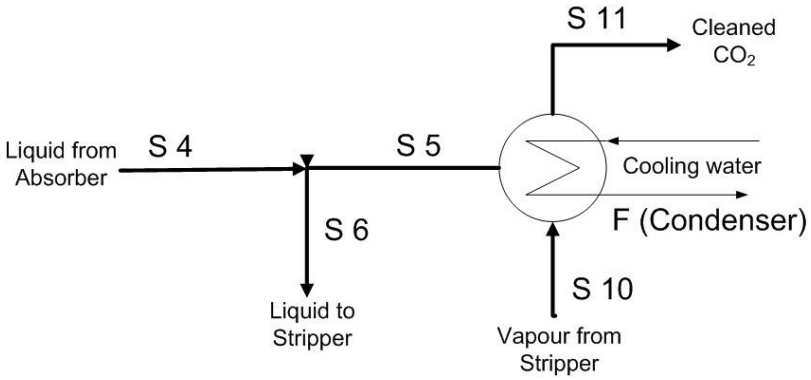

Figure2.8:Deabsortion tower Condenser process flow diagram

The molecular flows from the stripper into the condenser are calculated assuming the vapour volume flow rate from S10 is the same as S8 and $\dot{V}_{S8}^{v}$ is from the rebioiler calculations therefore:

$$n_{i,S10}^{v} = C_{i,S10}^{v}\dot{V}_{S10}^{v}$$

The condenser reflux rate is the percentage of the MEA and H_2O that is condensed in the condenser and returned to the stripper. The mol flow of this is given by:

$$\dot{n}_{H_2O,S5}^{l} = \dot{n}_{H_2O,S10}^{v} Reflux_{Condenser} \;\; and \; \dot{n}_{MEA,S5}^{l} = \dot{n}_{MEA,S10}^{v} Reflux_{Condenser}$$

The mol flow from the absorber is the mol flow of stream S3 which is the multiplication of the concentrations from the absorption tower and the volume flow rate of stream S3. The combined mol flow of S6 is S5 plus S4.

$$n_{i,S3}^{l} = n_{i,S4}^{l} = C_{i,S3}^{l}\dot{V}_{S3}^{l}$$

$$n_{i,S6}^{l} = n_{i,S4}^{l} + n_{i,S5}^{l}$$

The volume flow rate of S6 is calculated from the EOS which requires the mol fractions of the liquid of S6. The inlet concentrations into the stripper are the mol flows divided by the volume flow rate. The formulas are shown below.

$$x_{i,S6}^{l} = \frac{n_{i,S6}^{l}}{\sum_{i \in X} n_{i,S6}^{l}}$$

$$\dot{V}_{S6}^{l} = \frac{\dot{n}_{S6}^{l} R T_{S6}^{l} Z^{l}}{P_{Condenser}}$$

$$C_{i,S6}^{l} = \frac{\dot{n}_{i,S6}^{l}}{\dot{V}_{S6}^{l}} \; i \in X$$

The temperature of the inlet to the stripper is a combination of the temperature from flow S4 and flow S5. A simply mixing rule based on the mol flows, Cp values and temperatures of the flows was used. The outlet temperature of the condenser is an input and is controllable while the temperature from the absorber is varying as part of the system dynamics due to it being at

output of the rich-lean heat exchanger (C). The formula for the stripper inlet temperature is given below in equation 2.34

$$\dot{Q}_{S4} = \sum_{i \in X} \dot{n}^{l}_{i,S4}\, Cp^{l}_{i}\, T^{l}_{S4} \;\; and \;\; \dot{Q}_{S5} = \sum_{i \in MEA, H_2O} \dot{n}^{l}_{i,S5}\, Cp^{l}_{i}\, T^{l}_{S5}$$

$$T^{l}_{S6} = \frac{\dot{Q}_{S4} + \dot{Q}_{S5}}{\sum_{i \in X} \dot{n}^{l}_{i,S6}\, Cp^{l}_{i}} \quad \text{(Eq 2.34)}$$

Because the condenser cools the vapour and condenses some of the MEA and H_2O, a certain amount of cooling flow is required. This is made up of two parts like the reboiler.

1. Energy from cooling outlet vapours in the condenser
2. Energy released from the phase change of MEA and H_2O in the condenser.

The formulas for the two heat flows are given below.

$$\dot{Q}_{1,Co} = \sum_{i \in MEA, H_2O} \dot{n}^{l}_{i,S5} Cp^{l}_{i} \left(T^{l}_{S5} - T^{l}_{S10}\right) \; and \; \dot{Q}_{2,Co} = \sum_{i \in MEA, H_2O} \dot{n}^{l}_{i,S5} \Delta H^{lv}_{i}$$

The total energy is the sum of the two values i.e. $\dot{Q}_{Co} = \dot{Q}_{1,Co} + \dot{Q}_{2,Co}$

2.6 Heat Exchangers

There are two heat exchangers in the process C and H. The first heat exchange transfer heat from the hot stream S9 exiting the stripper to the cold stream S3 from the absorber. The stream S4 is the heated stream to the stripper and S12 is the cooled liquid flow back to the absorber. The second heat exchanger cools the flow to the absorber, to a set point temperature. An illustration of the process is shown in figure 2.9

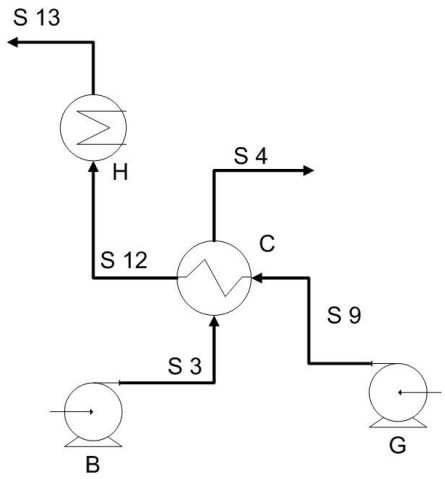

Figure 2.9: Heat Exchanger Network

The heat exchanger is modeled as a CSTR with a pinch of 10 K between streams S3 and S12. The amount of heat transferred from stream S9 is equal to the amount of heat received by stream S3. The pinch is set at 10K so T12 is T3 + 10. The amount of energy transfer from stream S9 is then:

$$\dot{Q}_{S9} = C_{S9} Cp^{l}_{S9-S12} \dot{V}_{S9} (T_{S9} - T_{S12}) \quad \text{(Eq 2.35)}$$

Where Cp^{l}_{S9-S12} is the heat capacity of the liquid evaluated at the mean temperature of S12 and S9 ie (T12+T9)/2. The log mean temperature between the hot and cold streams is given by the equation 2.36:

$$\Delta T_{LM} = \frac{(T_{S9} - T_{S4}) - (T_{S12} - T_{S3})}{ln\left(\frac{(T_{S9} - T_{S4})}{(T_{S12} - T_{S3})}\right)} \quad \text{(Eq 2.36)}$$

The heat transfer between the hot and cold stream s can also be calculated from the log mean temperature difference by equation 2.37:

$$\dot{Q}_{S9} = UA\Delta T_{LM} \quad \text{(Eq 2.37)}$$

Where UA is the overall heat transfer co-efficient and is assumed constant. This equation is rearranged so that the ΔT_{LM} is the unknown. Ie

$$\Delta T_{LM} = \frac{\dot{Q}_{S9}}{UA} \quad \text{(Eq 2.38)}$$

Knowing $\dot{Q}_{S9}$ from formula 2.38 then ΔT_{LM} can be calculated. The only unknown is T4 and this is iterated on to find when ΔT_{LM} from formula 2.36 is the same vale as ΔT_{LM} from formula 2.38

The second heat exchanger H cools stream S12 to temperature T13 which is the input to the absorber and the cooling requirements of this heat exchanger are

$$\dot{Q}_{S13} = C_{S13} Cp^{l}_{S13-S12} \dot{V}_{S13} (T_{S12} - T_{S13})$$

Where $Cp^{l}_{S13-S12}$ is the mean temperature between the two streams S12 and S13.

The power required by the rich and lean pumps is given by the formulas (Eq 2.29a and 2.39b)

$$P_{Rich} = \rho_{S3} \dot{V}_3 g H_{S3} \ (Eq\ 2.39a) \ \ and\ P_{Lean} = \rho_{S9} \dot{V}_{S9} g H_{S9} \ \ (Eq\ 2.39b) \ \ (W)$$

Where ρ_{S3} = density of stream S3 (kg/m^3)

ρ_{S9} = density of stream S9 (kg/m^3)

H_{S3} = Assumed pumping head of rich amine solution (taken as 20m)

H_{S9} = Assumed pumping head of lean amine solution (taken as 20m)

2.7 Pressure Drop

The pressure drop within the tower is assumed to be small and was not dynamically modeled. It is assumed the pressure drop is a linear pressure drop over the length of the towers of 2000 Pa. At the start when the initial conditions of the model are calculated the inlet pressure is the value assigned to the bottom of the columns and a ΔP is applied to each discretised volume so that the pressure at the top of the tower is the inlet pressure minus the overall pressure drop (in this case 2000Pa). For a more robust model the pressure drop could be allowed for by use of pressure drop equations which relate to the packing properties (Billet 1995) but was not considered needed in this model.

2.8 Velocity Correction

The Velocity of the liquid and the vapour in both columns is assumed to be constant. The previous work of Hansen (2004) developed a dynamic velocity from the momentum balance but the velocity only varied by less than 0.05% therefore this was not included in this model.

The velocity was calculated as the volume flow rate divided by the reduced cross sectional area of the tower. The cross sectional area of the tower is reduced in two ways.

1. Area is reduced due to volume of packing in tower therefore equation is divided by epslom (ε).
2. Area is reduced due to volume of liquid in the tower for the vapour phases therefore equation is divided by the liquid hold up (h_T). This is calculated as part of the formula for finding the mass transfer coefficient in the vapour phase.

$$u^l = \frac{\dot{V}^l}{\frac{A_c}{\epsilon}} \quad and \quad u^v = \frac{\dot{V}^v}{\frac{A_c}{\epsilon h_T}}$$

3. Model Validation

3.1 Parameters

The parameters for the model are listed in table 3.1. The parameters are constant.

Table 3.1: Model parameters used in this work

Parameter	value	Unit	Reference
Gravitational constant	9.81	$\frac{m}{s^2}$	
Diameter of absorption Tower	16	M	
Diameter of de-absorption tower	5	M	
Height of absortuion Tower	25	m	
Height of de-absorption Tower	15	m	
Inlet gas Pressure in absorption Tower	110000	Pa	
Inlet gas Pressure in de-absorption Tower	200000	Pa	
Pressure drop in de/Absorption tower(s)	2000	Pa	
Carbon dioxide critical temperature	304.2	K	Reid et al 1987
Carbon dioxide critical pressure	7.383	MPa	Reid et al 1987
Carbon dioxide acentric factor	0.228		Reid et al 1987
Monoethanolamine critical temperature	614.4	K	Kukoljac and Grozdanic 2000
Monoethanolamine critical pressure	4.45	MPa	Kukoljac and Grozdanic 2000
Monoethanolamine acentric factor	0.864	0.842	Reid et al 1987
Water critical temperature	645.	K	Reid et al 1987
Water critical pressure	22.12	MPa	Reid et al 1987
Water acentric factor	0.344		Reid et al 1987
Nitrogen critical temperature	126.1	K	Reid et al 1987
Nitrogen critical pressure	3.394	MPa	Reid et al 1987
Nitrogen acentric factor	0.040		Reid et al 1987
Oxygen critical temperature	154.6	K	Reid et al 1987
Oxygen critical pressure	5.043	MPa	Reid et al 1987
Oxygen acentric factor	0.022		Reid et al 1987
Heat of vapourization Monoethanolamine (assumed constant)	53700	$\frac{J}{mol}$	Scheiman 1962
Heat of vapourization for water (assumed constant)	40680	$\frac{J}{mol}$	Wikipedia/water
Heat of reaction 2MEA + CO_2	65000	$\frac{J}{mol\ CO_2}$	Akanksha et al 2007, Draxler et al
Heat of reaction $CO_2 + OH^-$	20000	$\frac{J}{mol\ CO_2}$	Pinsent et al 1950
Universal gas constant	8.314	$\frac{J}{mol\ K}$	

Packing surface area /volume (a_T) Note packing is Montz B 200 metal structured packing.	200	$\frac{m^2}{m^3}$	Billet 2005
Packing coefficient C_l	0.971		Billet 2005
Packing coefficient C_h	0.547		Billet 2005
Packing coefficient C_v	0.390		Billet 2005
Packing void fraction (ε)	0.979		Billet 2005
Heat exchanger area	$1.5x10^7$		

3.1.1 Interaction parameters

The interaction parameters for this work where include in the van der Waals mixing equation for formulation of the cubic equation of state. The interaction parameter of Mea and water was fitted to experimental data from Park and Lee (1997). The bubble point and dew point temperature were calculated for varying mol fraction of MEA with the Peng Robinson EOS. The binary interaction parameter was adjusted to fit the data and a value of -0.18 was found to be optimum. A plot of the experimental data and fitted curves are shown in figure 3.1.

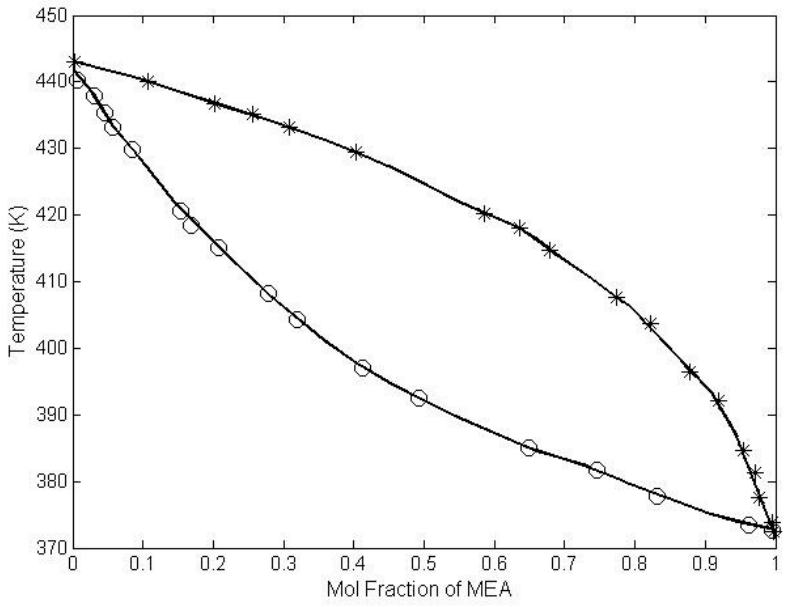

Figure 3.1: Bubble point and due point curves for MEA and water mixture

The values for other binary interaction parameters which were located from literature are included in table 3.2 and unknown values are set to zero.

Table 3.2: Binary inetraction parameters used in this work

	CO_2	MEA	H_2O	N_2	O_2
CO_2	0	0.16	0.065[b]	-0.0149[c]	-0.04838[c]
MEA		0	-0.18	0	0
H_2O			0	0	0
N_2				0	-0.00978[c]
O_2					

b=Paulus and Penoncello (2006) c=Stoll et al (2003) e=from this work

3.2 Inputs

The inputs are the adjustable values used in the model simulation are displayed in table 3.3

Table 3.3: Inputs used in this work

Input		
Mol flow of CO_2 into system	720	mol/s
Absorber gas inlet temperature*	313	K
Volume flow of liquid (stream S3)	0.8	m^3/s
Reflux percentage condenser	10	%
Reboiler pressure	200000	Pa
Reboiler Temperature	394.2	K
Absorber Liquid temperature	318	K
Condenser Liquid temperature	380	K
Lean pump Pressure	20	m
Rich pump Pressure	20	m

*note: The inlet gas from the post combustion process is cooled at a inlet heat exchanger beyond the scope of this model so the inlet temperature could be classed as a disturbance.

3.3 States

A summary of the states and the equations for the absorption and stripper PDE is listed below

$$\frac{dc_i^l}{dt} = u\frac{dc_i^l}{dz} - \dot{n}_{i,d} + R_{i,gen} \quad \text{(Eq 2.2)}$$

$$\frac{dc_i^v}{dt} = -u\frac{dc_i^v}{dz} + \dot{n}_{i,d} \quad \text{(Eq 2.3)}$$

$$\frac{dT^l}{dt} = -u\frac{\partial T^l}{\partial z} - \frac{[\dot{n}_d]^T\left[\Delta\tilde{H}_i^{vl}\right]}{[C_i^l]^T[\tilde{C}p_i^l]} - \frac{\dot{n}_{CO_2}\Delta H_{RE}}{[C_i^l]^T[\tilde{C}p_i^l]} - \frac{U_{T,lv}(T^l - T^v)}{[C_i^l]^T[\tilde{C}p_i^l]} \quad \text{(Eq 2.24)}$$

$$\frac{dT^v}{dt} = -u\frac{\partial T^v}{\partial z} - \frac{[\dot{n}_d]^T\left[\Delta\tilde{H}_i^{vl}\right]}{[C_i^v]^T[\tilde{C}p_i^v]} + \frac{U_{T,lv}(T^l - T^v)}{[C_i^v]^T[\tilde{C}p_i^v]} \quad \text{Eq (2.25)}$$

The table 3.4 shows which concentrations are modeled in which phase and what term are included..

Table 3.4: Included terms in the PDE equations 2.2,2.3,2.24 and 2.25.

Species	Gas phase	Liquid phase	Generation term	Diffusion term
CO_2	Yes	Yes	Yes	Yes
MEA	Yes	Yes	Yes	Yes
H_20	Yes	Yes	No	Yes
N_2	Yes	Yes	No	Yes
O_2	Yes	Yes	No	Yes
$MEAH^+$	No	Yes	Yes	No
$MEACOO^-$	No	Yes	Yes	No
HCO_3^-	No	Yes	Yes	No
OH^-	No	Yes	Yes	No
H_3O^+	No	Yes	Yes	No

3.4 Calculations

As a model validation some of the calculations and algebraic equations are evaluated in table 3.5. The properties of the fluids and the reaction rates and equilibrium values are the main values shown and have reference values when reference values were found.

Table 3.5: Validation Calculations

	313K	393K	Units	Range or typical value	Reference
Z^L	0.0012	0.0047			
Z^v	0.9991	0.9982			
Henrys water	2.32 $x10^8$	6.18 $x10^8$	Pa	1.65 $x10^8$-1.15 $x10^9$	Wikipedia/henry
Henrys MEA	1.210 $x10^8$	2.17 $x10^8$	Pa		
Henrys mix	2.19 $x10^8$	6.07 $x10^8$	Pa		
Ionic correction	1.0564	1.19			
Henrys corrected	5.28 $x10^3$	1.25 $x10^4$	$\frac{m^3 Pa}{mol}$		
H_2O liquid viscosity	6.53 $x10^{-4}$	2.25 $x10^{-4}$		1.0$x10^{-3}$-4.0$x10^{-4}$	Wikipedia/viscosity
MEA liquid viscosity	0.0101	0.0012	Pa s	0.007 @ 323K	AKZO Nobel
Mixture liquid viscosity	0.0019	5.86 $x10^{-4}$		6.1 $x10^{-4}$-2.6 $x10^{-2}$	Piche et al

					2007
CO_2 vapour viscosity	1.55 x10^{-5}	1.91 x10^{-5}	$\frac{kg}{m^2}$	1.26 x10^{-5} – 2.78 x10^{-5}	Perry and Green 1999
O_2 Vapour viscosity	2.12 x10^{-5}	2.53 x10^{-5}	$\frac{kg}{m^2}$	1.75 x10^{-5} – 3.48 x10^{-5}	Perry and Green 1999
N_2 vapour viscosity	1.84 x10^{-5}	2.17 x10^{-5}	$\frac{kg}{m^2}$	1.56 x10^{-5} – 2.95 x10^{-5}	Perry and Green 1999
H_2O vapour viscosity	9.28 x10^{-6}	1.29 x10^{-5}	$\frac{kg}{m^2}$	9.09 x10^{-6} – 2.27 x10^{-5}	Perry and Green 1999
Vapour mixture viscosity	1.98 x10^{-5}	1.36 x10^{-5}	$\frac{kg}{m^2}$	1.3-2.1 x10^{-5}	Piche et al 2003
Liquid density	1007	1160	$\frac{kg}{m^3}$	802-1190	Piche et al 2003
Vapour density	1.16	1.18	$\frac{kg}{m^3}$	0.18-16.1	Piche et al 2003
Column Reynolds number liquid	7.6	175			
Wetted surface area/ volume	64.8	120	$\frac{m^2}{m^3}$	7-244	Piche et al 2003
Diffusivity of CO_2 in H_2O	2.69 x10^{-9}	1.07 x10^{-8}			
Diffusivity of CO_2 in liquid mixture	1.57 x10^{-9}	1.59 x10^{-9}	$\frac{m^2}{m^3}$	1.42 x10^{-9} (298K)	Akanksha et al 2007
Diffusivity of H_2O in Vapour	2.59 x10^{-5}	2.08 x10^{-5}	$\frac{m^2}{s}$	0.7 x10^{-5} -8.4 x10^{-5}	Piche et al 2003
Diffusivity of MEA in vapour	1.14 x10^{-5}	9.26 x10^{-6}	$\frac{m^2}{s}$	0.7 x10^{-5} -8.4 x10^{-5}	Piche et al 2003
Mass transfer coefficient for CO_2 in liquid	8.61 x10^{-5}	4.09x10^{-4}		1 x10^{-5}- 8 x10^{-3}	Aroonwilas et al 2003
Mass transfer coefficient for H_2O in vapour	0.1350	0.134			
Mass transfer co-efficient for MEA in vapour	0.0785	0.0783			
Enhancement factor	117.4	208			
Forward reaction rate for reaction 1	14.15	5.13 x10^{2}	$\frac{m^3}{mol\ s}$	6.8-540	Jamal et al 2006
Forward reaction rate for reaction 2	0.024	0.024	$\frac{1}{s}$	0.024	Cents et al 2005
Forward reaction rate for reaction 3	25.16	2.11 x10^{3}	$\frac{m^3}{mol\ s}$	14.1 at 297K	Cents et al 2005
Forward reaction rate for reaction 4	2 x10^{-5}	2 x10^{-5}	$\frac{1}{s}$	2 x10^{-5}	Tanaka 2002

Forward reaction rate for reaction 5	0.1	0.1	$\frac{1}{s}$		
Forward reaction rate for reaction 6	0.1	0.1	$\frac{1}{s}$		
Equilibrium constant for reaction 1	623.85	0.3096			
Equilibrium constant for reaction 2	0.009	0.0052			
Equilibrium constant for reaction 3	6.26×10^{9}	1.40×10^{7}			
Equilibrium constant for reaction 4	1.44×10^{-12}	3.73×10^{-10}			
Equilibrium constant for reaction 5	1.25×10^{-6}	1.47×10^{-4}			
Equilibrium constant for reaction 6	11.54	114.3			

3.5 Reactions

The validation of the chemical reactions is an important part of the vapour liquid equilibrium model. Many different equilibrium constants from different authors where tried until the equilibrium constants from Liu et al (1999) were settled on. It is noted that to obtain accurate plots from the equilibrium constants the numerical values had to be multiplied by 1×10^{6} and the constant for equilibrium reaction 6 divided by 5. It is not known why the multiplication had to be applied this could be due to calculation errors within the numerical simulation. The validity of the equilibrium constants was tested by running a program which loaded a specific amount of CO_2 into a volume. At 15% MEA by weight the concentration of MEA is 2500 mol/m^3 and the concentration of water is 48000 mol/m^3. The program was then run with the reactions taking place in the liquid phase until steady state was achieved typically 10000s. The concentration of each species was noted and the amount of CO_2 increased and the simulation repeated. The loading was varied between 0 and 1 which corresponds to a CO_2 concentration of 0 at 0 loading and an MEA initial concentration of 2500 mol/m^3 at loading 1. Note loading is defined as mol$CO_{2,Total}$/mol MEA_{Total}. The CO_2 reacts with the MEA to form the various ions in solution. The concentration of the H_30^+ and OH^- ions are not indicated on the graph as are small values. The figures 3.2a and 3.2b are plots from the equilibrium constants from this work and figure 3.3a and 3.3b are the corresponding plots from Liu et al (1999). Figures 3.2a and

3.3a are for 313K while figures 3.2b and 3.3b are for 373K. The plots show good correlation so the author is confident the equilibrium constants are correct. It is noted that Hoff (2003) also obtained the same plots but using different equilibrium constants.

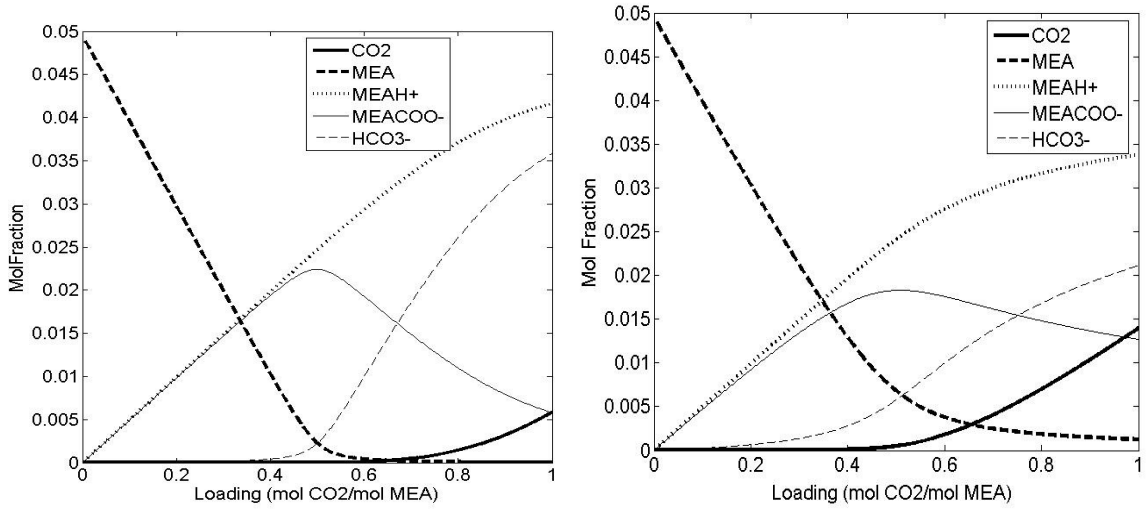

Figure 3.2a: Species composition at 313K and Figure 3.2b:Species composition at 373K. Plotted form modified equilibrium constants from Liu et al (1999)

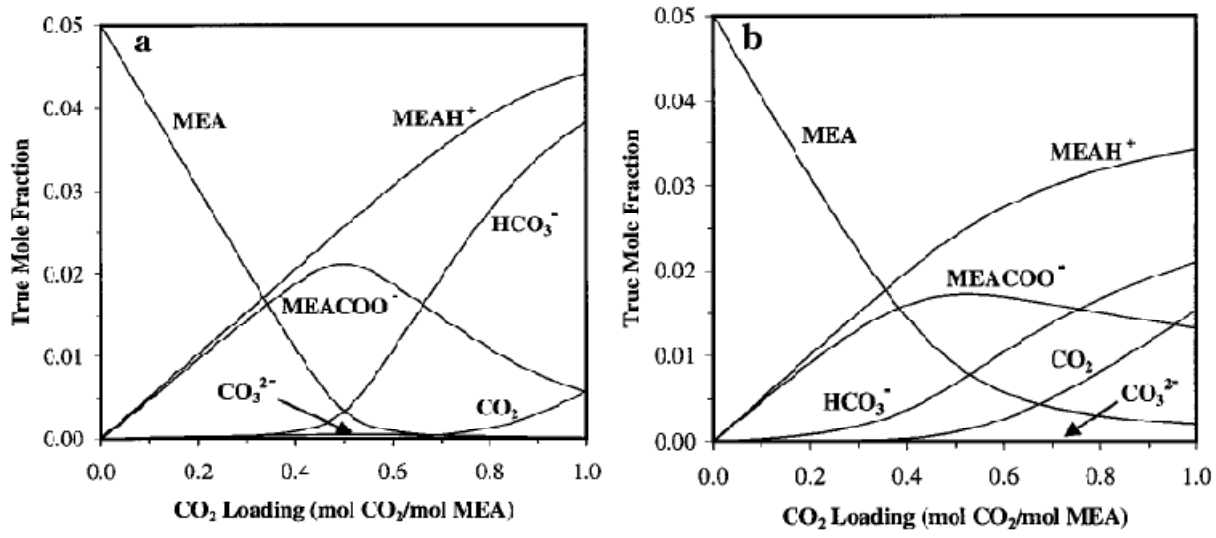

Figure 3.3a: Species composition at 313K and Figure 3.3b:Species composition at 373K. Taken from Liu et al (1999)

3.6 Vapour Liquid Equilibrium

The verification of the vapour liquid equilibrium is the next step in validating the model. The vapour liquid equilibrium is the relationship between the species in the liquid phase and the corresponding species in the vapour phase. The vapour-liquid equilibrium is between the 5

species (CO_2, MEA, H_2O, N_2 and O_2) which are present in both phases. The fugacity ratio was used to equate the mol fraction in the liquid phase to the mol fraction in the vapour for all species except CO_2 which used henrys constant. At steady state conditions the mass transfer between the phases can be considered to be equal and opposite and the reactions in the liquid phase to be in equilibrium. Taking a hypothetical $1m^3$ container with a 15% MEA (weight) solution at 313K temperature then there is approximately a H_2O concentration of 47200 mol/m^3 and a MEA concentration of 2500 mol/m^3. If one mol of CO_2 is added and allowed to react to steady state then according to the values for the equilibrium constants the concentration of all the species is shown in table 3.6

Table 3.6: sample calculation for partial pressure of CO_2 from CO_2 loading.(concentrations in mol/m^3)

K1	623	CO_2 Concentration vapour	$4.6x10^{-10}$
K2	0.009	MEA Concentration vapour	0.005
K3	$9.73 x10^{8}$	H_2O Concentration vapour	2.611
K4	$9.28 x10^{-12}$	N_2 Concentration vapour	37.5
K5	$1.25x10^{-6}$	Henrys Constant	4568 $\frac{Pa\,m^3}{mol}$
K6	11.5		
CO_2 Concentration liquid	$2.6x10^{-10}$		
MEA Concentration liquid	2498		
H_2O Concentration liquid	47198		
N_2 Concentration liquid	0.46		
$MEAH^+$ Concentration liquid	1		
$MEACOO^-$ Concentration liquid	0.99		
OH^- Concentration liquid	0.018		
H_3O^+ Concentration liquid	$5.1x10^{-10}$		
HCO_3^- Concentration liquid	0.004		

According to henrys law at 313K and the above ionic concentrations then the pressure of CO_2 in the vapour phase is found by solving the diffusion equation for zero mol flow

$$\dot{n}^l_{d,CO_2} = -kd^H_{CO_2} a_w \left(P^v_{CO_2} - H_{CO_2} C^l_{CO_2}\right)$$

$$\dot{n}^l_{d,CO_2} = 0 \;\Rightarrow P^v_{CO_2} = H_{CO_2} C^l_{CO_2}$$

$$P^v_{CO_2} = 4568x2.6x10^{-10}$$

$$P_{CO_2}^{v} = 1.18x10^{-6} \quad (Pa)$$

This can be expressed as a concentration also by using the ideal gas law

$$P_{CO_2}^{v} = C_{CO_2}^{v} RT^{v}$$

$$\Rightarrow C_{CO_2}^{v} = \frac{P_{CO_2}^{v}}{RT^{v}} = \frac{1.18x10^{-6}}{8.314x313} = 4.6x10^{-10}$$

CO_2 loading from 0 to 1 (which corresponds to a concentration of CO_2 from 0 to 2500 mol) was simulated to steady state and the partial pressure of the CO_2 plotted verse loading. The plots are shown in figure 3.4 for 30% MEA solution and figures 3.5 a and b for 15% MEA solution. The isotherm 313K is the line on the right in figurers 3.4a,3.4b and 3.5a while the other isotherm is at 373K on the left. Figure 3.5b has four isotherms of 298,313,333 qne 353K. The experimental points are from Mather et al (1975) for figures 3.4 a and 3.4b at 30% solution and Mather et al (1976) for 15% solution figure 3.5a and from Lee et al (1976) for figure 3.5b.

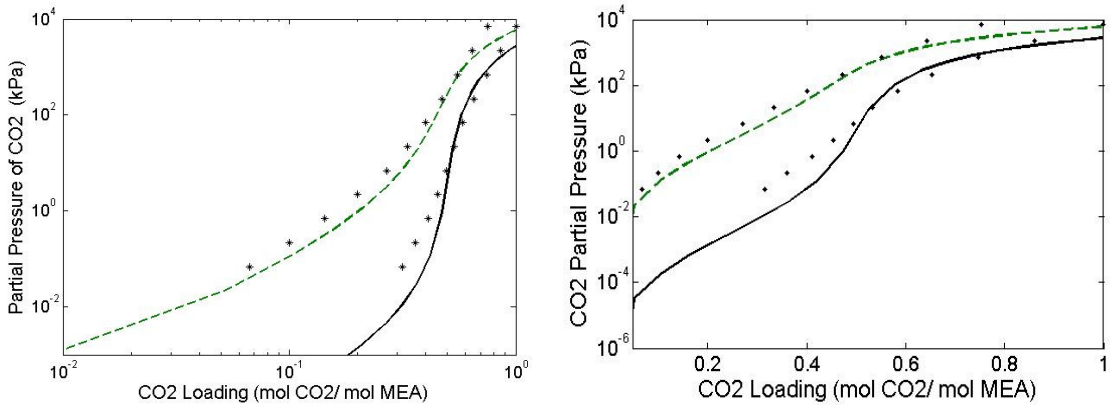

Figure 3.4a and b: Partial pressure of CO_2 for 30% Monoethanolamine solution

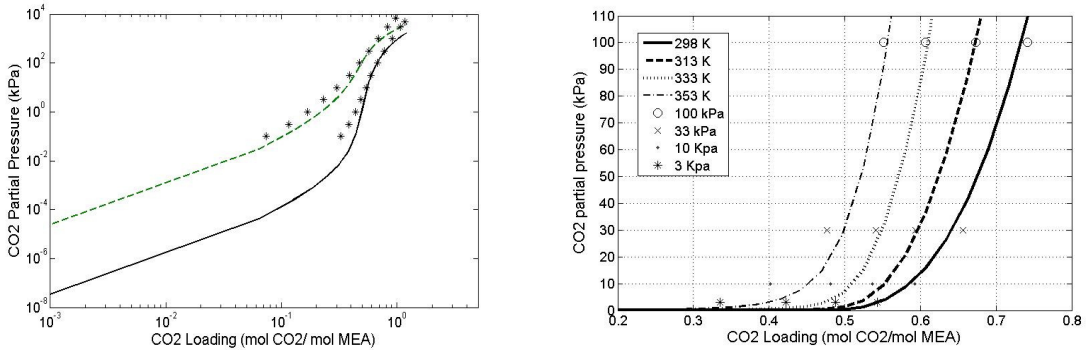

Figure 3.5a and b: Partial pressure of CO_2 for 15% Monoethanolamine solution

4 Implementation and Results

4.1 Model Simulation

The simulation of the system is undertaken in Matlab using the method of lines to discretise in the spatial direction along the length of the column and the numerical solver ODE15s to solve in the time direction. The system is characterized by the closed loop recirculation of the amine solution which means that outputs from one item of equipment are the inputs to another. The boundary conditions are the inlet conditions of the gas feed to the de-absorber. The model is simulated based on a 400 MW natural gas fired power station producing 1 million tones of CO_2 per year. This is a mol flow of CO of 720 mol/s which at 4% mol concentration is a total mol flow of 18009 mol/s. Using the ideal gas law (as the pressure is low and Z is typically 0.99) the volume flow rate at 313K and 110000 Pa is 426 m^3/s if the tower is selected as 16m diameter and the packing has a void fraction of 0.979 then the cross sectional area of the tower is 197m^2 and the velocity of the gas in the absorption tower is 2.21m/s (including for liquid holdup). A liquid flow rate of 0.8 m^3/s corresponds to a liquid velocity of 0.0041m/s. The details of the calculation are included in Appendix 3.

The Stripper has a diameter of 5m which corresponds to a cross-sectional area of 19m^2. A reboiler temperature of 394.2K produces flow which is a mol flow of 1300 mol/s for the vapour phase. At a pressure of two bars and a temperature of 393K this is a vapour volume flow rate of 20.5m^3/s and a gas H_2O concentration of approximately 60 mol/m^3.

The height of the absorber and stripper can be selected independently and the number of discretised zones within the tower can be changed. For reasonable speed 35 discretised zones was deemed acceptable but for higher accuracy more discretised zones are required. The computational time is exponentially related to the number of zones so to minimize simulation time 5 zones is used and then more can be used when the inputs and parameters have been set. The initial conditions within the towers dictate how long the system takes to simulate. If the system is far from equilibrium then the reaction rates are fast which results in large heats from the reactions affecting the temperature balance. The Matlab solver reduces the time step size resulting in a long simulation (up to 24 hours). This can be overcome by simulating for a

long time and using the steady state values as initial conditions for the start of the next simulation.

A list of the operator adjustable inputs and parameters are shown below

1. Absorption tower area which is a function of the tower diameter (if the tower is circular)
2. Packing properties (specific surface area ε, packing coefficients C_h C_l C_v etc)
3. Absorption tower diameter
4. Incoming gas mol composition
5. Incoming gas flow rate (in this model is set by mass flow of CO_2 into absorption tower)
6. Recycle rate of amine solution
7. Amine concentration of amine solution
8. De-absorption tower area (the tower area is set so the gas velocity is between 1-2 m/s)
9. De absorption tower height
10. Reflux rate from condenser
11. Pressure in reboiler and stripper
12. Reboiler temperature(sets amount of stripping steam) this also effects gas velocity
13. Pressure drop in absorption and stripping towers.

The model is made up of 14 Matlab files which are attached in appendix D a brief description of each Matlab function is listed below along with figure4.1 which is a flow chart of the simulation procedure.

- `carbon3.m`: This is the run file which the operator selects to start the process. This file contains the ODE solver and requires the initial conditions from `startvalues.m` and the inlet conditions at the boundary (`inletvalues.m`).
- `startvalues.m`: This file contains a previous simulation result which is saved as a .mat file. The file takes the results from the final time of the saved simulation and constructs a cubic spline of the values. This cubic spline can then be interpolated into a different length of tower and number of discretised zones. For example if the previous simulation had a tower height of 10m and is in 5 discretised zones then a new output

could be a height of 15m and 10 zones and the cubic functions fits the first to the second.

- `inletvalues.m`: The inlet conditions of the gas from the combustion process are calculated in this file from the mol fractions and mass flow of CO_2. The absorber tower velocities and liquid composition are also calculated in this file.
- `COabsorb.m`: This is the file that the ODE solve calls to run. In this file which calculates the ODE equations, The values from the previous time step are first extracted and ordered. Then the calculation of the `reboiler.m` is done which provides the inlet conditions into the stripper for the gas and the liquid flow back to the absorber. Then the calculation of the heat exchanger between the rich and lean amine solution is carried out by calling function `heatexlR.m` and this provides the inlet temperature to the absorber tower and condenser. The `condenser.m` file calculates the inlet conditions for the stripper for the liquid flow and the cleaned gas composition. The three sub routines are iterated to calculate the liquid volume flow into the de-absorber is the same as the liquid volume flow out

  As sub routines in the `COabsorb.m` file the PDE of the absorber and stripper are run and each tower is discretised into N slices. For each slice the functions `reactions.m`, `HEAT.m` and `vari.m` are called which calculate information about the reactions that take place, the heat transfer and the diffusion values respectively. It is also noted that their is a mol check of the water and MEA flowing back to the absorber as some MEA and water is lost from the system to the exhaust gas from both the stripper and the absorption tower. The mol check maintains the correct amount of MEA and H_2O in the process by adding extra if required.
- `reboiler.m`: Information from the stripper outlet conditions is used in the `reboiler.m` file to calculate the stripper gas inlet conditions and the liquid composition returning to the absorption tower. The energy requirements of the reboiler are also calculated.
- `heatexlR.m`: the heat exchanger calculation requires the temperatures and concentrations from the outlet of the absorption tower and stripper and calculates the inlet temperatures for each respective column. The pump power is also calculated for each liquid based on a volume flow rate and an assumed pressure drop set by the user.

- `Condenser.m`: taking the vapour conditions out of the stripper and the liquid from the absorption column, the condenser function calculates the inlet liquid conditions for the de-absorber and the cleaned gas composition. Also included in the `condenser.m` function is a calculation of the amount of CO_2 removed and the energy cost per kg.
- `Reactions.m`: In this function, the forward and backward reaction rates and the equilibrium constants which are used to calculate the overall reaction rate for each reaction. The overall reaction rate is multiplied with the stoichmetric matrix to calculated the rate of generation if each species in the liquid phase.
- `HEAT.m`: This file calculates the temperature change for the liquid and the gas in each discretized slice. For the liquid phase there is heat from the heat of reaction, heat of vapourization and the sensible heat transfer while the vapour phase does not have a heat of reaction term.
- `Vari.m`: This file calculates the diffusion mass transfer of the five species between the liquid and gas phase. The concentration in the bulk phase of the vapour and liquid is used in the subroutine `NLPE.m` to calculate the interface concentrations of the species and this is used as a driving force for the mass transfer calculation. Properties of the fluids are evaluated to find the mass transfer coefficients used in the calculation of mol transfer calculation. The diffusion of CO_2 from one phase to the other is calculated by henrys law.
- `NLPE.m`: this function is a sub routine for calculating the non linear solution to the concentrations at the vapour liquid interface. Successive approximation is used to calculate the roots to the five non linear equations which relate the mol fraction in the liquid to the mol fraction in the gas by the ratio of the fugacities. The `NLPE.m` functions calls the `PEA.m` function to calculate the fugacities.
- `PEA.m`: This is a function that calculates fugacities at the interface using the Peng Robinson equation of state. The mixing rules are applied to the components and the roots for the liquid and vapour phase calculated.
- `Para.m`: this file contains parameters of the system that are used in the functions within the calculation.
- `Output.m`: This file post processes the model information to show the energy consumed, loadings and cleaned gas composition.

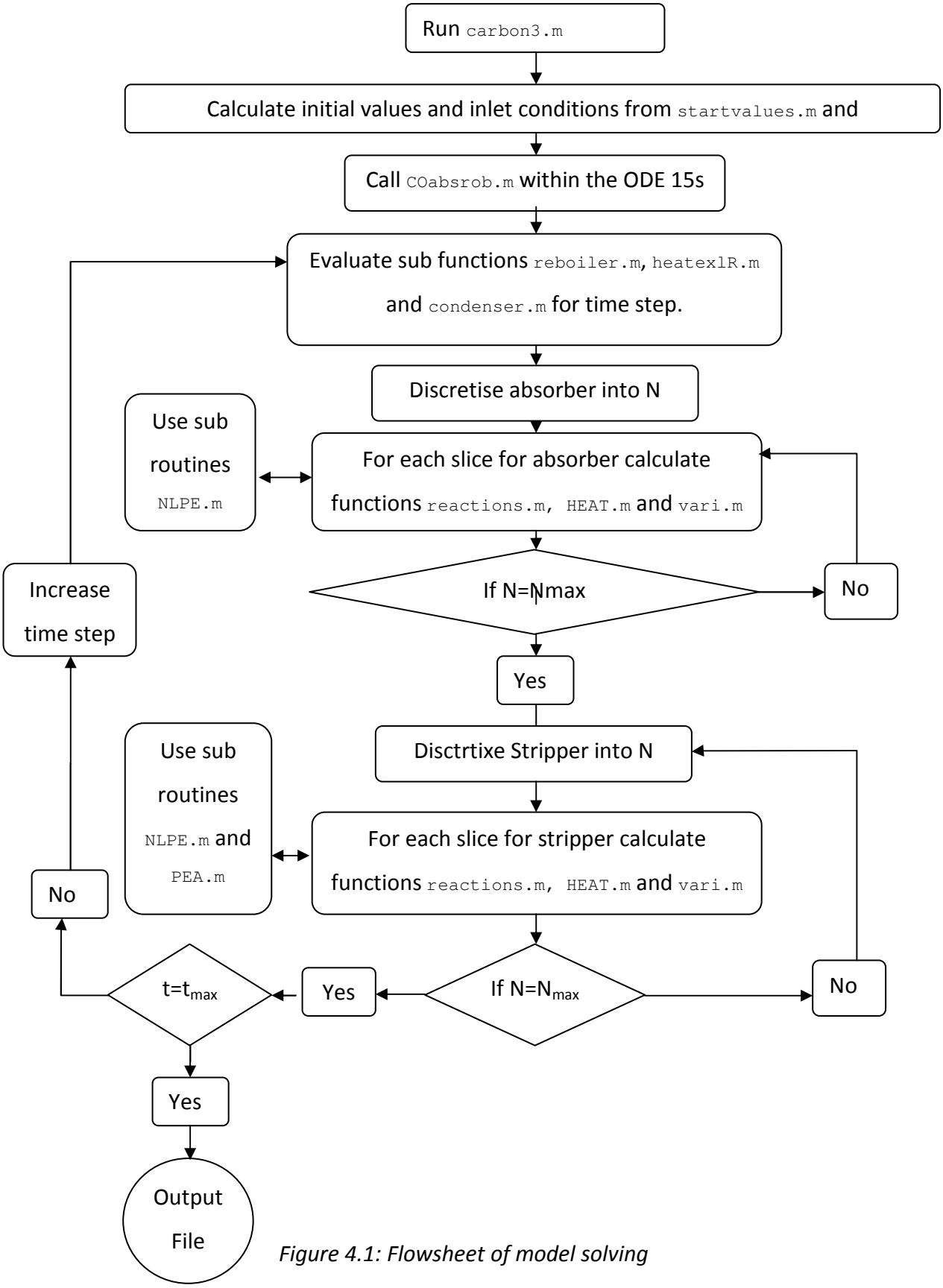

Figure 4.1: Flowsheet of model solving

4.2 Results

4.2.1 Graphical displays of Selected States

The simulation was run for 100000 seconds and 35 discretised control volumes for the inputs given in table 3.1 and 3.3 and 15 discretised zones. Graphical displays of the results for the absorber are shown in figures 4.2 to figures 4.8 and for the stripper in figures 4.9-4.13. The performance of the system is shown in table 4.1 as a function of the number of slices

Table 4.1: Process performance with varying number of discretised volumes

No of discretised volumes	CO_2 removal	Energy Consumption	Collected gas composition			Time of Simulation
			CO_2	MEA	H_2O	
	%	MJ/kg CO_2	%	%	%	S
5	78.7	4.02	37.6	0.16	62.2	76
10	83.1	4.01	36.6	0.17	63.4	360
15	84.9	4.79	29	0.22	70.75	862
20	86.2	5.96	22.5	0.27	77.2	1321
25	87.2	7.23	18	0.32	81.7	2377
35	88.5	9.35	13.3	0.38	86.3	5237

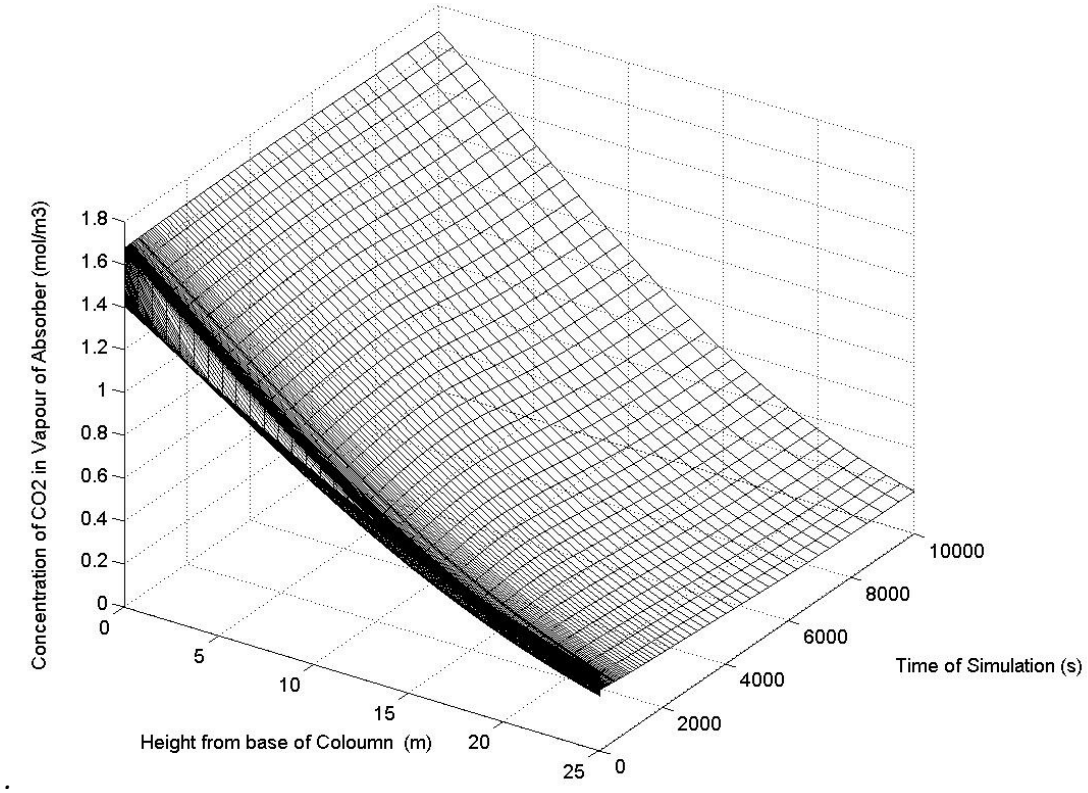

Figure 4.2: Concentration of CO2 in the vapour phase for the Absorber

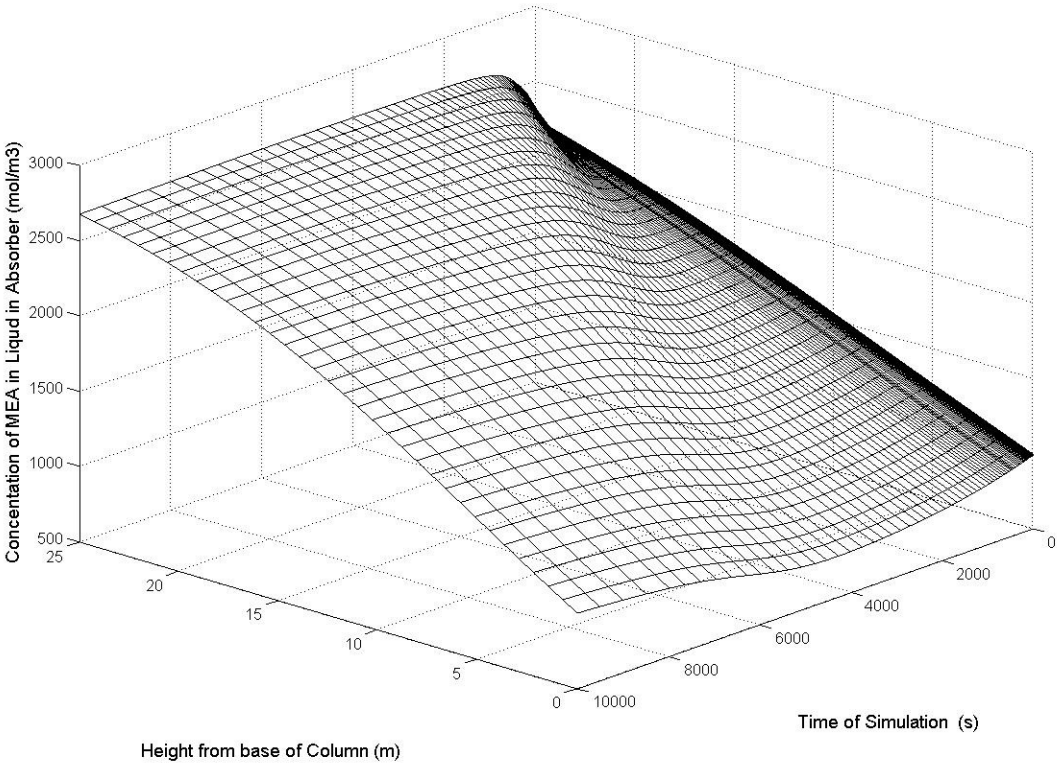

Figure 4.3: Concentration of MEA in liquid phase of Absorber

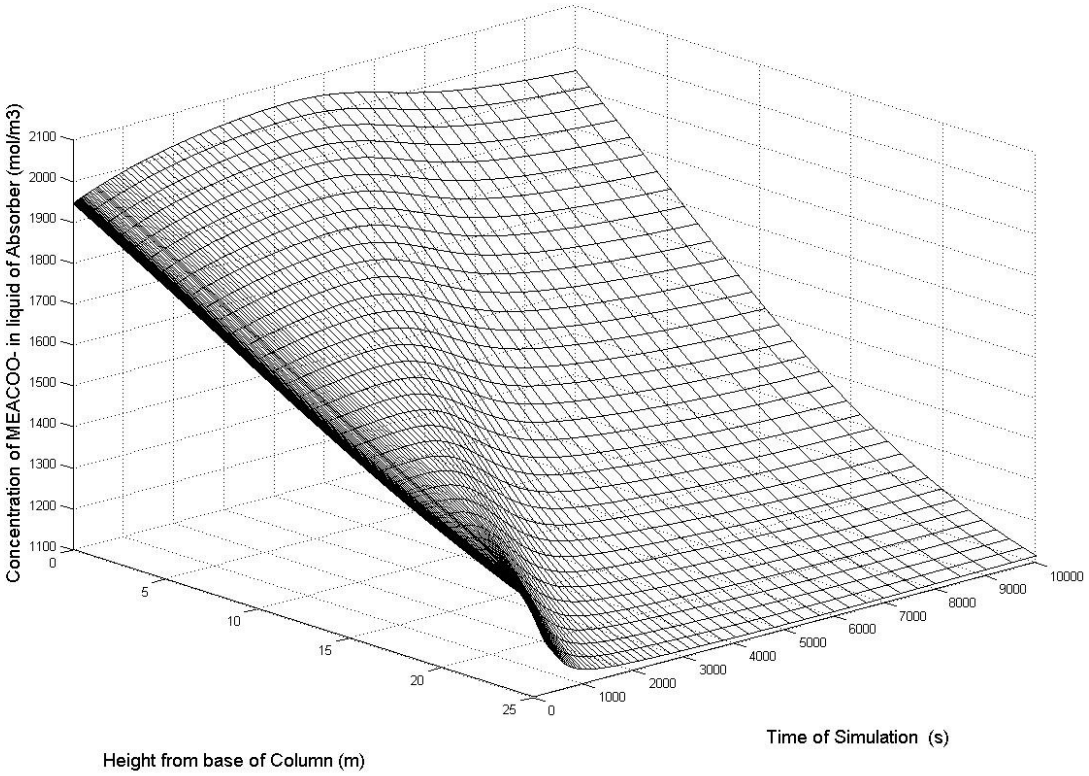

Figure 4.4: Concentration of MEACOO- in the liquid phase of the Absorber

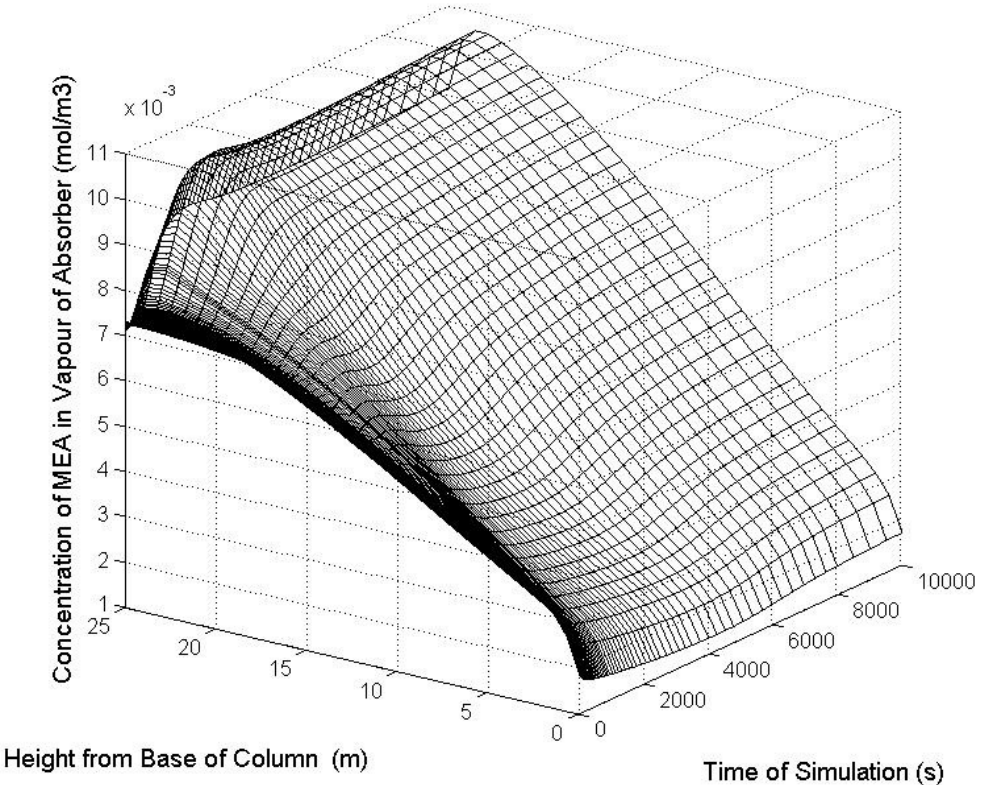

Figure 4.5: Concentration of MEA in the vapour phase of the absorber

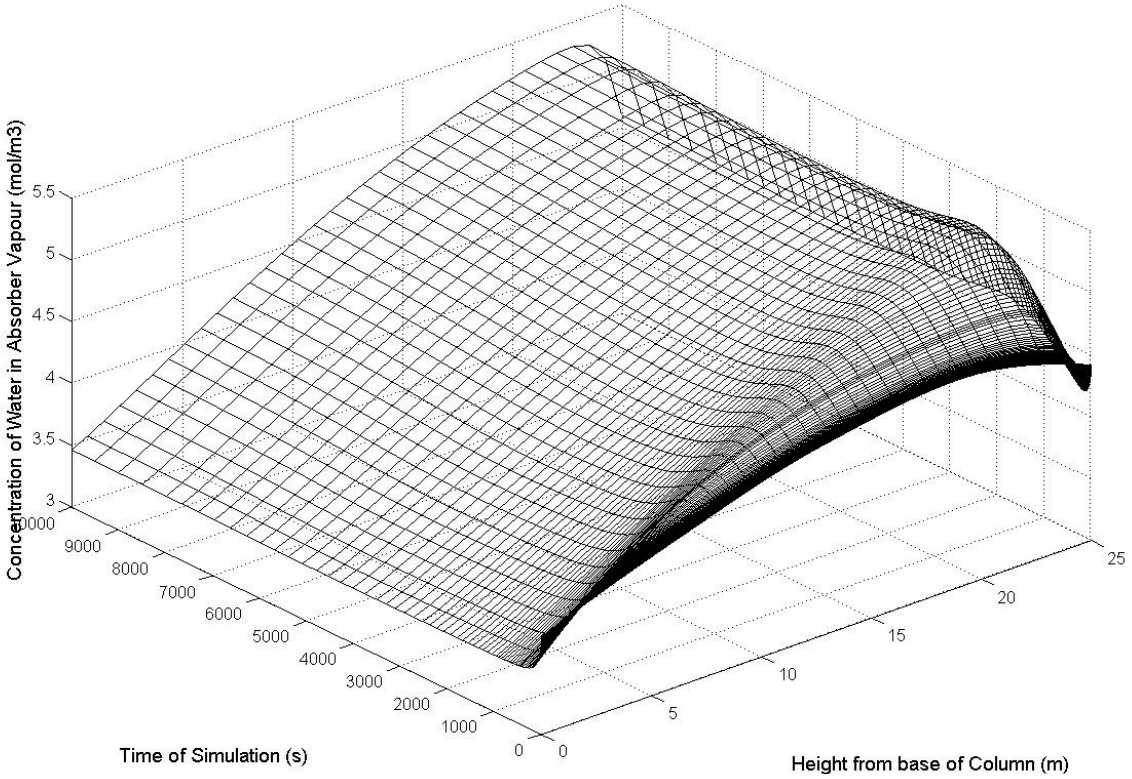

Figure 4.6: Concentration of H_2O in the vapour phase of the absorber

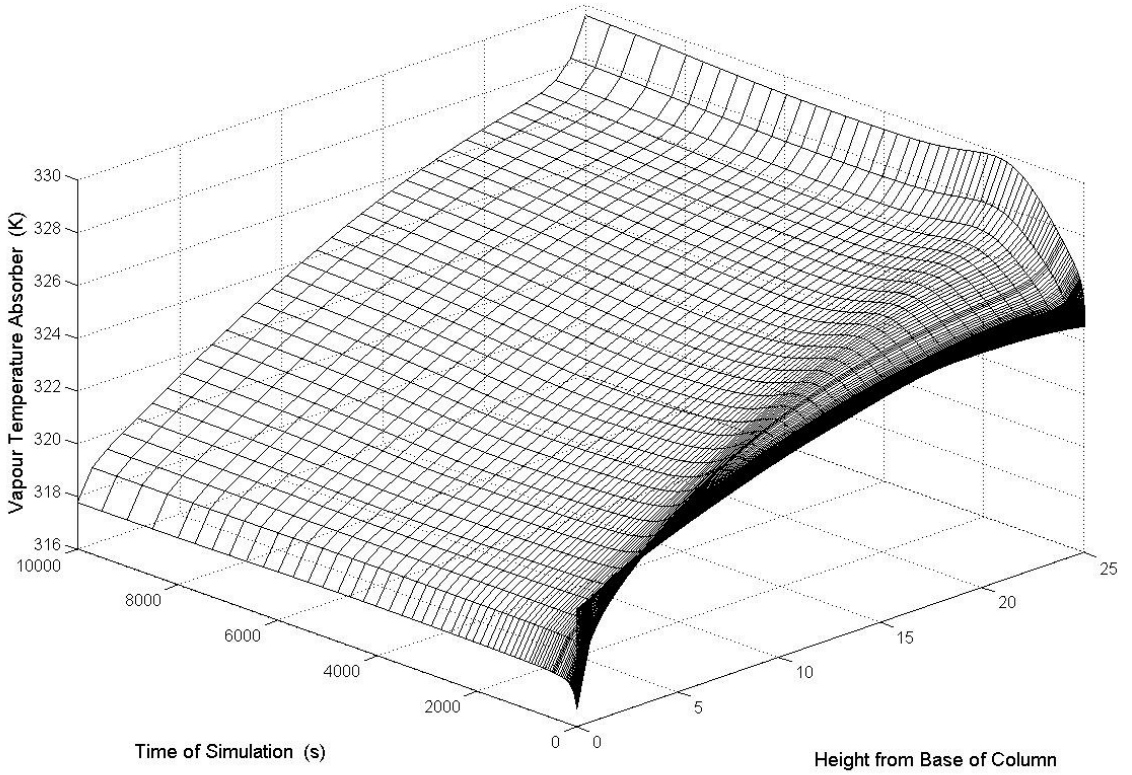

Figure 4.7: Temperature of the vapour phase in the absorber

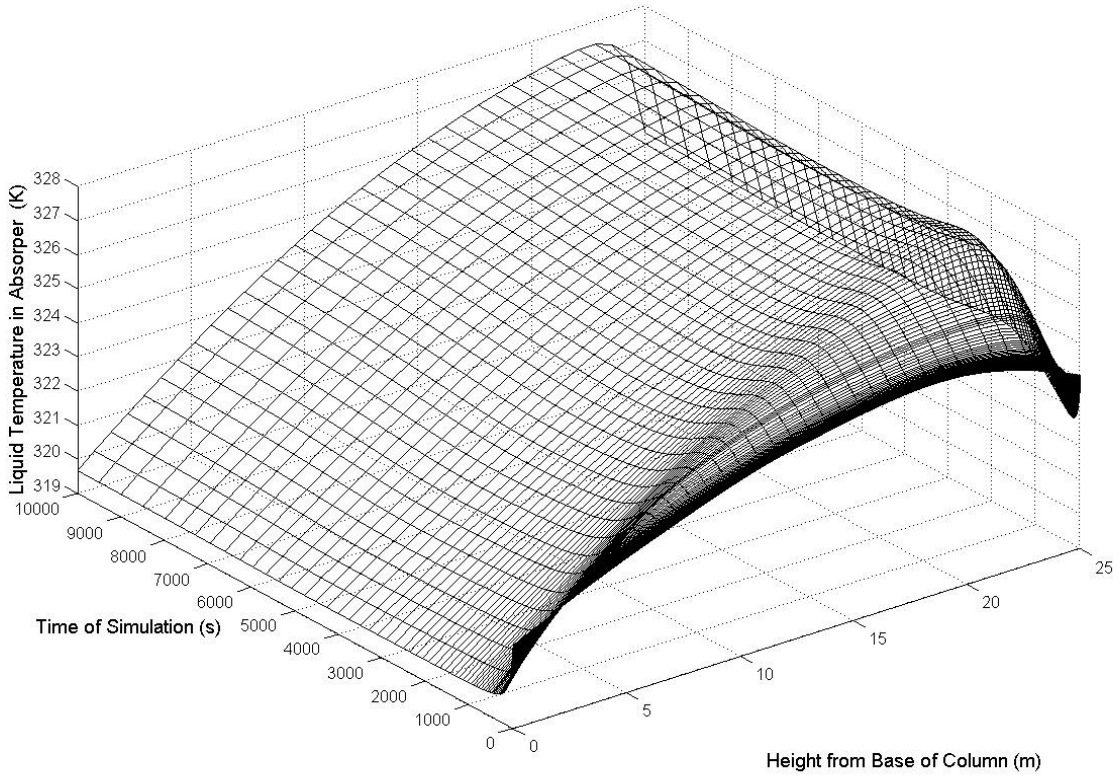

Figure 4.8: Temperature of the liquid in the absorber

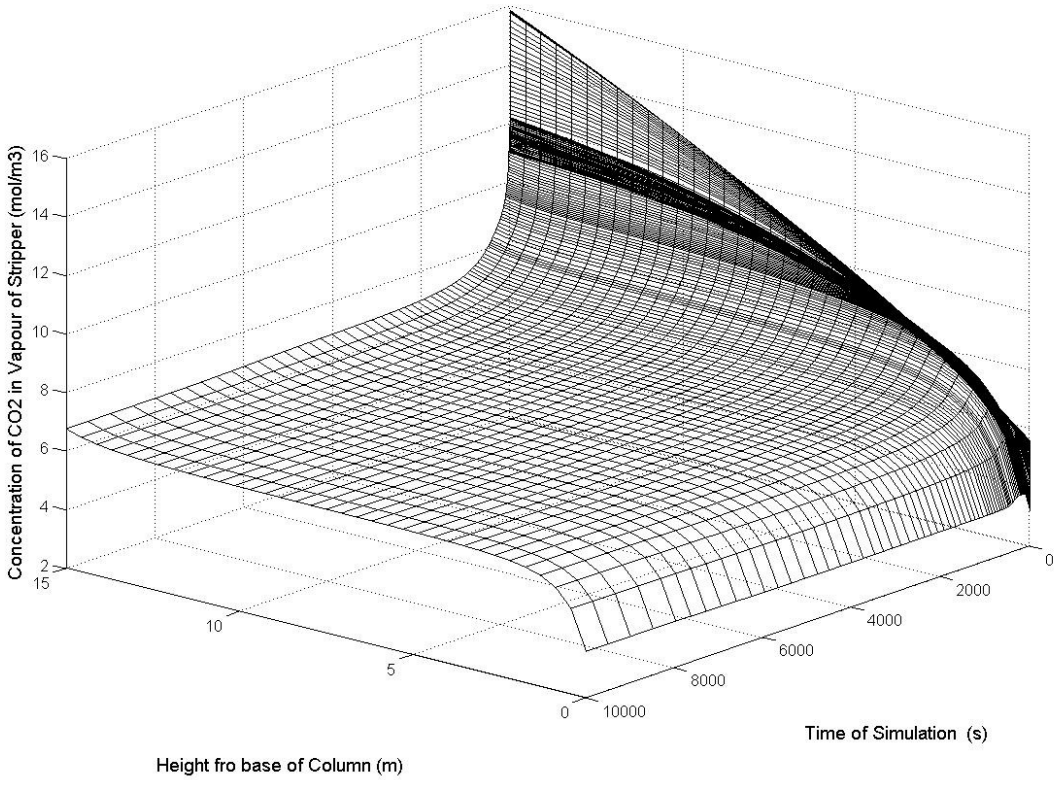

Figure 4.9: Concentration of CO2 in the vapour phase of the stripper

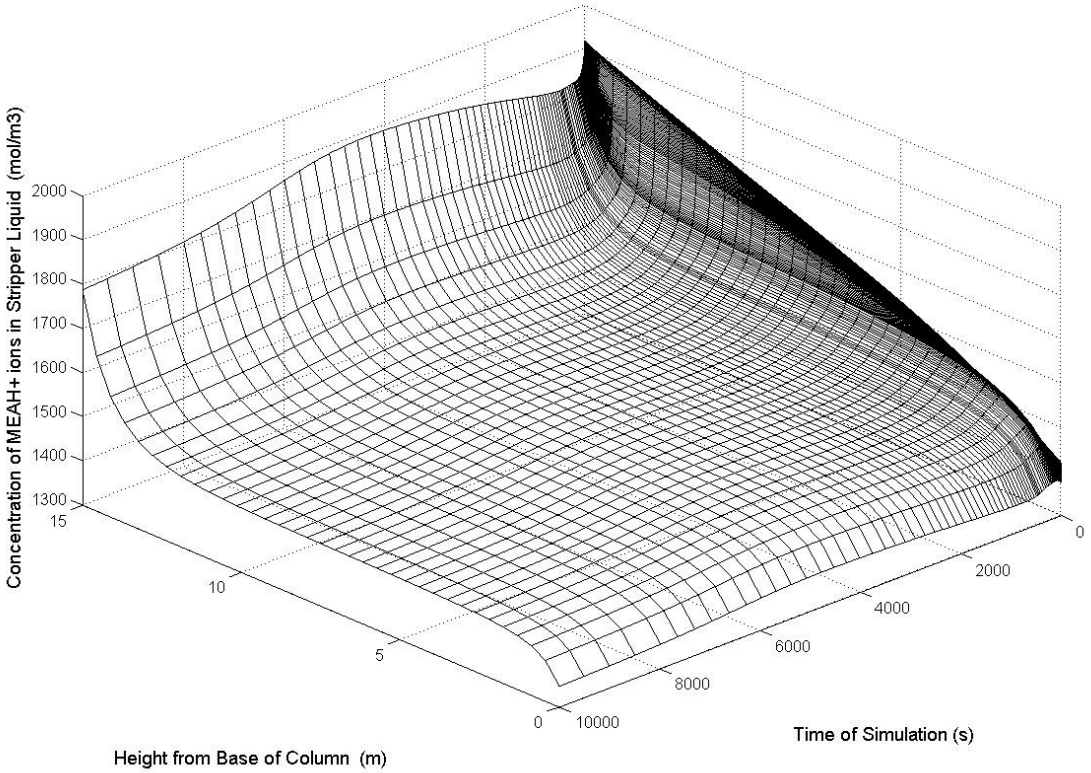

Figure 4.10: Concentration of the MEAH+ ions in the liquid phase of the stripper

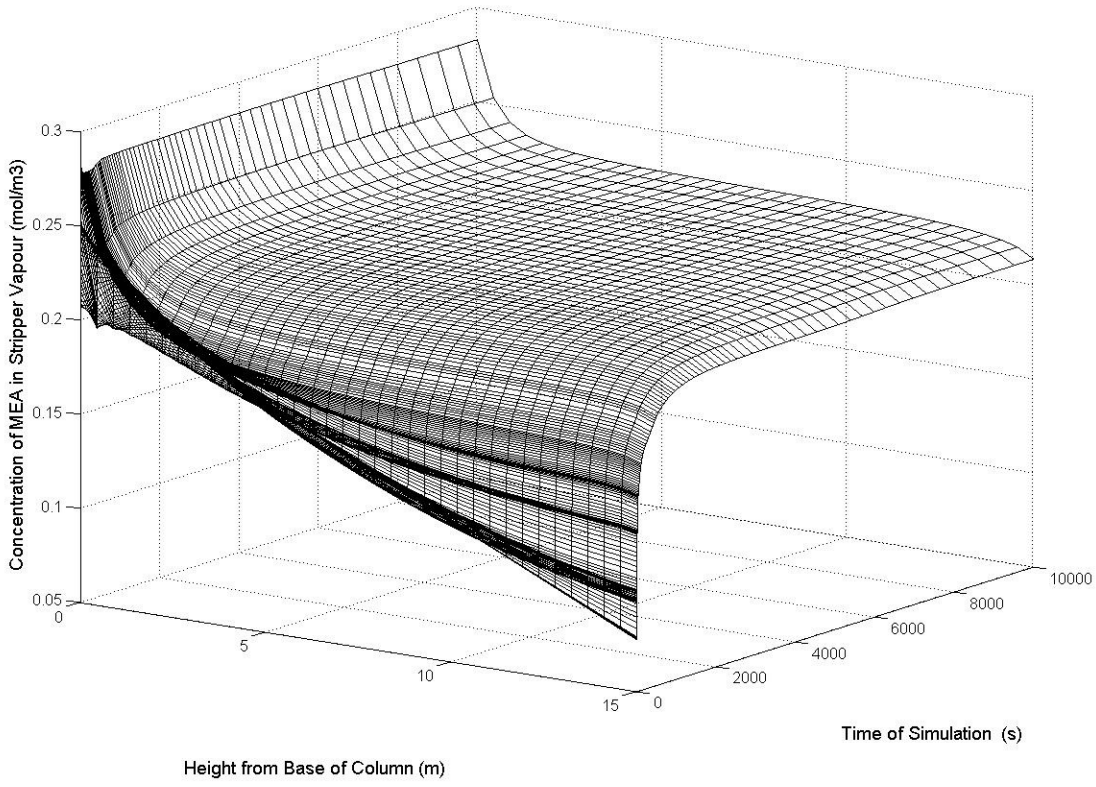

Figure 4.11: Concentration of MEA in the vapour phase of the Stripper

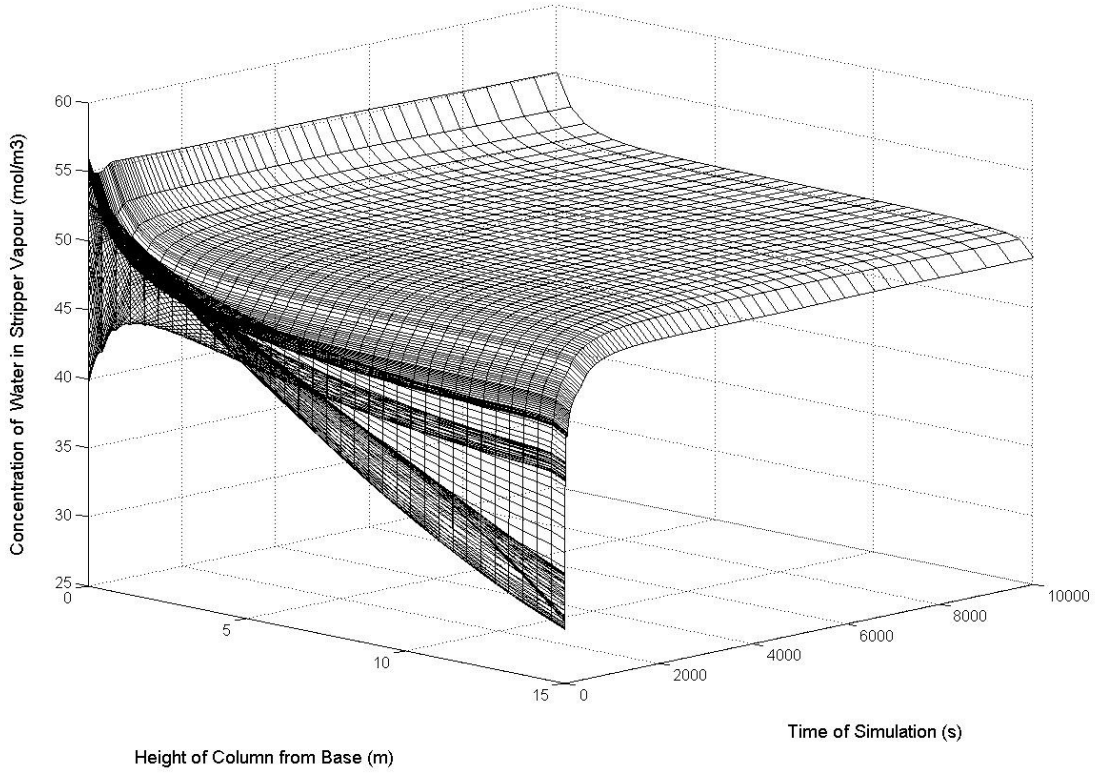

Figure 4.12: Concentration of H_2O in the vapour phase of the Stripper

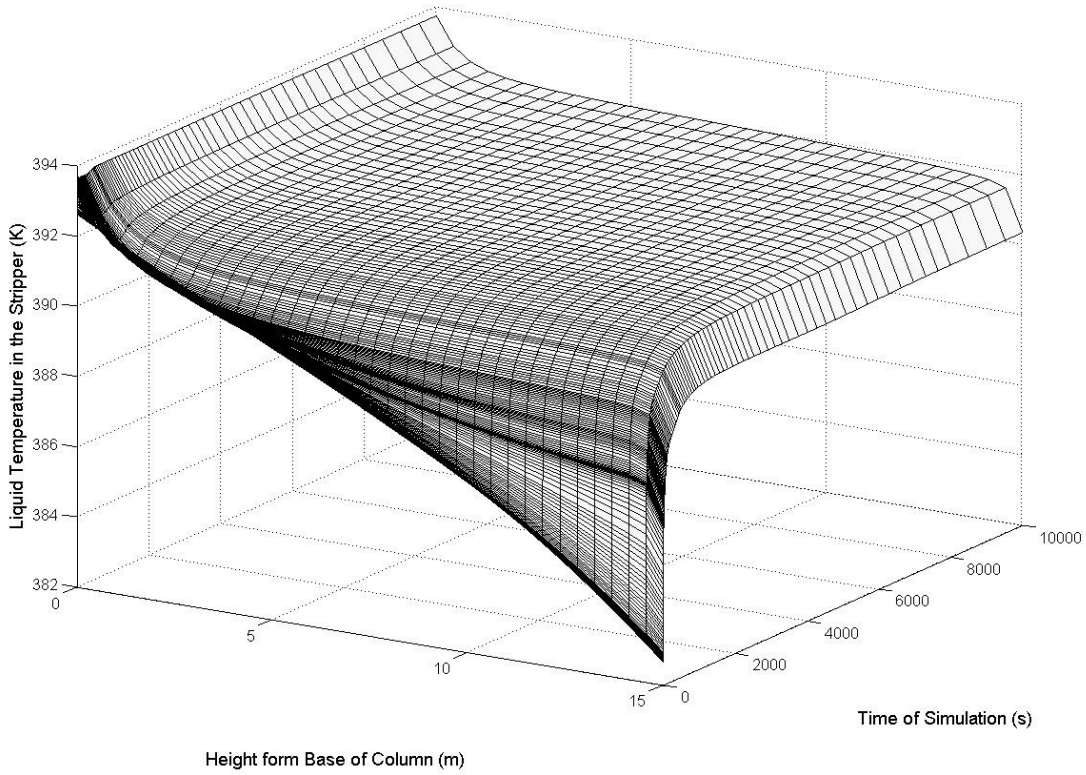

Figure 4.13: Liquid Temperature in the Stripper.

4.2.2 Perturbations

A serious or perturbations was taken from the base case where all values were held constant and then one parameter or input was changed. Table 4.2 shows the results of the perturbations. The data listed in the table is the percentage CO_2 removed; Energy consumed per kg of CO_2 removed the cleaned gas composition, the CO_2 loading in and CO_2 loading out. By looking at the table a quick overview of the cause and effect of changing the inputs can be seen. It is noted for computational speed reasons that only 5 discretised volumes were used.

Table 4.2: Perturbations in model parameters and inputs.

	Base case	Perturbation	CO_2 removal rate (%)	Energy consumed (MJ/kg CO_2)	Cleaned gas (%)			CO_2 Loading (mol CO_2/mol MEA)	
					CO_2	MEA	H_2O	Lean	Rich
Base case			***78.7***	***4.02***	***37.6***	***0.16***	***62.2***	***0.257***	***0.416***
Absorber height (m)	**25**	*30*	83.5	3.90	38.4	0.16	61.4	0.253	0.425
Absorber diameter (m)	**16**	*13*	72.3	4.25	35.9	0.17	63.8	0.252	0.40
Stripper height (m)	**15**	*10*	78.6	4.05	36.7	0.17	63.1	0.253	0.416
Stripper diameter (m)	**5**	*7*	78.4	3.82	40.1	0.15	59.4	0.255	0.418
Amine solution volume flow rate (m^3/s)	**0.8**	*0.6*	70.3	3.41	39.8	0.14	60.0	0.257	0.453
Heat exchanger ΔT (K)	**10**	*5*	78.4	3.92	34.8	0.18	64.9	0.255	0.415
Inlet gas temperature (absorber	**313**	*333*	77.4	4.03	37.3	0.16	62.5	0.254	0.415
Inlet liquid temperature (absorber) (K)	**318**	*333*	78.3	3.95	38.7	0.16	61.1	0.258	0.423
Condenser reflux rate (%)	**10**	*30*	78.9	4.05	43.2	0.15	56.6	0.251	0.413
Reboiler temperature	**394.2**	*394.5*	84.9	6.37	18.5	0.31	81.2	0.198	0.366
Pressure reboiler (Pa)	**20000**	*190000*	88.7	28.47	3.6	0.51	95.8	0.15	0.31
Temperature liquid exiting condenser (K)	**380**	*330*	78.7	4.02	37.6	0.16	62.2	0.253	0.416
Packing used	**Montz**	Pall	66.1	4.52	34.3	0.19	65	0.253	0.38

*Note the properties of plastic 50mm Pall ring packing are a=111 (m^2/m^3), ε=0.919, C_h=0.593, C_v=0.368 and C_l=1.239.

4.2.3 Discretised Volumes

The number of discretised volumes was increased from 5 to 35 slices and a plot of the removal percentage, energy consumed and time of simulation is given in figure 4.14. The simulations all used the base case parameters and inputs. When the number of discretised zones is 35 then each volume is 0.7m of packing.

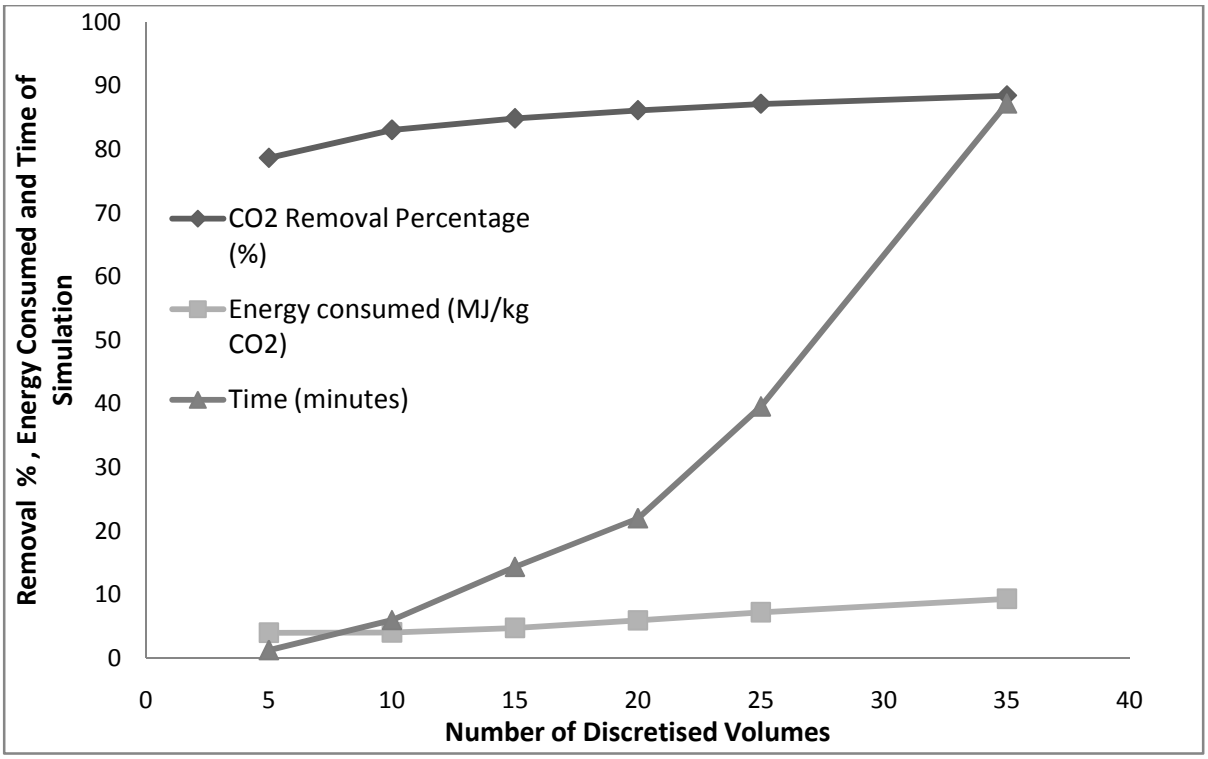

Figure 4.14: Effect on the number of slices in the performance of the simulation

5 Discussion and Conclusion

5.1 Chemical Reactions

5.1.1 Equilibrium Constants

The fundamental requirement of chemical absorption system model is to develop an accurate set of reactions which describe the chemical reactions taking place. From literature there were numerous values for the equilibrium constants (Liu et al 1990), (Cents et al 2000), (Hoff 2003) etc. In this work the author found it difficult to understand some of the equilibrium constants as not all agreed on the having the same numerical value. Some didn't allow for activity co-efficient and some did, while others had to be corrected for infinite dilution. The equilibrium constants from Liu et al (1999) where used in this work and the plots in figure 3.2a and 3.2b agree with other published figures. The equilibrium constants had to be multiplied by a factor of 1 million and the reason for this is unknown, it could be a computational problem in Matlab or an allowance for unit conversion that the paper publishers have not fully described.

5.1.2 Reaction Rates

The rate of reaction for CO_2 and MEA and for CO_2 and OH^- ion was important in this work as the reaction of CO_2 and MEA was the dominant reaction. A review of reaction rate constants for reaction 1 (k_{1f}) is well documented in Aboudheir et al (2003) with a variation in values at 298K of two fold. Most of the reaction rates from literature are developed from small scale lab work and most are derived from absorption experiments in the temperature range 280-313K. For this work an expression for the forward reaction rate is taken from Jamal et al (2006) as this was derived from both de-absorption and absorption experiments and covered the full temperature range. The forward reaction rate of CO_2 and MEA is one of the most important values within the model as it has a large influence on the rate of absorption and de-absorption as is used in calculating the enhancement factor. The reaction of CO_2 and OH^- was difficult to find a forward reaction rate that was adequate at elevated temperature as the values from literature were from absorption experiments. Because the CO_2-MEA reaction is the dominant reaction the effect of the reaction 3 was minimal so the system was not sensitive to the forward rate used. The other reaction rates are not that important as the reactions happen essentially instantaneous and it was found that the results were not sensitive to the selected values.

5.2 Vapour Liquid Equilibrium

5.2.1 Equation of State

The vapour liquid equilibrium between the species in the gas phase and the species in the liquid phase is the most difficult part of modelling the process. The method of residual thermodynamics was used in calculate the fugacities at the interface of the vapour and liquid. In researching the literature very few models where based on this method the noted exception being Solbraa (2002). Residual thermodynamics uses an equation of state to calculate both phase fugacities and the ratio of the two is the ratio of the mol fractions of the species in each phase. The majority of authors use the method of excess properties or sometimes called phi gamma approach where experimental data is used to fit interaction parameters. One of the more popular was the NRTL method from Augesten, Rochelle and Chen. The NRTL excess properties method allows for the interaction of all the ions in solution so is therefore more robust but is computationally demanding and also requires the fitting of 26 parameters (Liu et al 1999). The presence of ions in the solution and the modelling of polar substances such as water make the Peng Robinson equation of state inaccurate for some of the species. It was found that the binary interaction parameters greatly affected the accuracy of the model and also the binary interaction parameters are not as accurate when there are five species in the mixture. The Peng Robison equation of state still gave some reasonably accurate results based on the following reasons:

1. The ratio of CO_2 in the liquid phase to the vapour phase is modelled by henrys law which has a correction for ionic strength
2. The amount of MEA in the vapour phase is relatively small as volatility is low
3. The amount of Nitrogen and oxygen in the liquid phase is low and the accuracy of the liquid composition does not effect the model too much as long as the EOS is consistently used

The major weakness of the model is the choice of the equation of state. Sadus and Wei (2000) provide a detailed review of the various equations of states that can be used for electrolyte systems including the SAFT (Statistical associating Fluid Theory) and the SRK CPA which is a modified version of the SRK EOS with an ionic associating term which has been used by other authors (Solbraa 2002) to model systems with ions. The phi gamma approach is also an option

to use but it often has many parameters to fit and is a function of the quality of the experimental data used.

5.2.2 VLE Validation

The model is based on using henrys law to predict the ratio between the concentrations of CO_2 in each phase. The assumption that the majority of the resistance is in the liquid phase is very true for the physical absorption of CO_2 and is reasonably true for the chemical absorption. When the enhancement factor is allowed for the gas side resistance is between 2-15% of the total resistance. The equations below show typical values for the resistances.

$$\frac{1}{K_d^{overall}} = \frac{1}{\frac{H_{CO_2}}{Ekd_{CO_2}^l} + \frac{RT^vZ^v}{kd_{CO_2}^v}}$$

Typical values are H_i=2x10^4, E=100 $kd_{CO_2}^l$ =5x10^{-4} , T^v =400 Z^v =0.99 and $kd_{CO_2}^v$ =8x10^{-2}

Allowing for resistance in the gas phase

$$\frac{1}{K_d^{overall}} = \frac{1}{4x10^5 + 4.1x10^4}$$

$$K_d^{overall} = 4.41x10^5$$

Without resistance in the gas phase

$$K_d^{overall} = 4.0x10^5$$

Therefore the difference is up to 10% which can be considered substantial.

A typical method to validate the VLE model is a plot of the partial pressure of CO_2 versus CO_2 loading for a particular isotherm. The partial pressure of CO_2 varies from a few Pa at low loading up to many MPa at high loading therefore the accuracy of the experimental results used in fitting the VLE is important as a small error in the loading can lead to large errors in the partial a pressure. Liu et al (1999) notes that difference in experimental data between different authors was sometimes up to 40% so VLE model fitted to one set of data might not fit another. In this model the henrys law was used along with a correction for the ionic strength of the solution. By using this method the fit of the VLE could not be adjusted as the henrys constant and ionic correction are given. From the plots of the CO_2 verse loading it can be seen from

figure 3.5b that the model fits the data of lee et al (1976) reasonably accurately but the fit of the experimental data from Mather et al (1975 and 1976) is not as accurate in the other three figures (3.4a,3.4b and 3.5a). This is to be expected from using an empirical formula fitted to one set of data for henrys constant and compared to another set of experimental data. It was possible to not use henrys law and to use the fugacity ratio between the CO_2 in the liquid and vapour phases to fit to the curves. The binary interaction parameters could be adjusted to fit the experimental data. This was not used in this model as the Henrys constant gave a better fit and the Peng Robison EOS did not account for the short range interactions of the ions in solution so the results would have been inaccurate at best. The validation of the model to the partial pressure of MEA and H_20 in the vapour phase and the concentration of N_2 and O_2 in the liquid would also improve the accuracy of the model but was not done in this work. It is possible to model the diffusion of O_2 and N_2 into the liquid phase with henrys law but knowledge of henrys law of N_2 and O_2 in MEA is required which was not found in any papers. Strictly speaking there are reactions between MEA and O_2 leading to the degradation of amine and these also have not been accounted for either.

5.3 Fluid Properties

The properties of the fluids took a considerable amount of time to research and check against published data. The mol weights of the species and the density of the fluid where easily found.

5.3.1 Heat Capacity

The heat capacity in the vapour phase was taken from Reid et al (1987) based on ideal gas heat capacity. A polynomial function as a function of temperature was used to calculate the values. At constant pressure the assumption of the ideal gas in the vapour phase is adequate. For a more thermodynamic rigours approach the heat capacity could be calculated for a real case by a method such as the EOS. This was not done as it was deemed to add undue complexity to the model and the ideal gas assumption was adequate for the low pressure.

The heat capacity of the liquid had some larger assumptions. The H_2O was taken from the NIST web book and was considered accurate and the MEA heat capacity was from correlated data from Jolicouer et al (1993) but was only fitted in the range 25-40 °C so could be incorrect at elevated temperatures. The assumption that the OH^- ions and H_3O^+ ions had the same heat capacity as the water was reasonably acute because the mol weights are similar. The

assumption that the ions of $MEAH^+$ and $MEACOO^-$ had the same heat capacity as the MEA was not entirely correct but for the purposes of this study was considered adequate. A more robust heat capacity derived from an EOS would be the next step in the development of the model but the actual effect on the accuracy of the overall system is expected to be low as the majority of the energy required is in reversing the chemical and heating the water and MEA in the system which the heat capacities are well known for. The typical composition of the solution is 90% water,5% MEA and 5% ions (mol %) so it is not expected increased accuracy on the 5% ions will have a great effect.

5.3.2 Viscosity

The viscosity of the water is well known and correlated but the viscosity of MEA as a function of temperature was more difficult to evaluate. An expression from the previous masters students work (Hansen 2004) was used in this work as searching through literature found no other viable alternatives. The overall liquid mixture viscosity was a function of the two viscosities of water and MEA and also the CO_2 loading. The formula did not include allowance for the interactions of the ions in solutions but the results shown in table 3.5 where is the acceptable range.

The vapour viscosities were taken from Perry and Green (1999) and were fitted as a function of temperature. It is expected these values are accurate and the overall vapour viscosity is dominated by Nitrogen which makes errors in the other species not as significant.

5.3.3 Diffusivity

The diffusivity of CO_2 in the amine solution is difficult to measure experimentally as the MEA reacts with the CO_2. The N_2O analogy is typically used in calculating the diffusivity of CO_2 as N_2O has the same shape as the CO_2 molecule and does not react or be consumed in the experiment (Al-ghawas et al 1989). The diffusivity of N_2O is measured in the water and amine mixture and is correlated with the diffusivity of CO_2 in H_2O and the viscosity of the mixture. Because the diffusivity is difficult to measure in the amine solution the results from experimental results are varied. The values used in this model are in the range of other values in literature but there are still some errors. The CO_2 diffusivity in the liquid is important in the model as is apart of the enhancement factor which has a large bearing on the results. Because the system is chemical absorption with MEA reacting in the film boundary layer the diffusivity of the reproduced ions should be could be included in the model as was done by Hoff (2003) this adds another complexity to the model and was deemed beyond the scope of this project.

The vapours diffusivities for all five species in the vapour phase are taken from Reid et al(1987) and are derived from first principles and not from experimental data. They are modeled as a species diffusing in Air so there will be errors in the stripper vapour viscosities and for model completeness a more accurate diffusivity could be applied.

5.3.4 Thermal Conductivity

The thermal conductivity in the vapour phase is required to calculate the heat transfer coefficient for sensible heat transfer. The values for fitting the formula are taken from Dewitt and Incropera (2002) and are assumed accurate but the value for water was from extrapolated data. There maybe errors in using the extrapolated data but results were considered sufficient for this model.

5.4 Mass Transfer

The mass transfer coefficients where taken from Billet (1995) are from correlated experimental data. The formula is based on Higbie's penetration theory which is of the form:

$$k_d \approx \sqrt{\frac{D}{\pi t}}$$

Where the mass transfer co-efficient is proportional to the square root of diffusion coefficient of the species and the inverse square root of the time (t) it takes for a particle to move from the bulk liquid to the VLE interface. The actual formula is an empirical formula that has been derived from thousands of experiments over the years (Billet 1995). The formula for K_d fits many types of packing both structured and random and of various materials. Because the formula can be used for a large number of packing's the accuracy for a specific packing is typically within 8-10% (Billet 1995). For a more accurate model the empirical equation of the mass transfer co-efficients should be tuned to the type of packing.

The actual surface area of the wetted packing can be between 10-80% of the actual area depending on the liquid distribution system in the column (Billet 1995). An empirical formula was used to predict the ratio but this is difficult to measure and fit experimentally. Some modeling has been done by Aroonwilas et al (2003) and shows that the packing is typically least wet at the top of the column and is affected by the gas velocity. The formula was used in this

model as the wetted surface area had to be allowed for but the accuracy of the formula is unknown.

The largest effect on the system is the enhancement factor of the mass transfer co-efficient by the chemical reactions that occur in the film boundary layer. For modelling purposes the discretised volume of the liquid is considered a well mixed CSTR with concentrations equal though out the volume. In reality the reactions happen in the boundary layer of the film and not throughout the bulk liquid (for MEA-CO_2 anyway). The mass transfer coefficient assumes a particle enters the liquid from the vapour and diffuse through the boundary layer unreacted before entering the bulk fluid. The enhancement factor accounts for the reaction taking place in the boundary layer removing the species and maintaining a high driving force. The Hatta number is used by numerous authors in allowing for the chemical reactions (Hoff 2003), Solbraa (2002) Xiao (2000) etc and is considered the best method to avoid modelling the actual species in the boundary layer. This has been done by some authors (Jamal 2006) but is computationally demanding and is usually based on Ficks law which has the concentration gradient proportional to the diffusivity. In practise concentration gradient is proportional to the square root of the diffusivity as shown in Higbe's penetration method. The use of the enhancement factor seems adequate for this model to simplify the computational time but a more robust method maybe to use the Stefan Maxwell equations to model the boundary layer penetration. There is also the problem of the definition of direction where most theory is based on flow of gas up the tower and gas diffusion into the liquid which is often modelled as a flat plate. The liquid layer in a packed column filled with random packing is not a flat surface therefore detailed modelling of the diffusion in the packing can quickly become quite complex.

5.5 De-Absorption

5.5.1 Reboiler

The model of the reboiler includes a flash calculation of the liquid from the stripper into the reboiler at the reboiler temperature and pressure. It was found that the calculation is very closely related to the reboiler temperature and pressure and has problems converging. If the pressure is too high for the temperature then only very little of the feed flow rate flashes and the flash calculation has problems converging. Increasing the temperature to a value that allows flashing allows the calculation to take place. The amount of feed flow that is flashed is

strongly related to the temperature in the reboiler for example at 2 bar, 394.2K has a flashed vapour of 5% of the total mol flow while at 394.5 K this increases to 25%. The composition of the liquid feed also effects what percentage of the flow is flashed therefore as the simulation progresses at constant temperature and pressure, the vapour-liquid composition still varies. The solving of the flash calculation is closely related to the initial conditions chosen in the model so carful selection is required for convergence. A high vapour load in the stripper increases the amount of water vapour in the stripper and the energy requirements of the process. A vapour flow of 4-5% of the total feed mol flow seemed to give adequate results. The way in which the model is solved is for an initial guess for the liquid volume flow rate in the stripper for the reboiler calculation and then iterating on the liquid volume flow rate because the actual volume flow rate is calculated from the condenser sub function. This ended up being an inefficient method to solve the model as it required iterating the sub functions for the reboiler, heat exchanger and condenser. A more efficient method would be to use a DAE solution but the author did not have enough time to implement. The Volume flow rate from the stripper back to the absorber (S9) is calculated from the EOS and the compressibility factor Z. The Peng Robinson EOS is not as accurate for calculating the liquid compressibility factor but is used to make the model consistent.

5.5.2 Condenser

The model of the condenser is relatively simple with mol balances of the various streams being used to calculate the concentrations. The EOS is used to calculate the volume flow rate of the liquid at the elevated temperature which like the reboiler is consistent but maybe not entirely accurate as the Peng Robinson EOS is known to not calculate the liquid compressibility accurately. The temperature of the fluid returning from the condenser to the stripper is estimated but could be too high. Too make the model more accurate a flash calculation and heat exchanger model should be included. This was not implemented in this work as was considered not to have a large effect on the result.

5.5.3 Heat Exchanger

The model of the heat exchanger was simplified by taking the system as a CSTR. This was sufficient for this model but for a more rigorous model the heat exchanger should be modeled as a PDE so that it can be modeled in time and space. The inlet temperatures from the Absorber (Stream S3) and from the stripper (Stream S9) are known but the outlet temperatures

are unknown. The simple method of assuming a minimum ΔT of 10K between the streams S12 and S3 and then computing the unknown was applied in this model. The pump power required for the lean and rich amine liquids was calculated with a simple formula with an assumed pump head. The efficiency of the pump was corrected for by increasing the pump head. A PDE model of the heat exchanger would allow the outlet temperature of the two fluids to be calculated more accurately. The mass of steel within the heat exchanger should be allowed for as this will affect the temperature dynamics of the heat exchanger. It is also possible to solve the heat exchanger model as a DAE equation so that the two unknown temperature can be calculated analytically. The reader is referred to Lie (1995) for further reading.

5.6 Graphical Results

The graphical results are for a simulation with 35 discretised volumes so the accuracy is increased. The optimization of the equipment was not done in this project therefore the inputs and plant equipment sizes do not show the optimal solution. The removal percentage is higher than required and the energy consumption is double than literature values. The reboiler temperature should be reduced to lower energy consumption but this produces a lower stripping gas flow rate so the stripper diameter should also be reduced. The dynamic nature of the simulation results in a difficult optimization process as the performance of the plant changes over time. If for example the reboiler temperature is decreased then there will be less stripping steam which in turn reduces the amount of regeneration in the stripper effecting the feed composition back to the reboiler. The reboiler flash calculation is highly sensitive to pressure, temperature and composition so the process may move quite far from the desired out come.

The plot of the CO_2 concentration in the absorber (figure 4.2) shows clearly that the CO_2 is depleted from when it enters at the bottom of the absorption column until it leaves at the top. The removal percentage is estimated at 88% which is in the range expected from literature. The removal rate is greatest at the bottom of the tower decreasing as the concentration in the gas tends to zero. The height of the tower has a large effect on the removal rate as the higher the tower the greater the retention time of the liquid and the gas phases.

Figure 4.3 is a plot of the concentration of the free MEA in the liquid phase of the absorber. The plot shows a smooth curve as the MEA is consumed as it moves down the tower from the

inlet at the top. The inlet concentration is less than the 5000 mol/m^3 original solution concentration because not all the MEA is regenerated in the stripper. The outlet concentration of 1000 mol/m^3 indicates that only about $^1/_3$ of the MEA is consumed in the absorber. Decreasing the volume flow rate of the amine solution would increase this value but at the sacrifice of lowering the removal percentage form the absorption tower.

The concentration on the $MEACOO^-$ ion in the absorber liquid is shown in figure 4.4. The plot shows the opposite trend to that of the MEA as the $MEACOO^-$ is produced as the liquid travels down the column absorbing CO_2. The $MEAH^+$ ion concentration is the same shape and value as the $MEACOO^-$ ion and the level of increase is about ½ the consumption rate of the MEA because in the operating range of the tower, 2 moles of MEA is required to remove on mol of CO_2.

A certain amount of the MEA in the liquid phase in the absorber evaporates to the vapour phase as shown by figure 4.5. The shape of the graph is related to the liquid temperature as the higher the temperature, the more MEA transfers to the vapour phase. The fugacity at the interface is calculated with the liquid temperature as it is assumed the resistance to heat transfer is in the vapour phase. The concentration of the free MEA in the liquid is also a factor as the higher the concentration in the liquid phase then the higher the concentration in the vapour phase. The concentration may seem small at $1x10^{-2}$ mol/m^3, but at a gas volume flow rate of 420 m^3/s this is a mol flow of 4.2 mol/s or 900 kg/hr of MEA leaving the system therefore it is imperative a water wash is installed on the outlet gas to collect this “lost” MEA.

The concentration of the H_2O in the vapour follows the same profile as the liquid temperature and is shown in figure 4.6. At the bottom of the tower the inlet concentration is 3.6 mol/m^3 and then increases to a peak of nearly 5.5 mol/m^3, when the liquid temperature is at a maximum. The water then condenses back into the liquid phase at the top of the tower as the liquid temperature decreases. The shape of the graph following the liquid temperature is due to the vapor liquid interface temperature being taken as the water temperature.

Figure 4.7 is the vapour phase temperature profile which follows almost the same profile as the liquid temperature plot. At the bottom of the tower the gases receives heat from the liquid phase up until the maximum liquid temperature and then at the top of the tower the gas transfer heat to the liquid phase. The condensing water vapour also increases the gas

temperature due to the release of heat from the latent heat of vapourization. The choice of the heat transfer co-efficient for the sensible heat transfer has a major bearing on the result. In the model an h_v of about 120 $\left(\frac{J}{m^3 K\ s}\right)$ was used but increasing this result in the liquid and vapour phases having more the same temperature profiles. The choice of the heat transfer co-efficient requires more investigation.

Figure 4.8 is a plot of the temperature profile of the liquid temperature. It is characterized by an increase to a maximum value about a $^1/_5$ of the way down the tower and then a decrease. The increase is due to the heat supplied from the exothermic reaction between the MEA and the CO_2. The decrease in the bottom two thirds of the tower is due to the heat transfer to the vapour phase. When the liquid volume flow rate is decreased the maximum temperature moves to the top of the tower and an increase moves the maximum temperature down the tower.

The concentration in the cleaned gas in the stripper is shown in figure 4.9. The concentration increases quickly as the reaction spruced quickly at the bottom of the tower where the steam enters the tower supplying energy. The de-absorption process is controlled by the equilibrium constants which dictate how much aqueous CO_2 is released from the bound sources. Because the stripper reaches equilibrium so quickly (first 2-3m of tower) then this indicates the steam flow is too large and should be reduced. This also explains why increasing the height of the stripper doesn't have a large effect on the process.

The reversibility of the chemical reactions is indicated in figure 4.10 where the $MEAH^+$ ion is shown decreasing in concentration as the liquid enters the stripper. The oversupply of stipping steam results in the regeneration of the MEA taking place in the top 5 meter section of the tower. Entering at a concentration equal to the outlet value of the absorber, the $MEAH^+$ concentration is reduced to about 1200 mol/m^3. The concentration of the $MEACOO^-$ ion has the same profile.

Another point for the loss of MEA from the system is the flow leaving with the cleaned gas in the vapour phase. Figure 4.11 indicates this concentration to be quite significant due to the high temperature in the stripper vaporizing the MEA. Condensing of the cleaned gas stream to

remove the MEA and H_2O is important post processing parts of the plant to recover the MEA and to up concentrate the CO_2 to greater than 95% for compression.

Figure 4.12 is a plot of the water vapour concentration which is the stripping gas used in the de-absorption tower. The concentration decreases as it enters the bottom as some of the water vapour is condensed to provide energy to heat up the liquid and reverse the reactions. The concentration of the H_2O in the vapour phase is connected with the concentration of CO_2 as when the water vapour decreases the CO_2 increases. The water vapour is relatively constant over the length of the stripping column indicting that too much steam is being supplied.

The liquid temperature in the stripper is shown in figure 4.13. the shape is characterized by three zones. At the top of the tower the incoming liquid is quickly increased to the temperature of the gas within stripper. In the second zone the temperature is at at value equal to the gas temperature and is relatively constant only reducing slightly as the regeneration reactions require energy. At the bottom of the tower the decrease in H_2O vapour releases heat from the latent heat of vapourization and the liquid flow encounter the vapour exciting the reboiler which is at 394.2K. the constant liquid temperature is more evidence that the steam stripping flow is too large and the reboiler temperature is too high.

5.7 Perturbation

It is interesting to analysis the values in table 4.2 as they show the values for the CO_2 removal rate, Energy consume per kg CO_2, cleaned gas composition and CO_2 loading for different parameters and inputs. The perturbations were done with 5 slices in the towers so the results are not as accurate as with more slices but allow a quick overview of the controlling influences. The base case is the parameters and inputs used in modeling of the graphical results of section 5.6

Absorber height: Increasing the absorber height from 25 to 30 meters increases the removal percentage from 78.7 to 83.4%, the energy required per kg removed is decreased by 2.5% and the cleaned gas has a greater proportion of CO_2. The disadvantage of the higher tower is the increased capital cost.

Absorber diameter: Decreasing the absorber diameter from 16 m to 13m reduces the cross sectional area of the tower form 196m^2 to 136m^2, increasing the vapour and liquid velocities

and reducing the fluid retention time in the tower. The result is a drop in the removal efficiency of 6% and an increase in the energy used per kg recovered of 6%. The advantage is that the capital cost of the tower is cheaper.

Stripper height: Decreasing the stripper height from 15 to 10m drops the removal rate slightly and increases the cost per kg also. The reactions and mass transfer happen quickly at the elevated temperature in the stripper, therefore the controlling factor in the stripper is the equilibrium constants which dictate how much aqueous CO_2 is released from the bound CO_2 in the HCO_3^- and $MEACOO^-$ ions.

Stripper diameter: Increasing the stripper diameter from 5.0 to 7m increases the cross sectional area of the stripping column from 20.5m^2 to 37m^2, effectively halving the fluid velocities. The longer retention time removes a larger amount of the CO_2 increasing the cleaned gas proportion and decreasing the energy requirements by 5%. This is at the expense of increased capital cost.

Amine solution liquid volume flow rate: Decreasing the liquid volume flow rate from 0.8 m^3/s to 0.6 m^3/s decreases the removal efficiency from 78.7 to 70.3% , also reducing the energy consumption to 3.4 MJ/kg CO_2. The loading of the rich solution exiting the absorber increases to 0.45 as a smaller liquid volume flow rate increase the liquid retention time allowing more of the MEA to be consumed in the reactions. The energy requirement is less as the energy rate is proportional to the reboiler flow rate of steam which is a percentage of the liquid flow rate. The increase in energy efficiency comes at the sacrifice of CO_2 removal percentage.

Heat exchanger ΔT: Decreasing the heat exchanger Δt form 10 K to 5K requires increasing the overall heat transfer co-efficient of the heat exchanger (essentially the surface area of the heat exchanger) from $1.5x10^8$ to $3x10^8$ (W/K). This is a greater capital cost and the result is a higher temperature into the stripper of the rich mixture. This decreases the energy requirement of the process to 3.92 MJ/kg CO_2 by applieng more heat intergration.

Inlet gas temperature to Absorber: Increasing the inlet gas temperature from the combustion process from 313K to 333K increases the volume flow rate of the gas by approximately 6.5% which reduces the retention time of the gas in the absorption tower. The removal percentage decreases and the energy requirements increase as less CO_2 is removed. The smaller the inlet

gas temperature also allows the inlet fan to be sized for a smaller volume flow rate but the gas should not be cooled too much as the reactions in the absorption tower are faster at a higher temperature so rejected heat before the absorber is lost energy.

Inlet liquid temperature to absorber: Increasing the lean mixture temperature from 318K to 333K increases the removal percentage slightly as the reactions take place faster in the absorber increasing the rich loading value. The higher rich loading value also translates into a decrease in the energy consumption.

Condenser reflux rate: The reflux of the condenser is the percentage of the cleaned gas MEA and water mol flow which is returned to the stripper. The greater the percentage returned the higher the proportion of CO_2 in the cleaned gas. The energy consumption is slightly increased as the stripping steam must heat more of the liquid in the stripper. An increase from 10% to 30% reflux changes the energy consumption by 0.75%.

Reboiler Temperature: Increasing the reboiler temperature increases the amount of vapour that is flashed in the reboiler. A higher vapour load decreases the lean loading as more of the MEA is regenerated. This translated into an increased CO2 removal percentage and a higher energy cost . It is noted that increasing the temperature by only 0.3K increased the removal rate by 2.5% and the energy consumed by 12%. The oulet from the condenser alsocontains a larger proportion of water vapour.

Pressure reboiler: Operating the reboiler at a lower pressure of 1.9 bar increases the amout of liquid that is vapouised as the flash calculation. At 1.9 bar the vapour flow is 40% of the total feed compared to 5% at the base case 2 bar. This increased vapour load decreases the loading in the stripper to 0.15 which increases the perforemance in the stripper as more MEA is available. The cost of the etra removal is high as the energy consumption per kg of CO_2 sky rockets to 28.5 MJ/kg. This can be seen in the gas compostion out of the condenser wher the majpoity is water vapour.

Liquid returning from condenser temperature: The liquid from the condenser is set at 380K in the model but in reality this maybe too as high as other references have this value down to 330K (Kohl 1995). Decreasing the value to 330K has minimal effect on the process as the small inflow has a small effect on the liquid temperature to the stripper.

Packing material: The base case uses structured packing and this is replaced with pall ring random packing for a comparison simulation. The lower surface area of the random packing (111 m^2/m^3 compared to 200 m^2/m^3 for montz packing) reduces the area available for transfer and reduces the rate of mass transfer. The direct result is lower removal efficiency and greater energy consumption by a considerable amount. The choice of packing has a large effect on the results.

5.8 Control Philosophy

A typical control philosophy that could be implemented is:

- Rich amine pump B controls volumetric liquid flow rate to a set point
- Lean pump G is controlled to keep a constant level in the bottom of the stripper
- Stream 13 the inlet liquid to the absorber is controlled to a temperature set point by heat exchanger H
- The de absorption condenser F is used to control the temperature of S5 back to the stripper and the captured gas composition
- The temperature and heat load to the reboiler E, sets the temperature and flow rate of stream S8 which is the stripping steam.

5.9 Partial Differential Equation Solving.

The number of discretised volumes has an impact on the accuracy of the results. With only 5 slices in a 25m tall absorption tower each slice is 5m in height so the assumption of a well mixed control volume is not entirely correct. The boundary conditions have a large effect on the states at the top and the bottom of the tower. This is illustrated by figure 4.14 where the inputs and parameters are held constant and the number of discretised zones increased. The percentage removal approaches a maximum value of around 90% but the energy consumed is still increasing linearly. The time to simulate increase exponentially so it is advantageous to minimize the number of discretised volumes while maintaining accuracy. The method of lines is the simplest method for solving the PDE but is also the most inaccurate unless a large number of slices are used. A method such as the central difference method or higher order gradient approximations would be an improvement to the model.

5.6 Conclusion

A dynamic model of the removal of carbon dioxide from a post combustion process is developed in this work based on chemical absorption in Monoethanolamine solution. The model consists of an absorption tower, de-absorption tower, reboiler, condenser, heat exchangers and pumps. A summary of the main conclusions is listed below:

1. There is still disagreement on the actual Equilibrium constants and forward reaction rate constants for the reaction of CO_2 and MEA especially at the elevated temperature that is in the stripper.
2. The modeling of the vapour-liquid equilibrium is a difficult part of the process and the choice of a method (residual thermodynamics or excess thermodynamics) has a large effect on the results. The Peng Robinson used in this work was inaccurate in describing the ions in solution but was sufficient for this work
3. A henrys law for CO_2 as a function of temperature, solubility of CO_2 in water, solubility of CO2 in MEA and ionic strength was adequate at describing the vapour liquid equilibrium for Carbon dioxide.
4. Fluid properties as a function of temperature are time consuming to derive and verify. The system works over a temperature range from 300-400K and the effect of temperature on fluid properties is significant.
5. The majority of work for mass diffusion co-efficients can be traced back to one source (Billet 1995). From other authors working from first principle approaches the consensus is that the mass transfer coefficient is proportional to the square root of the diffusivity.
6. Allowing for chemical reactions in the film with the enhancement factor is the easiest and least computational demanding method. The accuracy of the enhancement factor is hard to qualify but should be quantified as the enhancement factor has a large effect on the system performance.
7. The residence time of the liquids in the absorption tower has a large effect on the result as the rate of CO_2 transfer is strongly dependent on the amount of surface area for transfer. Increasing the absorption tower diameter and height produce a higher removal rate as the volume of packing is increased
8. The de-absorption process is controlled by the equilibrium constants which dictate how much soluble CO_2 is released from the bound CO_2. At the elevated temperature in the

stripper the reactions precede faster, the enhancement factor is greater and the diffusion process is increased.

9. The heat of reaction in the absorber adds heat to the liquid and gas phase increasing the temperature. In the stripper the reactions are reversed and require energy as are endothermic. The greater the concentration of MEA the lower the energy requirements as less energy is required to heat the bulk fluid to a temperature to reverse the chemical reactions.
10. Representing the heat exchanger as a CSTR was adequate for the purpose of this model but could be improved on by also solving as a PDE.
11. The condenser and reboiler models are basic and adequate for this work. In this work the temperature of the reboiler was set as an input which was changed to minimize the amount of energy consumed removing each kg of CO_2, but still achieves an adequate stripping rate. The system is highly non linear and convergence is sometimes difficult.
12. The number of discretised volumes greatly affected the time of the simulations. For highest accuracy, the number of slices should be increased at the expense of computing time.
13. The overall system is very nonlinear with very fast reaction rates through to much slower diffusion rates and temperature transfer. The model is computationally demanding requiring upwards of 24 hours to run a simulation
14. Using the heat of reaction multiplied by the reaction rate took a long time to converge for the temperature from the heat of reaction. Multiplying the diffusion rate by the heat of reaction was an adequate simplification that reduced the simulation time.
15. There are many parameters and inputs which affect the results and finding an optimal solution is a challenging task especially if one includes the balance between capital and operational cost.
16. A significant amount of H_2O and MEA leaves the system with the exhaust gas and the purified stream. The addition of a water wash, make up water and MEA should be allowed for.
17. The model of a absorption and de-absorption process using amine solution is a complex problem with many interactions. In this model many assumptions and simplifications have been made but the results are still reasonable.

5.7 Future Work

This project was a major undertaking with many different facits such as chemical reactions, mass transfer, fugacity, EOS etc. Many areas where done very quickly in the simplest method therefore is major scope for investigation and development. A few possible areas are listed below:

- A more accurate equation of state such as the SAFT or CPA where the electrolytes of the liquid are accounted for.
- Investigate other mixing rules for the equation of state. Sadus, R,J. and Wei Y.S. (2000) provide a through review.
- Applying the gamma phi method of excess thermodynamics to sole for the VLE.
- Modeling of the CO_2 in the film boundary layer to compare against the enhancement factor.
- Modeling of the temperatures within the heat exchangers
- Better model for the condenser c/w flash calculation and heat exchanger.
- Model the reboiler with steam flow as a control input rather than reboiler temperature.
- Addition of water wash, inlet fan, post process compression equipment to include for the peripheral equipment.
- Modeling of pressure drop within the tower.
- Investigate diffusion properties of O_2 and N_2 in the amine solution to increase the accuracy of the model.
- Include chemical reactions of amine with oxygen to allow for oxygen degradation.
- Include other amine products in the model.
- Examine the heat of reaction for the amine and what the actual value is for each individual reaction.
- Examination of the equilibrium constants in detail and compare to other literary values
- Investigation into the forward reaction constants most notably at elevated temperatures.
- Develop the mass transfer coefficient with the Stefan Maxwell equations.
- Detailed control philosophy.

- Add pump head loss calculation to model.

References

Aboudheir A., Tontiwachwuthikula P., Chakma A. and Idem R. (2003). Kinetics of the reactive absorption of carbon dioxide in high CO2-loaded, concentrated aqueous Monoethanolamine solutions. *Chemical Engineering Science*, volume 58, pp5195 – 5210. Available from *www.elsevier.com/locate/ces.*

Aroonwilas, A, Chakma,A, Tontiwachwuthikul,P, and Veawab, A. (2003) Mathematical modelling of mass-transfer and hydrodynamics in CO_2 absorbers packed with structured packing's. *Chemical Engineering Science*, volume 58,pp 4037 – 4053. Available from *www.elsevier.com/locate/ces.*

Akzo Nobel. (2008). Monoethanolamine datasheet. Aker Nobel.org. [Online]. September 2005. Available from *http://www.ethyleneamines.com/NR/rdonlyres/C9D13174-A9F4-4A4E-B3E2-9843D266804E/0/ MEA.pdf*. [accessed 18.03.08]

Billet R.H. (1995). Packed towers in processing and environmental technology. First edition, Weinheim, VCH Verlagsgesellschaft.

Billet, R and Schultes, M. (1999). Prediction of mass transfer columns with dumped and arranged packing's: Updated Summary of the Calculation Method of Billet and Schultes. *Trans IChemE* , volume 77.

Carleton (2008) Global Climate change. [Online]. Available from *http://http-server. carleton.ca/~msmith2/45315/gcc_06.html.* [Accesed:21.05.2008]

Cents A.H.G., Brilman D.W.F. and Versteeg G.F.(2005). CO_2 absorption in carbonate/ bicarbonate solutions: The Danckwerts-criterion revisited. *Chemical Engineering Science* volume 60 pp 5830 – 5835 available at *www.elsevier.com/locate/ces.*

Chembuddy. Activation coefficient. Chembuddy.com. [Online]. July 2005. Available from *http://www.chembuddy.com/?left=pH-calculation&right=ionic-strength-activity-coefficients*. [accessed 20.04.08]

DeWitt D.P. and Incropera T.P. (2002). Fundamentals of Heat and Mass Transfer. Fifth edition, John Wiley & Sons, p981

Draxler J., Stevens G. And Kentish S. (2007). Criteria for the selection of reagents for CO2 absorption. Co-operative Research Centre for Greenhouse Gas Technologies. [Online]. February 2007. Available from *https://extra.co2crc.com.au/modules/pts2/download.php?file_id=847&rec_id=215.*

Elliott, J.R Lira, C.T. (1998). Introductory Chemical Engineering Thermodynamics. Prentice-Hall, London.

Freguia S. And Rochelle G.T. (2003). Modelling of CO Capture by Aqueous Monoethanolamine. *AIChE Journal*, volume 49.

Green facts. (2005). Scientific facts on CO_2 Capture and storage. Greenfacts.org. [Online]. September 2005. Available from *http://www.greenfacts.org/en/co2-capture-storage*. [accessed 20.04.08]

Hansen D.K. (2004). Dynamic modeling of an absorption tower for the removal of carbon dioxide from exhaust gas by means of Monoethanolamine. Telemark University College, Faculty of Technology. Thesis carried out at NTNU.

Hoff K.A. (2003). Modelling and experimental study of carbon dioxide absorption in a membrane contactor. NTNU pHd Thesis. Trondheim , Norway. P224 available from *http://www.diva-portal.org/ntnu/searchresult.xsql.* Accessed [22.1.2008].

IPCC. (2007). Climate change 2007 Syntheses report. Intergovernmental Panel on Climate Change. [Online]. November 2007. Available from *http://www.ipcc.ch/ipccreports/ar4-syr.htm*. [accessed 23.04.08]

IPCC, (2005): IPCC Special Report on Carbon Dioxide Capture and Storage. Prepared byWorking Group III of the Intergovernmental Panel on Climate Change [Metz, B.,O. Davidson, H. C. de Coninck, M. Loos, and L. A. Meyer (eds.)]. Cambridge UniversityPress, Cambridge, United Kingdom and New York, NY, USA, 442 pp.. Available from *http://www.ipcc.ch/pdf/special-reports/srccs/srccs_wholereport.pdf*. [accessed 23.04.08]

Jamal, A., Meisen, A. and Jim Lim, C. (2006) Kinetics of carbon dioxide absorption and desorption in aqueous alkanolamine solutions using a novel hemispherical contactor—II: Experimental results and parameter estimation. *Chemical Engineering Science*, volume 61 ,pp 6590 – 6603. Available from *www.elsevier.com/locate/ces.*

Jolicouer C., Page M. And Huot J.Y. (1993). A comprehensive thermodynamic investigation of water-ethanolamine mixtures at 10, 25, and 40°C. Canadian Journal of chemistry, volume 71,pp 1064-1072

Kohl A.L. and Nielsen R.B. Gas Purification, 5th Edition, Gulf Publishing, Houston, TX, 1997.

Kukoljac, M.D and Grozdanic. D.K. (2000). New values of the polarity factor. *Journal of Serbian chemical society*. Volume 65, pp 899-904

Lie B. (1995). Kompendium i prosessmodellering 2. Telemark University College, Norway

Lie B. (2005). Modeling of Dynamic Systems. Telemark University College, Norway

Lee J.L., Otto F.D and Mather A.E. (1976). Equilibrium between carbon dioxide and aqueous Monoethanolamine solution. *Journal of applied chemistry Biotechnology*. Vol 26 pp 541-549.

Li Y. G and Mather A. E. (1994). Correlation and Prediction of the Solubility of Carbon Dioxide in a Mixed Alkanolamine Solution. *Industrial Engineering Chemistry Research*, Volume 33, pp2006-2015

Liu, Y., Zhang, L and Watanasiri, S. (1999). Representing Vapour-Liquid Equilibrium for an Aqueous MEA-CO2 System Using the Electrolyte Non-random-Two-Liquid Model. *Industrial Engineering Chemical Research*, volume 38, pp 2080-2090.

Maceiras R., Alvarez E. and Cancela M.A. (2007). Effect of temperature on carbon dioxide on absorption in Monoethanolamine solutions. *Chemical Engineering Journal*, volume 56, pp 987-996.

Mather A., Otto F.D and Lee .J. (1975). Solubility of Mixtures of Carbon Dioxide and Hydrogen Sulfide in *5.O N* Monoethanolamine Solution. *Journal of Chemical and Engineering Data,* Vol. *20*

Mather A., Otto F.D and Lee .J. (1976). The measurement and prediction of the Solubility of Mixtures of Carbon Dioxide and Hydrogen Sulfide in 2.*5 N* Monoethanolamine Solution. *The Canadian Journal of chemical Engineering ,* Vol. *54, pp 214-219*

Munoz E., Diaz E., Ordonez S. and Vega A. (2006). Adsorption of Carbon Dioxide on Alkali Metal Exchanged Zeolites. AICHE Conference, San Francisco USA.

NIST. (2008). [Online]. Available from, *www://webbook.nist.gov/chemistry*. Accessed [12.03.2008].

Park S.B. and Lee H. Vapour-Liquid equilibria for the binary Monoethanolamine + water and Monoethanolamine + ethanol systems. (1997). *Korean Journal of chemical engineering*, volume 14, pp 146-148

Perry R.H. and Green D.W. (1999), Chemical Engineers Handbook. 7th edition McGrawHill, NewYork.

Paulus, M.E. and Penoncello S.G. (2006). Correlation for the Carbon Dioxide and Water Mixture based on The Lemmon–Jacobsen Mixture Model and the Peng–Robinson Equation of State. *International Journal of Thermo physics,* volume 27. Available from *www.springerlink.com*.

Peng, D.Y. and Robinson D.B. (1976). A New two constant equation of state. *Industrial Engineering Chemical Fundamentals*. Volume 15.

Piche´, S., Le´vesque, S., Grandjean, B.P.A. and Larachi F.(2003). Prediction of HETP for randomly packed towers operation:integration of aqueous and non-aqueous mass transfer characteristics into one consistent correlation. *Separation and Purification Technology*, volume 33 ,pp 145-162. Available from *www.elsevier.com/locate/seppur*

Pinsent B.R.W., Pearson L and Roughton F. J. W.. (1956). The kinetics of combination of carbon dioxide with hydroxide ions. *Journal of the Chemical Society, Faraday Transactions* 52 (1956), pp. 1512–1520

Reid R.C., Prausnitz J.M. and Poling B.E. (1987). The Properties of Gases and Liquids. New York: McGraw-Hill. Fourth edition.

Royal Society. (2005). Ocean acidification due to increasing atmospheric carbon dioxide. The Royal Society. [Online]. June 2005. Available from *http://royalsociety.org/ displaypagedoc.asp?id=13314* [accessed 20.04.08].

Sadus, R,J. and Wei Y.S. (2000).Equations of State for the Calculation of Fluid-Phase Equilibria. *AIChE Journal*, volume 46 ,

Scheiman M.A. (1962). A Review of Monoethanolamine chemistry. [Online]. Surface chemistry branch US army. Available from *http://stinet.dtic.mil/oai/oai?verb=getRecord &metadataPrefix=html& identifier=AD0277031.* accessed [21.02.2008]

Smith R. (20050. Chemical Process Design and Integration. First edition, John Wiley & sons, Chichester, England.

Solbraa E. (2002). Equilibrium and Non-Equilibrium Thermodynamics of Natural Gas Processing Measurement and Modelling of Absorption of Carbon Dioxide into Methyldiethanolamine Solutions at High Pressures. NTNU pHd Thesis. Trondheim , Norway. P348 available from *http://www.diva-portal.org/ntnu/searchresult.xsql.* Accessed [10.2.2008]

Stoll J., Vrabec J., and Hasse H. Vapour–Liquid Equilibria of Mixtures Containing Nitrogen, Oxygen, Carbon Dioxide, and Ethane (2003). *AIChE Journal*, Volume 49 pp2187-2198

Svendsen H.F. and. da Silva E. F. (2007). Computational chemistry study of reactions, equilibrium and kinetics of chemical CO2 absorption. [Online]. International journal o f greenhouse gas control, pp151 – 157. Available from *www.elsevier.com/locate/ijggc.*

Svendsen H.F. and Kim I. (2007). Heat of Absorption of Carbon Dioxide (CO2) in Monoethanolamine (MEA) and 2-(Aminoethyl)ethanolamine (AEEA) Solutions. Industrial engineering Chemical Research. Volume 46, pp 5803-5809.

Tanaka Y. (2002). Water dissociation in ion-exchange membrane electro dialysis. *Journal of Membrane Science,volume 2*03 pp 227–244 available from *www.elsevier.com/locate/memsci*

Twidell J. and Weir T. (2006). Renewable Energy Resources. 2nd edition, Taylor & Francis, London, p601

Vaidya P.D. and Kenig E.Y. (2007). CO_2-Alkanolamine Reaction Kinetics: A Review of Recent Studies. *Chemical Engineering Technology*, volume 30, No. 11, pp1467–1474

Versteeg, G.F., Snijder E.D., te Reile M.J.M and van SwaaiJ, W.P.M. (1993). Diffusion Coefficients of several aqueous alkanolamine solutions. *Journal of Chemical Engineering data*, volume 38 ,pp 475-480.

Versteeg, G.F. and. van SwaaiJ, W.P.M. (1988) Solubility and Diffusivity of Acid Gases *(CO_2,* N_20) in Aqueous Alkanolamine Solutions Journal of *Chemical Engineering*, volume 33 ,pp 29-34.

Versteeg G.F., Holst J.V., Politiek P.P, and Niederer J.P. (2006). CO_2 capture from flue gas using amino acid salt solutions, [Online] June 2006 available from *http://www.co2-cato.nl/doc.php?lid=317* accessed [12.04.2008]

Wallace, D. (2000). Capture and Storage of CO_2 what needs to be done?. IEA [online]. November 2000. Available from *http://www.iea.org/textbase/papers/2000/capstor.pdf*. Accessed [23.04.08]

Whitman W.G and Lewis W.K. (1924). The two-film theory of gas absorption. *Industrial engineering chemistry*, volume 16 p1215.

Wikipedia/absorption. (2008). [Online]. Available from, *http://en.wikipedia.org/wiki/absorption*. Accessed [12.05.2008].

Wikipedia/adsorption. (2008). [Online]. Available from, *http://en.wikipedia.org/wiki/adsorption*. Accessed [14.05.2008].

Wikipedia/greenhouse. (2008). [Online]. Available from, *http://en.wikipedia.org/wiki /Greenhouse _effect*. Accessed [12.05.2008].

Wikipedia/Henry. (2008). [Online]. Available from, http://en.wikipedia.org/wiki/Henry's_law. Accessed [12.03.2008].

Xiao J., Li C.W. and Li M.H. (2000). Kinetics of absorption of carbon dioxide into aqueous solutions of 2-amino-2-methyl-1-propanol + Monoethanolamine. *Chemical Engineering Science*, volume 55, pp 161-175.

Øi L.E. Aspen. (2007) HYSYS simulation of CO_2 removal by amine absorption from a gas based power plant. SIMS 2007 Conference proceedings, Goteborg Sweden.

Appendix A

The fugacity can be used as a measure of the driving force for the transfer of a component form one phase to another. By applying the assumptions for the vapour phase that CO_2, $O_2$and N_2 have negligible resistance to mass transfer and the bulk vapour concentration (or fugacity) is the same as the interface value. The concentration of the vapour phase can be related to the partial pressure by the equation

$$P_i^v = Z^v c_i^v R T^v$$

The fugacity of the vapour phase is given by the equation $f_i^v = \varphi_i^v y_i P$ and the partial pressure is defined as $P_i=y_iP$. Rewriting the expression for mass transfer in terms of fugacity's. In the derivation of the diffusion molecular flow the molecular flow from the liquid to the gas is defined as positive

$$\dot{n}_{d,i}^v = k d_i^v a_w (C_i^{v*} - C_i^v)$$

$$\dot{n}_{d,i}^v = k d_i^v a_w \left(\frac{P_i^{v*}}{R T^v Z^v} - \frac{P_i^v}{R T^v Z^v} \right)$$

$$\dot{n}_{d,i}^v = k d_i^v a_w \left(\frac{f_i^{v*}}{\varphi_i^{v*} R T^v Z^{v*}} - \frac{f_i^v}{\varphi_i^v R T^v Z^v} \right)$$

At the interface the fugacity of the liquid is equal to the fugacity of the vapour hence $f_i^{v*} = f_i^{l*}$. For the water and MEA components the interface fugacity is assumed to be equal to the bulk liquid fugacity $f_i^l = f_i^{l*}$. This can be substituted into the above equation which leads to the expression.

$$\dot{n}_{d,i}^v = \frac{k d_i^v a_w}{\varphi_i^v Z^v R T^v} \left(f_i^l - f_i^v \right)$$

This expression for the diffusion flux is valid for the MEA and H_20 components when the resistance is assumed to be in the gas liquid film. A similar expression for CO_2, $O_2$and N_2 can be also be derived by

$$\dot{n}_{d,i}^l = -k d_i^l a_w (C_i^{l*} - C_i^l)$$

Substituting the expressions $x_i = \frac{C_i^l}{C_T^l}$ and $f_i^l = x_i \varphi_i^l P$

$$\dot{n}_{d,i}^{l} = -kd_i^l a_w (x_i^* C_T^{l*} - x_i C_T^l)$$

$$\dot{n}_{d,i}^{l} = -kd_i^l a_w \left(\frac{f_i^{l*}}{\varphi_i^{l*} P} C_T^{l*} - \frac{f_i^l}{\varphi_i^l P} C_T^l \right)$$

At vapour equilibrium $f_i^{v*} = f_i^{l*}$ and for CO_2, $O_2$and N_2 , $f_i^{v*} = f_i^v$ as there is negligible resistance in the vapour phase. In the liquid phase the bulk concentration and interface concentration are dominated by water and MEA which are assumed not to change therefore it is assumed the concentrations and fugacity co-efficient the same This reduces the above equation to:

$$\dot{n}_{d,i}^{l} = \frac{-kd_i^l a_w C_T^l}{\varphi_i^l P} \left(f_i^v - f_i^l \right)$$

The advantage of using the liquid and gas fugacity's is that the interface concentrations and molecular fractions are not required therefore no iteration is required to solve for these values.

The fugacity of the liquid can be calculated with an activity coefficient method for the mol transfer of the water and MEA in the vapour phase which allows the liquid fugacity coefficient to be eliminated. This is an advantage as the Peng Robinson EOS lacks accuracy when applied to on electrolyte containing ionic solution. For the activity co-efficient method to be applied to the system an alternative form is required for the diffusion mol transfer of the CO_2, $O_2$and N_2 in the liquid phase.

Appendix B

Fitting of Perry data for gas viscosity

Temperature (K)	H_2O	CO_2	O_2	N_2
250		0.0000126	1.79E-05	1.56E-05
300	9.09E-06	0.000015	2.07E-05	0.000018
400	1.31E-05	0.0000196	2.58E-05	2.23E-05
500	1.66E-05	0.0000239	3.06E-05	2.61E-05
600	2.27E-05	0.0000278	3.48E-05	2.95E-05

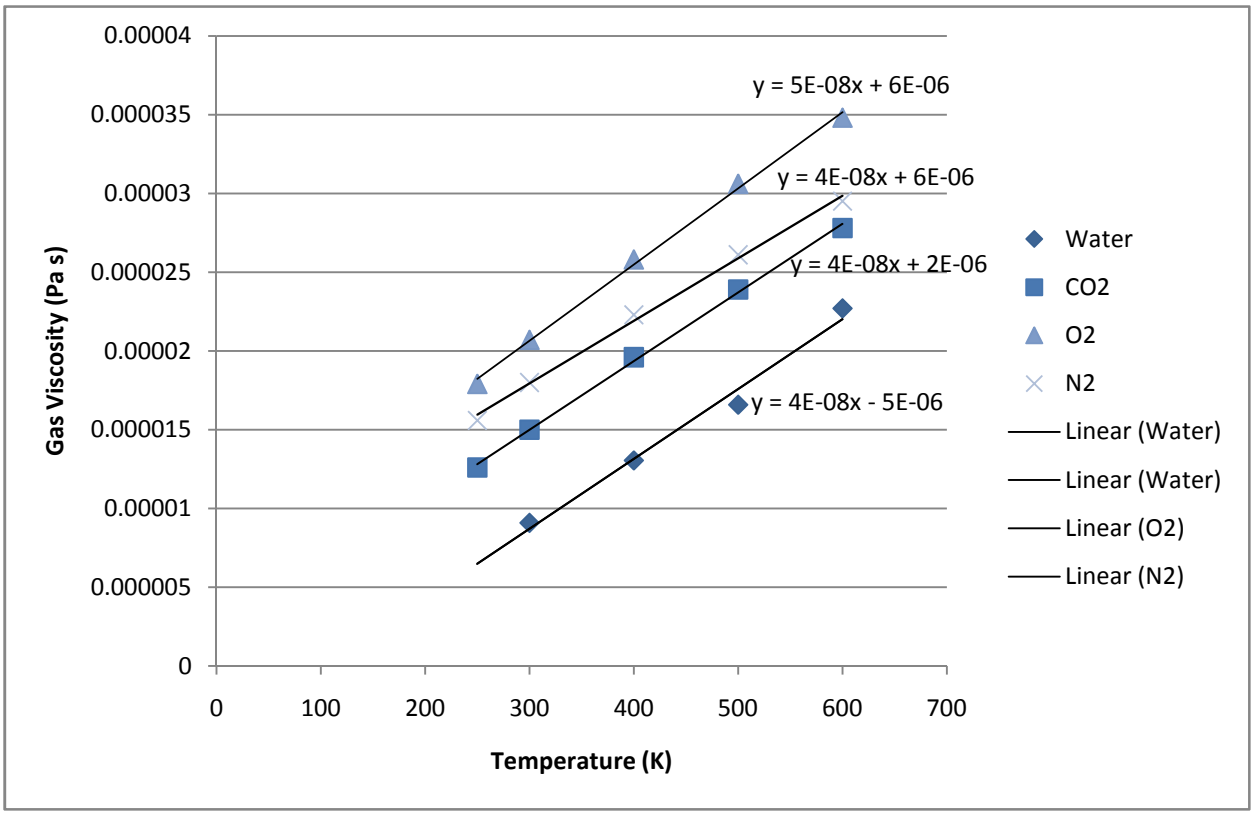

Figure B1:Gas viscosity fitted to experimental data from Perry et al

Fitting of gas thermal conductivity data from Dewitt and Incropera (2005)

T (K)	CO_2 (W/mK) x 10^{-3}	T (K)	N_2(W/mK) x 10^{-3}	T(K)	H_2O(W/mK) x 10^{-3}
280	15.2	250	22.2	380	24.6
300	16.55	300	25.9	400	26.1
320	18.05	350	29.3		
340	19.7	400	32.7		
360	21.2				
380	22.75				
400	24.3				

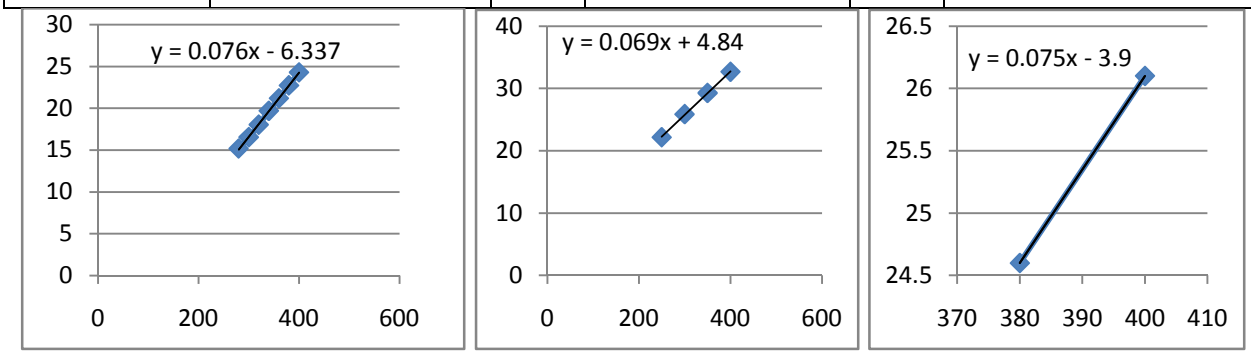

Figure B2 (a,b,c) Thermal condicityof CO_2, N_2 and H_20 c/w linea eqyaion as a function of temperature.

Appendix C

Initial and inlet conditions of gas and liquid for absorber.

Gas	weight	mass flow	mol weight	mol flow	Velocity	Mass flow	Volume flow	concentration	Mol Fraction
	%	g/s	g/mol	Mol/s	m/s	g/s	m^3/s	mol/m^3	
CO_2	0.04	31700	44	720	2.16	196.8	426.1	1.7	0.04
MEA	0			0	2.16	196.8	426.1	0.0	0.00
H_20	0.08	25936	18	1441	2.16	196.8	426.1	3.4	0.08
N_2	0.76	383282	28	13689	2.16	196.8	426.1	32.1	0.76
O_2	0.12	34582	16	2161	2.16	196.8	426.1	5.1	0.12
Total	1	475500		18011	2.16	196.8	426.1	42.3	
				Epslom	0.979	T (K)	313		
				D (m)	16	P (Pa)	110000		
Liquid									
	weight	mass flow	mol weight	mol flow	Velocity	Mass flow	Volume flow	concentration	Mol Fraction
	%	g/s	g/mol	Mol/s	m/s	g/s	m^3/s	mol/m^3	
CO_2	0	0	44	0	0.0041	800000	0.8	0	0.00
MEA	0.3	240000	61	3934	0.0041	800000	0.8	4918	0.11
H_20	0.7	560000	18	31111	0.0041	800000	0.8	38889	0.89
N_2		0	28	0	0.0041	800000	0.8	0	
O_2		0	16	0	0.0041	800000	0.8	0	
Total	1	800000		35046			0.8	43807	1.00

Appendix D

Matlab code:

Carbon3.m

```
clear all
clc
tic
% Number of subvolumes in discretization
Ns= 5;
B=18*Ns;
% Final ti0me of simulationvv
tf =10000;
LA = 25; % Height of absorber (m)
LS=15;  %height of Stripper
% Setting up initial value function
% Spatial positions of discretized subvolumes:
zA = (linspace(0,LA,Ns));  %absorber volumes)
zS = (linspace(0,LS,Ns));   %stripper volumes
% Spatial step length
dxA = LA/Ns;
dxS =LS/Ns;
para
H=1;
for h=1:H;

[C0,uAB]=inletvalues;  %inlet values

% intial values in the ode  nnote not used if using prevois model
CLABCO2i = C0(1).*ones(Ns,1);
CGABCO2i = C0(2).*ones(Ns,1);
CLABMEAi = C0(3).*ones(Ns,1);
CGABMEAi= C0(4).*ones(Ns,1);
CLABH20i = C0(5).*ones(Ns,1);
CGABH20i = C0(6).*ones(Ns,1);
CLABN2i = C0(7).*ones(Ns,1);
CLABN2i = C0(8).*ones(Ns,1);
CLABO2i = C0(9).*ones(Ns,1);
CGABO2i = C0(10).*ones(Ns,1);
CLABHi = C0(11).*ones(Ns,1);
CLABOHi= C0(12).*ones(Ns,1);
CLABMEAHi = C0(13).*ones(Ns,1);
CLABMEACOOi =C0(14).*ones(Ns,1);
CLABHCO3i = C0(15).*ones(Ns,1);

delP=dP/Ns;
PTABi=1;

for d=1:Ns;
PTABi(d)= C0(16)-d*delP;  %give linera pressure drop
end

TGABi = C0(17).*ones(Ns,1);
TLABi = C0(18).*ones(Ns,1);
CLSCO2i = C0(19).*ones(Ns,1);
CGSCO2i = C0(20).*ones(Ns,1);
CLSMEAi = C0(21).*ones(Ns,1);
CGSMEAi= C0(22).*ones(Ns,1);
CLSH20i = C0(23).*ones(Ns,1);
```

```
CGSH20i = C0(24).*ones(Ns,1);
CLSN2i = C0(25).*ones(Ns,1);
CLSN2i = C0(26).*ones(Ns,1);
CLSO2i = C0(27).*ones(Ns,1);
CGSO2i = C0(28).*ones(Ns,1);
CLSHi = C0(29).*ones(Ns,1);
CLSOHi = C0(30).*ones(Ns,1);
CLSMEAHi = C0(31).*ones(Ns,1);
CLSMEACOOi =C0(32).*ones(Ns,1);
CLSHCO3i = C0(33).*ones(Ns,1);

PTSi=1;
for d=1:Ns;
PTSi(d)= C0(34)-d*delP;  %linear pressure drop
end

TGSi = C0(35).*ones(Ns,1);
TLSi = C0(36).*ones(Ns,1);

%Intial condition vector
Ci=[CLABCO2i CGABCO2i CLABMEAi CGABMEAi CLABH20i CGABH20i CLABN2i CLABN2i
CLABO2i CGABO2i CLABHi CLABOHi CLABMEAHi CLABMEACOOi CLABHCO3i PTABi' TGABi
TLABi CLSCO2i CGSCO2i CLSMEAi CGSMEAi CLSH20i CGSH20i CLSN2i CLSN2i CLSO2i
CGSO2i CLSHi CLSOHi CLSMEAHi CLSMEACOOi CLSHCO3i PTSi' TGSi TLSi];

% intila conditiond from previous simullation
[INT]=startvalues(Ns,LA,LS);
 Ci=INT;
 Ci(:,34)=PTSi';

[time,Cc] = ode15s(@COabsorb,[0,tf],Ci,[],C0,dxA,dxS,uAB);

%Produces a 3D plot of the results
clf;
Cc;
time;
%B=18*Ns;
CLABCO2=Cc(:,1:Ns);
CGABCO2=Cc(:,Ns+1:2*Ns);
CLABMEA=Cc(:,2*Ns+1:3*Ns);
CGABMEA=Cc(:,3*Ns+1:4*Ns);
CLABH2O=Cc(:,4*Ns+1:5*Ns);
CGABH2O=Cc(:,5*Ns+1:6*Ns);
CLABN2=Cc(:,6*Ns+1:7*Ns);
CGABN2=Cc(:,7*Ns+1:8*Ns);
CLABO2=Cc(:,8*Ns+1:9*Ns);
CGABO2=Cc(:,9*Ns+1:10*Ns);
CLABH=Cc(:,10*Ns+1:11*Ns);
CLABOH=Cc(:,11*Ns+1:12*Ns);
CLABMEAH=Cc(:,12*Ns+1:13*Ns);
CLABMEACOO=Cc(:,13*Ns+1:14*Ns);
CLABHCO3=Cc(:,14*Ns+1:15*Ns);
PTAB=Cc(:,15*Ns+1:16*Ns);
TGAB=Cc(:,16*Ns+1:17*Ns);
TLAB=Cc(:,17*Ns+1:18*Ns);

CLSCO2=Cc(:,18*Ns+1:19*Ns);
CGSCO2=Cc(:,19*Ns+1:20*Ns);
CLSMEA=Cc(:,20*Ns+1:21*Ns);
CGSMEA=Cc(:,21*Ns+1:22*Ns);
CLSH2O=Cc(:,22*Ns+1:23*Ns);
```

```
CGSH2O=Cc(:,23*Ns+1:24*Ns);
CLSN2=Cc(:,24*Ns+1:25*Ns);
CGSN2=Cc(:,25*Ns+1:26*Ns);
CLSO2=Cc(:,26*Ns+1:27*Ns);
CGSO2=Cc(:,27*Ns+1:28*Ns);
CLSH=Cc(:,28*Ns+1:29*Ns);
CLSOH=Cc(:,29*Ns+1:30*Ns);
CLSMEAH=Cc(:,30*Ns+1:31*Ns);
CLSMEACOO=Cc(:,31*Ns+1:32*Ns);
CLSHCO3=Cc(:,32*Ns+1:33*Ns);
PTS=Cc(:,33*Ns+1:34*Ns);
TGS=Cc(:,34*Ns+1:35*Ns);
TLS=Cc(:,35*Ns+1:36*Ns);

percentageremovedAB=100*(C0(2)-CGABCO2(end,Ns))/C0(2)
PD(h,1)=1;
PD(h,2)=percentageremovedAB;
End

figure(1);
surf(zA,time,CLABCO2);
xlabel('x')
ylabel('t')
zlabel('Cco2l')

figure(2);
surf(zA,time,CGABCO2);
xlabel('x')
ylabel('t')
zlabel('Cgco2g')

figure(3);
surf(zA,time,CLABMEA);
xlabel('x')
ylabel('t')
zlabel('Cmeal')

figure(4);
surf(zA,time,CGABMEA);
xlabel('x')
ylabel('t')
zlabel('Cgmeag')

figure(5);
surf(zA,time,CLABH2O);
xlabel('x')
ylabel('t')
zlabel('Ch2ol')

figure(6);
surf(zA,time,CGABH2O);
xlabel('x')
ylabel('t')
zlabel('Ch2og')

figure(7);
surf(zA,time,CLABH);
xlabel('x')
ylabel('t')
zlabel('ClH')
```

```
figure(8);
surf(zA,time,CLABOH);
xlabel('x')
ylabel('t')
zlabel('CLOH')

figure(9);
surf(zA,time,CLABMEAH);
xlabel('x')
ylabel('t')
zlabel('ClMEAH')

figure(10);
surf(zA,time,CLABHCO3);
xlabel('x')
ylabel('t')
zlabel('CLHCO3')

figure(11);
surf(zA,time,CLABMEACOO);
xlabel('x')
ylabel('t')
zlabel('CLMEAC00')


figure(12);
surf(zA,time,TGAB);
xlabel('x')
ylabel('t')
zlabel('Tg')

figure(13);
surf(zA,time,TLAB);
xlabel('x')
ylabel('t')
zlabel('Tl')


figure(14);
surf(zS,time,CLSCO2);
xlabel('x')
ylabel('t')
zlabel('Cco2l')

figure(15);
surf(zS,time,CGSCO2);
xlabel('x')
ylabel('t')
zlabel('Cgco2g')

figure(31);
surf(zS,time,CLSMEA);
xlabel('x')
ylabel('t')
zlabel('Cmeal')

figure(41);
surf(zS,time,CGSMEA);
xlabel('x')
ylabel('t')
zlabel('Cgmeag')
```

```
figure(51);
surf(zS,time,CLSH2O);
xlabel('x')
ylabel('t')
zlabel('Ch2ol')

figure(61);
surf(zS,time,CGSH2O);
xlabel('x')
ylabel('t')
zlabel('Ch2og')

figure(71);
surf(zS,time,CLSH);
xlabel('x')
ylabel('t')
zlabel('ClH')

figure(81);
surf(zS,time,CLSOH);
xlabel('x')
ylabel('t')
zlabel('CLOH')

figure(91);
surf(zS,time,CLSMEAH);
xlabel('x')
ylabel('t')
zlabel('ClMEAH')

figure(101);
surf(zS,time,CLSHCO3);
xlabel('x')
ylabel('t')
zlabel('CLHCO3')

figure(111);
surf(zS,time,CLSMEACOO);
xlabel('x')
ylabel('t')
zlabel('CLMEAC00')


figure(121);
surf(zS,time,TGS);
xlabel('x')
ylabel('t')
zlabel('Tg')

figure(113);
surf(zS,time,TLS);
xlabel('x')
ylabel('t')
zlabel('Tl')

[Vdot7]=Output(Cc,C0,dxA,dxS,uAB,tf,Ns)   %output file


toc
```

COabsorb.m

```
function [dCdt]=COabsorb(t,Y,C0,dxA,dxS,uAB)

para;  %pull in parameters

size(Y);
B = length(Y);
Ns=B/36;

% extract states
CLABCO2 = Y(1:Ns);
CGABCO2 = Y(Ns+1:2*Ns);
CLABMEA = Y(2*Ns+1:3*Ns);
CGABMEA= Y(3*Ns+1:4*Ns);
CLABH2O = Y(4*Ns+1:5*Ns);
CGABH2O = Y(5*Ns+1:6*Ns);
CLABN2 = Y(6*Ns+1:7*Ns);
CGABN2 = Y(7*Ns+1:8*Ns);
CLABO2 = Y(8*Ns+1:9*Ns);
CGABO2 = Y(9*Ns+1:10*Ns);
CLABH = Y(10*Ns+1:11*Ns);
CLABOH = Y(11*Ns+1:12*Ns);
CLABMEAH = Y(12*Ns+1:13*Ns);
CLABMEACOO =Y(13*Ns+1:14*Ns);
CLABHCO3 = Y(14*Ns+1:15*Ns);
PTAB = Y(15*Ns+1:16*Ns);
TGAB = Y(16*Ns+1:17*Ns);
TLAB = Y(17*Ns+1:18*Ns);
CLSCO2 = Y(18*Ns+1:19*Ns);
CGSCO2 = Y(19*Ns+1:20*Ns);
CLSMEA = Y(20*Ns+1:21*Ns);
CGSMEA= Y(21*Ns+1:22*Ns);
CLSH2O = Y(22*Ns+1:23*Ns);
CGSH2O = Y(23*Ns+1:34*Ns);
CLSN2 = Y(24*Ns+1:25*Ns);
CGSN2 = Y(25*Ns+1:26*Ns);
CLSO2 = Y(26*Ns+1:27*Ns);
CGSO2 = Y(27*Ns+1:28*Ns);
CLSH = Y(28*Ns+1:29*Ns);
CLSOH = Y(29*Ns+1:30*Ns);
CLSMEAH = Y(30*Ns+1:31*Ns);
CLSMEACOO =Y(31*Ns+1:32*Ns);
CLSHCO3 = Y(32*Ns+1:33*Ns);
PTS = Y(33*Ns+1:34*Ns);
TGS = Y(34*Ns+1:35*Ns);
TLS = Y(35*Ns+1:36*Ns);

%values for the reboiler  T and C
TPRBin(1)=TGS(1);
TPRBin(2)=TLS(1);
TPRBin(3)=PTS(1);

CLRBin(1)=CLSCO2(1);
CLRBin(2)=CLSMEA(1);
CLRBin(3)=CLSH2O(1);
CLRBin(4)=CLSN2(1);
CLRBin(5)=CLSO2(1);
CLRBin(6)=CLSMEAH(1);
CLRBin(7)=CLSMEACOO(1);
CLRBin(8)=CLSHCO3(1);
```

```
CLRBin(9)=CLSOH(1);
CLRBin(10)=CLSH(1);

%outlet values from absorber
CLAB(1)=CLABCO2(1);
CLAB(2)=CLABMEA(1);
CLAB(3)=CLABH2O(1);
CLAB(4)=CLABN2(1);
CLAB(5)=CLABO2(1);
CLAB(6)=CLABMEAH(1);
CLAB(7)=CLABMEACOO(1);
CLAB(8)=CLABHCO3(1);
CLAB(9)=CLABOH(1);
CLAB(10)=CLABH(1);

%initial guess for Vdot 7
Vdot7=Vdot3*(1+(0.05));
%iterate on Vdot7 so doesnt change
for i=1:M

% reboiler calculation
    [CGRB,uvS,VGS,QRb,CLSout,Vdot9,n9] = reboiler(TPRBin,CLRBin,Vdot7);
% values for heat exchanger
    CGSCO20=CGRB(1);
    CGSMEA0=CGRB(2);
    CGSH2O0=CGRB(3);
    CGSN20=CGRB(4);
    CGSO20=CGRB(5);
    TGS0=TGRBOUT;


% values for the condenser
    TPCoin(1)=TGS(Ns);
    TPCoin(2)=TLS(Ns);
    TPCoin(3)=PTS(Ns);

    CGSCoin(1)=CGSCO2(Ns);
    CGSCoin(2)=CGSMEA(Ns);
    CGSCoin(3)=CGSH2O(Ns);
    CGSCoin(4)=CGSN2(Ns);
    CGSCoin(5)=CGSO2(Ns);

    TLABout=TLAB(1);
    TLSout=TLS(1);
% heat exchanger calc
    [TLSin,Richpumppower,Leanpumppower,molflow3,n3] =
HeatexlR(TLSout,TLABout,CLAB,CLSout,Vdot9);
% condenser calc
    [TlSIN,CLSin,ulS,Vdot6,n11] =
condenser(TPCoin,CGSCoin,VGS,QRb,TLSin,CLAB,molflow3,Richpumppower,Leanpumppo
wer);

    Del=Vdot7-Vdot6;  % difference in liquid flow into and out of stripper

    if abs(  Del ) <  eps_abs;
        break;
    elseif j == M;
        error( 'Ns method nverge' );
    end
    Vdot7=Vdot6;
```

```
end

% boundary condtiions for stripper
CLSCO20=CLSin(1);
CLSMEA0=CLSin(2);
CLSH2O0=CLSin(3);
CLSN20=CLSin(4);
CLSO20=CLSin(5);
CLSMEAH0=CLSin(6);
CLSMEACOO0=CLSin(7);
CLSHCO30=CLSin(8);
CLSOH0=CLSin(9);
CLSH0=CLSin(10);
TLS0=TlSIN;
PTS0=C0(34);

uS=[ulS,uvS];
uAB;

% vector of each state in stripper repernenting the control volumes
CLSCO2p= [CLSCO2;CLSCO20];
CGSCO2p= [CGSCO20;CGSCO2];
CLSMEAp= [CLSMEA;CLSMEA0];
CGSMEAp= [CGSMEA0;CGSMEA];
CLSH2Op= [CLSH2O;CLSH2O0];
CGSH2Op= [CGSH2O0;CGSH2O];
CLSN2p= [CLSN2;CLSN20];
CGSN2p= [CGSN20;CGSN2];
CLSO2p= [CLSO2;CLSO20];
CGSO2p= [CGSO20;CGSO2];
CLSHp= [CLSH;CLSH0];
CLSOHp= [CLSOH;CLSOH0];
CLSMEAHp= [CLSMEAH;CLSMEAH0];
CLSMEACOOp= [CLSMEACOO;CLSMEACOO0];
CLSHCO3p= [CLSHCO3;CLSHCO30];
PTSp= [PTS0;PTS];
TGSp=[TGS0;TGS];
TLSp=[TLS;TLS0];

% inlet for stripper
CLABCO20=CLSout(1);
CGABCO20=C0(2);
CLABMEA0=CLSout(2);
CGABMEA0=C0(4);
CLABH2O0=CLSout(3);
CGABH2O0=C0(6);
CLABN20=CLSout(4);
CGABN20=C0(8);
CLABO20=CLSout(5);
CGABO20=C0(10);
CLABMEAH0=CLSout(6);
CLABMEACOO0=CLSout(7);
CLABHCO30=CLSout(8);
CLABOH0=CLSout(9);
CLABH0=CLSout(10);
PTAB0=C0(16);
TGAB0=TGABin;
TLAB0=TLABin;

%MEA check and replenishment
```

```
MEA=C0(3)+C0(11)+C0(12);
CLABMEA0;
CLABMEA0=MEA-CLABMEAH0-CLABMEACOO0;
%water check and add makeup
CLABH2O0;
CLABH2O0=C0(5);
%calculation of loadings
LOADINGABin=(CLABCO20+CLABHCO30+CLABMEACOO0)/MEA;
LOADINGSin=(CLSCO20+CLSHCO30+CLSMEACOO0)/MEA;

%set up nodes in absorber
CLABCO2p= [CLABCO2;CLABCO20];
CGABCO2p= [CGABCO20;CGABCO2];
CLABMEAp= [CLABMEA;CLABMEA0];
CGABMEAp= [CGABMEA0;CGABMEA];
CLABH2Op= [CLABH2O;CLABH2O0];
CGABH2Op= [CGABH2O0;CGABH2O];
CLABN2p= [CLABN2;CLABN20];
CGABN2p= [CGABN20;CGABN2];
CLABO2p= [CLABO2;CLABO20];
CGABO2p= [CGABO20;CGABO2];
CLABHp= [CLABH;CLABH0];
CLABOHp= [CLABOH;CLABOH0];
CLABMEAHp= [CLABMEAH;CLABMEAH0];
CLABMEACOOp= [CLABMEACOO;CLABMEACOO0];
CLABHCO3p= [CLABHCO3;CLABHCO30];
PTABp= [PTAB0;PTAB];
TGABp=[TGAB0;TGAB];
TLABp=[TLAB;TLAB0];

%for each slice calculate state gradient
for i = 1:Ns;
 %extract Concentrations  and temp
Cl(1)=CLABCO2(i);
Cl(2)=CLABMEA(i);
Cl(3)=CLABH2O(i);
Cl(4)=CLABN2(i);
Cl(5)=CLABO2(i);
Cl(6)=CLABMEAH(i);
Cl(7)=CLABMEACOO(i);
Cl(8)=CLABHCO3(i);
Cl(9)=CLABOH(i);
Cl(10)=CLABH(i);

Tg=TGAB(i);
Tl=TLAB(i);
PAB=PTAB(i);

Cg(1)=CGABCO2(i);
Cg(2)=CGABMEA(i);
Cg(3)=CGABH2O(i);
Cg(4)=CGABN2(i);
Cg(5)=CGABO2(i);

TP(1)=Tg;
TP(2)=Tl;
TP(3)=PAB;

[Rgen,Ra]= reactions(Cl,TP,t);  % calc rate of speies gen

[nd,Z,aw,rhov,mewg,ht,E] = vari(TP,Cg,Cl,uAB);  % cal rate of diffuison
```

```
[Tld,Tgd] = HEAT(TP,uAB,Cl,Cg,aw,rhov,nd,Ra,mewg,ht,t,E);  % calc heat change

ulAB=uAB(1);
uvAB=uAB(2);
uvAB=uvAB/(1-ht); %corect velocity for liquid hold up

     % calc esach species change in concentation
    dCLABCO2dt(i) = ulAB*(CLABCO2p(i+1) - CLABCO2p(i))/dxA - nd(1)  +
Rgen(1);

    dCGABCO2dt(i) = -uvAB*(CGABCO2p(i+1) - CGABCO2p(i))/(dxA) + nd(1);

    dCLABMEAdt(i) = ulAB*(CLABMEAp(i+1) - CLABMEAp(i))/dxA - nd(2) + Rgen(2);

    dCGABMEAdt(i) = -uvAB*(CGABMEAp(i+1) - CGABMEAp(i))/(dxA) + nd(2);

    dCLABH2Odt(i) = ulAB*(CLABH2Op(i+1) - CLABH2Op(i))/dxA - nd(3);

    dCGABH2Odt(i) = -uvAB*(CGABH2Op(i+1) - CGABH2Op(i))/(dxA) + nd(3);

    dCLABN2dt(i) = ulAB*(CLABN2p(i+1) - CLABN2p(i))/dxA - nd(4);

    dCGABN2dt(i) = -uvAB*(CGABN2p(i+1) - CGABN2p(i))/(dxA) + nd(4);

    dCLABO2dt(i) = ulAB*(CLABO2p(i+1) - CLABO2p(i))/dxA - nd(5);

    dCGABO2dt(i) = -uvAB*(CGABO2p(i+1) - CGABO2p(i))/(dxA) + nd(5);

     dCLABMEAHdt(i) = ulAB*(CLABMEAHp(i+1) - CLABMEAHp(i))/dxA + Rgen(6);

     dCLABMEACOOdt(i) = ulAB*(CLABMEACOOp(i+1) - CLABMEACOOp(i))/dxA +
Rgen(7);

     dCLABHCO3dt(i) = ulAB*(CLABHCO3p(i+1) - CLABHCO3p(i))/dxA + Rgen(8);

     dCLABOHdt(i) = ulAB*(CLABOHp(i+1) - CLABOHp(i))/dxA + Rgen(9);

     dCLABHdt(i) = ulAB*(CLABHp(i+1) - CLABHp(i))/dxA + Rgen(10);

     dPABdt(i) = 0;

     dTGABdt(i) = -uvAB*(TGABp(i+1) - TGABp(i))/dxA + Tgd;

     dTLABdt(i) = ulAB*(TLABp(i+1) - TLABp(i))/dxA  +  Tld;

end

% collect in outputt vector
dABdt=[dCLABCO2dt';dCGABCO2dt';dCLABMEAdt';dCGABMEAdt';dCLABH2Odt';dCGABH2Odt
';dCLABN2dt';dCGABN2dt';dCLABO2dt';dCGABO2dt';dCLABHdt';dCLABOHdt';dCLABMEAHd
t';dCLABMEACOOdt';dCLABHCO3dt';dPABdt';dTGABdt';dTLABdt'];

% repeat above for stripper
for i = 1:Ns;

Cl(1)=CLSCO2(i);
Cl(2)=CLSMEA(i);
Cl(3)=CLSH2O(i);
Cl(4)=CLSN2(i);
Cl(5)=CLSO2(i);
```

```
Cl(6)=CLSMEAH(i);
Cl(7)=CLSMEACOO(i);
Cl(8)=CLSHCO3(i);
Cl(9)=CLSOH(i);
Cl(10)=CLSH(i);

Tg=TGS(i);
Tl=TLS(i);
PS=PTS(i);

Cg(1)=CGSCO2(i);
Cg(2)=CGSMEA(i);
Cg(3)=CGSH2O(i);
Cg(4)=CGSN2(i);
Cg(5)=CGSO2(i);

TP(1)=Tg;
TP(2)=Tl;
TP(3)=PS;

[Rgen,Ra]= reactions(Cl,TP,t);

[nd,Z,aw,rhov,mewg,ht,E] = vari(TP,Cg,Cl,uS);

[Tld,Tgd] = HEAT(TP,uS,Cl,Cg,aw,rhov,nd,Ra,mewg,ht,t,E);

    uvS=uvS/(1-ht);
    dCLSCO2dt(i) = ulS*(CLSCO2p(i+1) - CLSCO2p(i))/dxS - nd(1)  + Rgen(1);

    dCGSCO2dt(i) = -uvS*(CGSCO2p(i+1) - CGSCO2p(i))/(dxS) + nd(1);



    dCLSMEAdt(i) = ulS*(CLSMEAp(i+1) - CLSMEAp(i))/dxS - nd(2) + Rgen(2);

    dCGSMEAdt(i) = -uvS*(CGSMEAp(i+1) - CGSMEAp(i))/(dxS) + nd(2);



    dCLSH2Odt(i) = ulS*(CLSH2Op(i+1) - CLSH2Op(i))/dxS - nd(3);

    dCGSH2Odt(i) = -uvS*(CGSH2Op(i+1) - CGSH2Op(i))/(dxS) + nd(3);


    dCLSN2dt(i) = ulS*(CLSN2p(i+1) - CLSN2p(i))/dxS - nd(4);

    dCGSN2dt(i) = -uvS*(CGSN2p(i+1) - CGSN2p(i))/(dxS) + nd(4);


    dCLSO2dt(i) = ulS*(CLSO2p(i+1) - CLSO2p(i))/dxS - nd(5);

    dCGSO2dt(i) = -uvS*(CGSO2p(i+1) - CGSO2p(i))/(dxS) + nd(5);



     dCLSMEAHdt(i) = ulS*(CLSMEAHp(i+1) - CLSMEAHp(i))/dxS + Rgen(6);

     dCLSMEACOOdt(i) = ulS*(CLSMEACOOp(i+1) - CLSMEACOOp(i))/dxS + Rgen(7);

     dCLSHCO3dt(i) = ulS*(CLSHCO3p(i+1) - CLSHCO3p(i))/dxS + Rgen(8);
```

```
     dCLSOHdt(i) = ulS*(CLSOHp(i+1) - CLSOHp(i))/dxS + Rgen(9);

     dCLSHdt(i) = ulS*(CLSHp(i+1) - CLSHp(i))/dxS + Rgen(10);

     dPSdt(i) = 0;

      dTGSdt(i) = -uvS*(TGSp(i+1) - TGSp(i))/dxS + Tgd;

     dTLSdt(i) = ulS*(TLSp(i+1) - TLSp(i))/dxS  +  Tld;

end


dSdt=[dCLSCO2dt';dCGSCO2dt';dCLSMEAdt';dCGSMEAdt';dCLSH2Odt';dCGSH2Odt';dCLSN
2dt';dCGSN2dt';dCLSO2dt';dCGSO2dt';dCLSHdt';dCLSOHdt';dCLSMEAHdt';dCLSMEACOOd
t';dCLSHCO3dt';dPSdt';dTGSdt';dTLSdt'];
%final output vector for ode
dCdt=[dABdt;dSdt];
```

Condenser.m

```
function [TlSIN,ClSin,ulS,Vdot6,n11] =
condenser(TPCoin,CGSCoin,VGS,QRb,TLSin,CLAB,molflow3,Richpumppower,Leanpumppo
wer);

% call in inforamtion
TgC=TPCoin(1);
TlC=TPCoin(2);
P=TPCoin(3);
para;

%5 calculate cp vvalues
Ttg=[1 TgC TgC^2 TgC^3]';
Cpg=Cpgi*Ttg;

Ttl=[1 TlCoout/1000 (TlCoout/1000)^2 (TlCoout/1000)^3 1/((TlCoout/1000)^2)]';
Cpl=Cpli*Ttl;   %J/molK

% flow from absorber
molflABout=molflow3;
n4=sum(molflABout);

% flow into stripper from condenser
for i=1:5
    molflgCoin(i)=VGS*CGSCoin(i);
end
n10=sum(molflgCoin);

% reflux flow to top of stripper
molfllCoout=[0 molflgCoin(2)*refluxrat molflgCoin(3)*refluxrat 0 0 0 0 0 0
0];
n5=sum(molfllCoout);
% flow to stripper
molflSin=molflABout+molfllCoout;
n6=sum(molflSin);

n11=n10-n5;

% heat from cooling gas and condensing
Cpcg=CGSCoin*Cpg*VGS; %J/Ks
```

```
dTg=TlCoout-TgC;
heatcpg=Cpcg*dTg;
heatvap=molfllCoout*delHlv'; %J/s
QC=(heatcpg-heatvap);

% consumed energy and cost per kg
Cons=Richpumppower+Leanpumppower+QRb;
molflowCO2=CGSCoin(1)*VGS;  %mol/s
masflowCO2=molflowCO2*MW(1);  %g/s
remoavalcost=(Cons/masflowCO2); %J/g
remcostMJKg=remoavalcost*1e-3;

% temp calc for liquid entering stripper
QABout=molflABout*Cpl*TLSin;
QCoout=molfllCoout*Cpl*TlCoout;
QS=QABout+QCoout;
TlSIN=QS/(molflSin*Cpl);

% calculation of collect gas compostion
for i=1:5
    molflgCoout(i)=molfllCoout(i);

end
molflClean=molflgCoin-molflgCoout;

for i=1:5
    yclean(i)=molflClean(i)/sum(molflClean);
end

% calclation of volume flow rate of liquid into stripper
for i=1:10
    x(i)=molflSin(i)/sum(molflSin);
end

y=x;
TP(1)=TlSIN;
TP(2)=TlSIN;
TP(3)=P;

[K,Z,fhi] = PEA(TP,y,x);

Vdot6=Z(1)*sum(molflSin)*R*TlSIN/P;

% stripper velocity and concentration
ulS=Vdot6/AStripper;
for i=1:10
    ClSin(i)=molflSin(i)/(Vdot6);
end
```

Heat.m

```
function [Tld,Tgd] = HEAT(TP,u,Cl,Cg,aw,rhov,nd,Ra,mewg,ht,t,E)

Tg=TP(1);
Tl=TP(2);
P=TP(3);

para;
ul=u(1);
ug=u(2);
```

```
% calculate Cp values
Ttg=[1 Tg Tg^2 Tg^3]';
Ttl=[1 Tl/1000 (Tl/1000)^2 (Tl/1000)^3 1/((Tl/1000)^2)]';
Cpg=Cpgi*Ttg;  %J/molK
Cpl=Cpli*Ttl;   %J/molK

for i=1:10
Cplma(i)=Cpl(i)/MW(i);  %maybe no 1000   J/g K
end
for i=1:5
Cpgma(i)=Cpg(i)/MW(i);  %maybe no 1000   J/g K
end

% co2 loading
CO2=Cl(1)+Cl(7)+Cl(8);
MEA=Cl(2)+Cl(6)+Cl(7);

load=CO2/MEA;

%alternative function for heat heat of reaction
% Hr=-(65.7-(73.725*(Cl(1)/Cl(2))^1)+(154.03*(Cl(1)/Cl(2))^2)-
(147.06*(Cl(1)/Cl(2))^3)+(52.75*(Cl(1)/Cl(2))^4))*1000;

% function of heat of reaction
Hy = -2.798*(load^5) + 1.6545*(load^4)-0.1686*(load^3) -0.04535*(load^2)
+0.00839*load + 0.085017;
Hy2 =-0.1256*(load^5) + 0.6377*(load^4)-1.2818*(load^3) + 1.2757*(load^2) -
0.6319*load + 0.129077;

if load<0.55
    Hr2=-Hy*1e6;
else Hr2=-Hy2*1e7;
end

if load<1.2
    Hr3=Hr2;
else Hr3=-2e4;
end

% thermal mass of system ( concentation x cp)
for i=1:N
CCg(i)=Cpg(i)*Cg(i); %J/m3K
CCl(i)=Cpl(i)*Cl(i);   %J/m3K
end

CCgt=sum(CCg);  %J/m3K
CClt=sum(CCl);    %J/m3K

diff=nd(1);
%gas mol fraction
for i=1:5
    yg(i)=Cg(i)/sum(Cg);
end
% thermal conductivity
kCO2=0.076*Tg-6.337;
kN2=0.069*Tg+4.84;
kH2O=0.075*Tg-3.9;

kT=(yg(1)*kCO2+yg(2)*kH2O+yg(3)*kH2O+yg(4)*kN2+yg(5)*kN2)*0.001;
```

```
% covert cp to J/kg K
CpvT=CCgt/sum(Cg);   %J/mol K
MWkg=sum(Cg)/rhov ;  %mol/kg
CpvTkg=CpvT*MWkg;   %J/kg K

% diffusvity
DvCO2=(8.65e-5*Tg^1.75)/P;
Dvmea=(5.33e-5*Tg^1.75)/P;
Dvh2o=(1.2e-4*Tg^1.75)/P ; %as per reid
DvN2=(9.5e-5*Tg^1.75)/P;
DvO2=(1.16e-4*Tg^1.75)/P;
DvT=(yg(1)*DvCO2+yg(2)*Dvmea+yg(3)*Dvh2o+yg(4)*DvN2+yg(5)*DvO2);

%  combined mass transfer coefficient
ug=ug/(1-ht);
kdvT=((Cv*a*DvT)/((4*(epslom^2)-
(4*epslom*ht))^(1/2)))*((ug*rhov/(a*mewg))^(3/4))*(mewg/(rhov*DvT))^(1/3);

% heat transfre coefficeient
hv=kdvT*((rhov*CpvTkg)^(1/3))*((kT/DvT)^(2/3));

q=aw*hv*(Tl-Tg);  % sensible heat

% Rea=(Hr*diff);
Rea=(Hr3*diff);  % heat of reaction

Hdf=nd*delHlvv;       % heat of dif

Tl1=(Rea-q-Hdf)/CClt;  % change in heat liquid
Tg1=(q-Hdf)/CCgt;       %change in heat gas


Hdiff=nd*delHlvv;

Hreact=delHr*Ra;  % heat from reaction using rate of reaction
% change in heat 2nd method
Tl2=(-Hdiff-Hreact-q)/CClt;
Tg2=(-Hdiff+q)/CCgt;


% selection of method
if t<1e8
   Tgd=Tg1;

else Tgd=Tg2;
end

if t<1e8
    Tld=Tl1;


else Tld=Tl2;

end
```

HeatexlR.m

```
function [TLSin,Richpumppower,Leanpumppower,molflow3,n3] =
HeatexlR(TLSout,TLABout,CLAB,CLSout,Vdot9)

para;
%  assigne temperatures
Tl9=TLSout;
Tl3=TLABout;
% calculate pinch
Tl12=Tl3+10;

% calculate Cp
Tl=(Tl12+Tl9)/2;
Ttl=[1 Tl/1000 (Tl/1000)^2 (Tl/1000)^3 1/((Tl/1000)^2)]';
Cpl=Cpli*Ttl;   %J/molK

% heat removed from lean stream
qHX=(Tl9-Tl12)*CLSout*Cpl*Vdot9;

% log mean temp difference of heat
dtlog=(qHX/(UA));

%iterate on Tl4 to find log mean temp diff with other formula
Tl4=Tl9-13.5;

for j=1:M

    dt1=Tl9-Tl4;
    dt2=Tl12-Tl3;

    dTlog=(dt1-dt2)/log(dt1/dt2); % other log mean temp formula
    Del=dtlog-dTlog;

    if abs(  Del ) <  eps_abs;
        break;
    elseif j == M;
        error( 'Ns method nverge' );
    end
    Tl4=Tl4-Del/10;
end

% CP and heat of second heat exchanger
Tl2=(TLABin+Tl12)/2;
Ttl2=[1 Tl2/1000 (Tl2/1000)^2 (Tl2/1000)^3 1/((Tl2/1000)^2)]';
Cpl2=Cpli*Ttl2;   %J/molK
QHX=(CLSout*Cpl2*Vdot3)*(TLABin-Tl12);

% liquid density
for i=1:10
    denlAb(i)=CLAB(i)*MW(i)/1000;
end
rholAb=sum(denlAb);

Richpumppower=Vdot3*rholAb*PRichPres*g;  %Pump power Watts

for i=1:10
    denlS(i)=CLSout(i)*MW(i)/1000;
end
rholS=sum(denlS);
```

```
Leanpumppower=Vdot9*rholS*PleanPres*g;  %pump power watts

% mol flow of stream from absorber to condenser
for i=1:10
    molflow3(i)=CLAB(i)*Vdot3;
end
n3=sum(molflow3);
n4=n3;

TLSin=Tl4;
```

inletvalues.m

```
function [C0,uAB]=inletvalues;

para;
%mol fraction inlet gas
y0(1)=0.04;
y0(2)=0.0;
y0(3)=0.08;
y0(4)=0.76;
y0(5)=0.12;

%Mass flow CO2
mafg(1)=32000; %g/s   0
molfg(1)=mafg(1)/MW(1);
tmolfg =molfg(1)/y0(1);
% mol flow of each species in gas
for i=1:5
    molfg(i)=tmolfg*y0(i);
    molfrac(i)=molfg(i)/tmolfg;
end

% volume flow of gas
VGAB=tmolfg*R*TGABin/PrAB;

for i=1:5
    Cg0(i)=molfg(i)/VGAB;
end

uvAB=VGAB/AreaAB; %gas velocity

% weight fractions of liquid
x0(1)=0.0;
x0(2)=0.3;
x0(3)=0.7;
x0(4)=0;
x0(5)=0;
x0(6)=0;
x0(7)=0;
x0(8)=0;
x0(9)=0;
x0(10)=0;

masflt=Vdot3*1e6;  % mass flow  total

for i=1:10
    masfl(i)=masflt*x0(i);  % mass flow each species
end
```

```
for i=1:10
    molfl(i)=masfl(i)/MW(i);  % mol flow each species
end

for i=1:10
    Cl0(i)=molfl(i)/Vdot3;  % consentration each species
end

ulAB=Vdot3/AreaAB;
uAB=[ulAB,uvAB];
Cl0';
Cg0';
PrAB;
CAB0=[Cl0(1),Cg0(1),Cl0(2),Cg0(2),Cl0(3),Cg0(3),Cl0(4),Cg0(4),Cl0(5),Cg0(5),C
l0(6),Cl0(7),Cl0(8),Cl0(9),Cl0(10),PrAB,TGABin,TLABin]';

ClC02i=1.5e-1;
CgC02i=0.1;
Clmeai=2600;
Cgmeai=0.4;
Clh2oi=38000;
Cgh2oi=60;  %
ClN2i=0;
CgN2i=0;
ClO2i=0;
CgO2i=0;
ClHi=3.2e-5;
ClOHi=7.5e-6;
ClMEAHi=1100;
ClMEACOOi=1100;
ClHCO3i=10;
Pti=PrRB;
Tgi=TGRBOUT;
Tli=TGRBOUT;
CS0=[ClC02i,CgC02i,Clmeai,Cgmeai,Clh2oi,Cgh2oi,ClN2i,CgN2i,ClO2i,CgO2i,ClHi,C
lOHi,ClMEAHi,ClMEACOOi,ClHCO3i,Pti,Tgi,Tli]';

C0=[CAB0;CS0];
```

NPLE.m

```
function [xi,yi,Z,K,fhi]=NLPE(TP,xl,yg,Cl);
para;

Tg=TP(1);
Tl=TP(2);
P=TP(3);
eps_abs=1e-10;
% set values for first iteration
xi=xl;
yi=yg;

  % iterate on 5 unknowns to find values when then dont change
     for j=1:M

         [K,Z,fhi] = PEA(TP,yi,xi);

             xi(1)=yi(1)/K(1);
             yi(2)=K(2)*xi(2);
             yi(3)=K(3)*xi(3);
```

```
            xi(4)=yi(4)/K(4);
            xi(5)=yi(5)/K(5);
            yi(4)=1-yi(1)-yi(2)-yi(3)-yi(5);
            xi(3)=1-xi(1)-xi(2)-xi(4)-xi(5)-xi(6)-xi(7)-xi(8)-xi(9)-xi(10);

         AS(j+1)=xi(1);
         Del=AS(j+1)-AS(j);

        if abs(  Del ) <  eps_abs;
        break;
        elseif j == M;
        error( 'Ns method nverge' );
        end

   end
```

Output.m

```
function [Vdot7]=Output(Cc,C0,dxA,dxS,uAB,tf,Ns)

t=tf;%extract simulation end values
OUT(1,:)=Cc(end,1:Ns);
for i=1:35
    x=Ns*i;
    OUT(i+1,:) = Cc(end,x+1:x+Ns);
end
OUT=OUT';
para;
DD=size(OUT);
B = DD(1);
Ns=B;

% reperat one time step to find result
CLABCO2 = OUT(:,1);
CGABCO2 = OUT(:,2);
CLABMEA = OUT(:,3);
CGABMEA= OUT(:,4);
CLABH2O =OUT(:,5);
CGABH2O = OUT(:,6);
CLABN2 = OUT(:,7);
CGABN2 = OUT(:,8);
CLABO2 = OUT(:,9);
CGABO2 = OUT(:,10);
CLABH = OUT(:,11);
CLABOH = OUT(:,12);
CLABMEAH = OUT(:,13);
CLABMEACOO =OUT(:,14);
CLABHCO3 = OUT(:,15);
PTAB = OUT(:,16);
TGAB = OUT(:,17);
TLAB = OUT(:,18);
CLSCO2 = OUT(:,19);
CGSCO2 = OUT(:,20);
CLSMEA = OUT(:,21);
CGSMEA= OUT(:,22);
CLSH2O = OUT(:,23);
CGSH2O = OUT(:,24);
CLSN2 = OUT(:,25);
CGSN2 = OUT(:,26);
CLSO2 = OUT(:,27);
```

```
CGSO2 = OUT(:,28);
CLSH = OUT(:,29);
CLSOH = OUT(:,30);
CLSMEAH = OUT(:,31);
CLSMEACOO =OUT(:,32);
CLSHCO3 = OUT(:,33);
PTS = OUT(:,34);
TGS = OUT(:,35);
TLS = OUT(:,36);

TPRBin(1)=TGS(1);
TPRBin(2)=TLS(1);
TPRBin(3)=PTS(1);

CLRBin(1)=CLSCO2(1);
CLRBin(2)=CLSMEA(1);
CLRBin(3)=CLSH2O(1);
CLRBin(4)=CLSN2(1);
CLRBin(5)=CLSO2(1);
CLRBin(6)=CLSMEAH(1);
CLRBin(7)=CLSMEACOO(1);
CLRBin(8)=CLSHCO3(1);
CLRBin(9)=CLSOH(1);
CLRBin(10)=CLSH(1);

CLAB(1)=CLABCO2(1);
CLAB(2)=CLABMEA(1);
CLAB(3)=CLABH2O(1);
CLAB(4)=CLABN2(1);
CLAB(5)=CLABO2(1);
CLAB(6)=CLABMEAH(1);
CLAB(7)=CLABMEACOO(1);
CLAB(8)=CLABHCO3(1);
CLAB(9)=CLABOH(1);
CLAB(10)=CLABH(1);


Vdot7=Vdot3*(1+(0.05));

for i=1:M


    [CGRB,uvS,VGS,QRb,CLSout,Vdot9,n9] = reboiler(TPRBin,CLRBin,Vdot7);

    CGSCO20=CGRB(1);
    CGSMEA0=CGRB(2);
    CGSH2O0=CGRB(3);
    CGSN20=CGRB(4);
    CGSO20=CGRB(5);
    TGS0=TGRBOUT;

    TPCoin(1)=TGS(Ns);
    TPCoin(2)=TLS(Ns);
    TPCoin(3)=PTS(Ns);

    CGSCoin(1)=CGSCO2(Ns);
    CGSCoin(2)=CGSMEA(Ns);
    CGSCoin(3)=CGSH2O(Ns);
    CGSCoin(4)=CGSN2(Ns);
    CGSCoin(5)=CGSO2(Ns);
```

```
    TLABout=TLAB(1);
    TLSout=TLS(1);

    [TLSin,Richpumppower,Leanpumppower,molflow3,n3] =
HeatexlR2(TLSout,TLABout,CLAB,CLSout,Vdot9);

    [TlSIN,CLSin,ulS,Vdot6,n11] =
condenser2(TPCoin,CGSCoin,VGS,QRb,TLSin,CLAB,molflow3,Richpumppower,Leanpumpp
ower);

    error=n3-n9-n11;

    Del=Vdot7-Vdot6;

    if abs(  Del ) <  eps_abs;
        break;
    elseif j == M;
        error( 'Ns method nverge' );
    end
    Vdot7=Vdot6;


end

CLSCO20=CLSin(1);
CLSMEA0=CLSin(2);
CLSH2O0=CLSin(3);
CLSN20=CLSin(4);
CLSO20=CLSin(5);
CLSMEAH0=CLSin(6);
CLSMEACOO0=CLSin(7);
CLSHCO30=CLSin(8);
CLSOH0=CLSin(9);
CLSH0=CLSin(10);
TLS0=TlSIN;
PTS0=C0(34);

uS=[ulS,uvS]
uAB

CLSCO2p= [CLSCO2;CLSCO20];
CGSCO2p= [CGSCO20;CGSCO2];
CLSMEAp= [CLSMEA;CLSMEA0];
CGSMEAp= [CGSMEA0;CGSMEA];
CLSH2Op= [CLSH2O;CLSH2O0];
CGSH2Op= [CGSH2O0;CGSH2O];
CLSN2p= [CLSN2;CLSN20];
CGSN2p= [CGSN20;CGSN2];
CLSO2p= [CLSO2;CLSO20];
CGSO2p= [CGSO20;CGSO2];
CLSHp= [CLSH;CLSH0];
CLSOHp= [CLSOH;CLSOH0];
CLSMEAHp= [CLSMEAH;CLSMEAH0];
CLSMEACOOp= [CLSMEACOO;CLSMEACOO0];
CLSHCO3p= [CLSHCO3;CLSHCO30];
PTSp= [PTS0;PTS];
TGSp=[TGS0;TGS];
TLSp=[TLS;TLS0];

CLABCO20=CLSout(1);
```

```
CGABCO20=C0(2);
CLABMEA0=CLSout(2);
CGABMEA0=C0(4);
CLABH2O0=CLSout(3);
CGABH2O0=C0(6);
CLABN20=CLSout(4);
CGABN20=C0(8);
CLABO20=CLSout(5);
CGABO20=C0(10);
CLABMEAH0=CLSout(6);
CLABMEACOO0=CLSout(7);
CLABHCO30=CLSout(8);
CLABOH0=CLSout(9);
CLABH0=CLSout(10);
PTAB0=C0(16);
TGAB0=TGABin;
TLAB0=TLABin;

MEA=C0(3)+C0(11)+C0(12);
CLABMEA0;
CLABMEA0=MEA-CLABMEAH0-CLABMEACOO0;  %do by molflow
CLABH2O0;
CLABH2O0=C0(5);
LOADINGABin=(CLABCO20+CLABHCO30+CLABMEACOO0)/MEA
LOADINGSin=(CLSCO20+CLSHCO30+CLSMEACOO0)/MEA

CLABCO2p= [CLABCO2;CLABCO20];
CGABCO2p= [CGABCO20;CGABCO2];
CLABMEAp= [CLABMEA;CLABMEA0];
CGABMEAp= [CGABMEA0;CGABMEA];
CLABH2Op= [CLABH2O;CLABH2O0];
CGABH2Op= [CGABH2O0;CGABH2O];
CLABN2p= [CLABN2;CLABN20];
CGABN2p= [CGABN20;CGABN2];
CLABO2p= [CLABO2;CLABO20];
CGABO2p= [CGABO20;CGABO2];
CLABHp= [CLABH;CLABH0];
CLABOHp= [CLABOH;CLABOH0];
CLABMEAHp= [CLABMEAH;CLABMEAH0];
CLABMEACOOp= [CLABMEACOO;CLABMEACOO0];
CLABHCO3p= [CLABHCO3;CLABHCO30];
PTABp= [PTAB0;PTAB];
TGABp=[TGAB0;TGAB];
TLABp=[TLAB;TLAB0];



for i = 1:Ns;

    Cl(1)=CLABCO2(i);
    Cl(2)=CLABMEA(i);
    Cl(3)=CLABH2O(i);
    Cl(4)=CLABN2(i);
    Cl(5)=CLABO2(i);
    Cl(6)=CLABMEAH(i);
    Cl(7)=CLABMEACOO(i);
    Cl(8)=CLABHCO3(i);
    Cl(9)=CLABOH(i);
    Cl(10)=CLABH(i);

    Tg=TGAB(i);
```

```
    Tl=TLAB(i);
    PAB=PTAB(i);

    Cg(1)=CGABCO2(i);
    Cg(2)=CGABMEA(i);
    Cg(3)=CGABH2O(i);
    Cg(4)=CGABN2(i);
    Cg(5)=CGABO2(i);

    TP(1)=Tg;
    TP(2)=Tl;
    TP(3)=PAB;

    [Rgen,Ra]= reactions(Cl,TP,t);

    [nd,Z,aw,rhov,mewg,ht,E] = vari(TP,Cg,Cl,uAB);

    [Tld,Tgd] = HEAT(TP,uAB,Cl,Cg,aw,rhov,nd,Ra,mewg,ht,t,E);

    ulAB=uAB(1);
    uvAB=uAB(2);
 end


for i = 1:Ns;

    Cl(1)=CLSCO2(i);
    Cl(2)=CLSMEA(i);
    Cl(3)=CLSH2O(i);
    Cl(4)=CLSN2(i);
    Cl(5)=CLSO2(i);
    Cl(6)=CLSMEAH(i);
    Cl(7)=CLSMEACOO(i);
    Cl(8)=CLSHCO3(i);
    Cl(9)=CLSOH(i);
    Cl(10)=CLSH(i);

    Tg=TGS(i);
    Tl=TLS(i);
    PS=PTS(i);

    Cg(1)=CGSCO2(i);
    Cg(2)=CGSMEA(i);
    Cg(3)=CGSH2O(i);
    Cg(4)=CGSN2(i);
    Cg(5)=CGSO2(i);

    TP(1)=Tg;
    TP(2)=Tl;
    TP(3)=PS;

    [Rgen,Ra]= reactions(Cl,TP,t);

    [nd,Z,aw,rhov,mewg,ht,E] = vari(TP,Cg,Cl,uS);

    [Tld,Tgd] = HEAT(TP,uS,Cl,Cg,aw,rhov,nd,Ra,mewg,ht,t,E);

end
```

PEA.m

```
function [K,Z,fhi] = PEA(TP,y,x);
%call in temp and pressure
Tg=TP(1);
Tl=TP(2);
P=TP(3);
para;
T=Tl;

R = 8.314; % gas constant [=] J/(mol K)
q=size(Q);
N=q(1);

for j=1:N;

    % Reduced variables
    Tc(j)=Q(j,1);
    Pc(j)=Q(j,2);
    w(j)=Q(j,3);
    Tr(j)= T/Tc(j);
    Pr(j)= P/Pc(j);
    % Parameters of the EOS for a pure component
    m(j) = 0.37464 + 1.54226*w(j) - 0.26992*w(j)^2;
    alfa(j) = (1 + m(j)*(1 - sqrt(Tr(j))))^2;
    a(j) = 0.45724*((R*Tc(j))^2/Pc(j))*alfa(j);
    b(j) = 0.0778*R*Tc(j)/Pc(j);

    A(j)= a(j)*P/(R*T)^2;
    B(j)= b(j)*P/(R*T);
end

i=1;
j=1;
%set up mixing matrix
for j=1:N

    for i=1:N

        E(i,j)=y(i)*y(j)*(1-delta(i,j))*(A(i)*A(j))^0.5;
        EE(i,j)=(1-delta(i,j))*(A(i)*A(j))^0.5;
    end
    F(j)=B(j)*y(j);
end
% calculate mixed parameters
e=sum(E);
AA=sum(e);
BB=sum(F);

% Compressibility factor
Z = roots([1 -(1-BB) (AA-3*BB^2-2*BB) -(AA*BB-BB^2-BB^3)]);

ZR = [];

for i = 1:3;
    if isreal(Z(i));
        ZR(i) = Z(i);
    end
end

ZZ = max(ZR);  %max root for vapour
```

```
for i=1:N;

    for k=1:N;

        Ay(k)=y(k)*EE(i,k);
        AY=sum(Ay);
    end

    %calculate fugacity for each species
    fhi(i,2) = exp((B(i)/BB)*(ZZ- 1)- log(ZZ-BB) -
(AA/(2*BB*sqrt(2)))*log((ZZ+(1+sqrt(2))*BB)/(ZZ+(1-sqrt(2))*BB))*((2*(AY/AA)-
(B(i)/BB))));

end
ZZg=ZZ;


%repeat for liquid phase
for j=1:N

    for i=1:N
            El(i,j)=x(i)*x(j)*(1-delta(i,j))*(A(i)*A(j))^0.5;
            EEl(i,j)=(1-delta(i,j))*(A(i)*A(j))^0.5;
    end
    F(j)=B(j)*x(j);
end
e=sum(El);
AA=sum(e);
BB=sum(F);

% Compressibility factor
Z = roots([1 -(1-BB) (AA-3*BB^2-2*BB) -(AA*BB-BB^2-BB^3)]);

ZR=[];
for i = 1:3;
    if isreal(Z(i));
        ZR(i) = Z(i);
    end
end
ZZ = abs(min(ZR));
if ZZ==0
    ZZ = abs(max(ZR));
end

for i=1:N;

    for k=1:N;
        Ax(k)=x(k)*EEl(i,k);
        AX(i)=sum(Ax);
    end

    fhi(i,1) = exp((B(i)/BB)*(ZZ- 1)- log(ZZ-BB) -
(AA/(2*BB*sqrt(2)))*log((ZZ+(1+sqrt(2))*BB)/(ZZ+(1-
sqrt(2))*BB))*((2*(AX(i)/AA)-(B(i)/BB))));

end

ZZl=ZZ;
Z=[ZZl',ZZg'];
%calclate phi ratio which is ratio of liquid to gas
```

```
for i=1:N
    K(i)=fhi(i,1)/fhi(i,2);
end
```

reactions.m

```
function [Rgen,Ra]=reactions(Cl,TP,t)
%
Tl=TP(2);  %liquid temp

kf=zeros(6,1);

%forward reaction rates
kf(1)=4.4e8*exp(-5400/Tl );
kf(2)=0.024;%  m3/mol s;
kf(3)=4.3e8*exp(-6668/Tl);
kf(3)=10^(13.65-2895/Tl)*1e-3;
kf(4)=2e-5; %;
kf(5)=1e-1;
kf(6)=1e-1;
kf(1)=3.951e10*exp(-6863/Tl);  %Jamal

%li mather  (Liu) equilbruim constants
K2=1e6*exp(231.465-(12092.1/Tl)-36.7816*log(Tl));
K4=1e6*exp(132.899-13445.9/Tl-22.4773*log(Tl));
K5=1e6*exp(0.79960-8094.81/Tl-0.007484*Tl);
K6=1e6*exp(1.282562-(3456.179/Tl))/5 ; %5
K1=K2/(K5*K6);
K3=K2/K4;

%actula concentration equilbruim
Kee1=(Cl(6)*Cl(7)/(Cl(1)*Cl(2)^2));
Kee2=Cl(8)*Cl(10)/(Cl(1));
Kee3=Cl(8)/(Cl(1)*Cl(9));
Kee4=Cl(9)*Cl(10);
Kee5=(Cl(2)*Cl(10))/Cl(6);
Kee6=(Cl(2)*Cl(8))/Cl(7);

%reversre reaction rate
kr(1)=kf(1)/K1;
kr(2)=kf(2)/K2;
kr(3)=kf(3)/K3;
kr(4)=kf(4)/K4;
kr(5)=kf(5)/K5;
kr(6)=kf(6)/K6;

% forward and reverse reaction rates
Rf(1)=Cl(1)*(Cl(2)^2)*kf(1);
Rr(1)=Cl(6)*Cl(7)*kr(1);

Rf(2)=Cl(1)*kf(2);
Rr(2)=Cl(8)*Cl(10)*kr(2);

Rf(3)=Cl(1)*Cl(9)*kf(3);
Rr(3)=Cl(8)*kr(3);

Rf(4)=kf(4);
Rr(4)=Cl(9)*Cl(10)*kr(4);

Rf(5)=Cl(6)*kf(5);
Rr(5)=Cl(2)*Cl(10)*kr(5);
```

```
Rf(6)=Cl(7)*kf(6);
Rr(6)=Cl(2)*Cl(8)*kr(6);


Ra=Rf'-Rr';  % overall reaction rate

%actual eq constant minus nummerical value at eq are equal
Kt1=Kee1-K1;
Kt2=Kee2-K2;
Kt3=Kee3-K3;
Kt4=Kee4-K4;
Kt5=Kee5-K5;
Kt6=Kee6-K6;
%stiochmetric matrix
ST=[-1 -2 0 0 0 1 1 0 0 0
    -1 0 0 0 0 0 0 1 0 1
    -1 0 0 0 0 0 0 1 -1 0
    0 0 0 0 0 0 0 0 1 1
    0 1 0 0 0 -1 0 0 0 1
    0 1 0 0 0 0 -1 1 0 0];


Rgen=ST'*Ra; % rate of generation vector

tr=1/(kf(1)+kr(1)); %time for reaction to take place
```

reboiler.m

```
function [CGRB,uvS,VGS,QRb,CLSout,Vdot9,n9T]=reboiler(TPRBin,CLRBin,Vdot7)

TgRB=TPRBin(1);
TlRB=TPRBin(2);
PRB=TPRBin(3);
para;

Tl1=(TlRB+TGRBOUT)/2;
Ttl=[1 Tl1/1000 (Tl1/1000)^2 (Tl1/1000)^3 1/((Tl1/1000)^2)]';

Cpl=Cpli*Ttl;  %J/molK

for i=1:10
    molflRBin(i)=CLRBin(i)*Vdot7;

end

for i=6:10
    n9(i)=molflRBin(i);
end

for i=1:5
    n71(i)=CLRBin(i)*Vdot7;
end

 for i=1:5
    z(i)=molflRBin(i)/sum(n71);
end
n7=sum(molflRBin);
```

```
n7x=sum(n71);
x=z;
y=x;
TP(1)=TGRBOUT;
TP(2)=TGRBOUT;
TP(3)=PrRB;
LF=0.5;

for k=1:M

[K,Z,fhi] = PEA(TP,y,x);


for j=1:M

for i=1:5
    a(i)=1-K(i);
    ob(i)=(z(i)*a(i));
    oj(i)=K(i)+(LF*a(i));
    obj(i)=ob(i)/oj(i);
end


    Del=sum(obj);

    if abs(  Del ) <  eps_abs;
        break;
    elseif i == M;
        error( 'Ns method nverge' );
    end

   LF=LF+Del/1;
end


for i=1:5
    bo(i)=K(i)+(LF*(1-K(i)));
    x(i)=z(i)/bo(i);
    y(i)=x(i)*K(i);
end

    AS(k+1)=x(2);

         Del=AS(k+1)-AS(k);

        if abs(  Del ) <  eps_abs;
        break;
        elseif j == M;
        error( 'Ns method nverge' );
        end
end

n92=n7x*LF;
n8=n7x-n92;

for i=1:5
    n9(i)=x(i)*n92;
end
```

```
VGS=n8*R*TGRBOUT/PrRB;
uvS=VGS/AStripper;

for i=1:5
    n8g(i)=y(i)*n8;
    CGRB(i)=n8g(i)/VGS;
end

dTl=(TGRBOUT-TlRB);%K
Cpcl=molflRBin*Cpl;

heatcpl=Cpcl*dTl; %J/s
heatvap=n8g*delHlvv;

QRb=(heatcpl+heatvap);

n9T=sum(n9);
for i=1:10
    x(i)=n9(i)/n9T;
end

y=x;
TP(1)=TGRBOUT;
TP(2)=TGRBOUT;
TP(3)=PrRB;

[K,Z,fhi] = PEA(TP,y,x);

Vdot9=Z(1)*n9T*R*TGRBOUT/PrRB;


for i=1:10
    CLSout(i)=n9(i)/Vdot9;
end
LF
end
```

startvalues.m

```
function [INT]=startvalues(Ns,LA,LS);
load 2;
INT(1,:)=Cc(end,1:5);
for i=1:35
    x=5*i;
INT(i+1,:) = Cc(end,x+1:x+5);
end
INT;

N=Ns-1;
dxA=LA/N;
dxS=LS/N;

xA=[0:(25/4):25];
xS=[0:(15/4):15];
xxA=[0:dxA:LA];
xxS=[0:dxS:LS];
```

```
for i=1:36
y(i,:)=INT(i,:);
if i<19
yy(i,:)=interp1(xA,y(i,:),xxA,'cubic');
else
yy(i,:)=interp1(xS,y(i,:),xxS,'cubic');
end
end
yy;

INT=yy';
```

Vari.m

```
function [nd,Z,aw,rhov,mewg,ht,E] = vari(TP,Cg,Cl,u)

Tg=TP(1);
Tl=TP(2);
P=TP(3);


TP=[Tg,Tl,P];
para;
ul=u(1);
uv=u(2);

 for i=1:5
    yg(i)=Cg(i)/sum(Cg);
end

for i=1:10
    xl(i)=Cl(i)/sum(Cl);
end

[xi,yi,Z,K,fhi]=NLPE(TP,xl,yg,Cl);


AA=[1-xi(1),0,0,-xi(1),-xi(1);0,1-yi(2),-yi(2),0,0;0,-yi(3),1-yi(3),0,0;-
xi(4),0,0,1-xi(4),-xi(4);-xi(5),0,0,-xi(5),1-xi(5)];
BB=[xi(1)*(Cl(2)+Cl(3));yi(2)*(Cg(1)+Cg(4)+Cg(5));yi(3)*(Cg(1)+Cg(4)+Cg(5));x
i(4)*(Cl(2)+Cl(3));xi(5)*(Cl(2)+Cl(3))];

Cint=AA\BB;
Cgi=[Cg(1),Cint(2),Cint(3),Cg(4),Cg(5)]';
Cli=[Cint(1),Cl(2),Cl(3),Cint(4),Cint(5)]';

xmea1=xl(2);
xwat1=xl(3);
xt=xmea1+xwat1;
xmea=xmea1/xt;
xwat=xwat1/xt;

Hwat=1*exp(170.7126-(8477.7771/Tl)-21.95743*log(Tl)+0.005781*Tl);  %Pa
Hmea=1*exp(89.452-(2934.6/Tl)-11.592*log(Tl)+0.01644*Tl);          %Pa
Hmix=(xwat*Hwat+xmea*Hmea);
H(1)=Hmix/sum(Cl); %Pa m3/mol
H(4)=(1639.34)*101.325*exp(-1300*((1/Tl)-(1/298)));    %Pa m3/mol
H(5)=(769.23)*101.325*exp(-1700*((1/Tl)-(1/298)));     %Pa m3/mol

z=[0 0 0 0 0 1 -1 -1 -1 1];
```

```
for i=1:7
    ion(i)=Cl(i)*z(i)^2;
    I=0.5*sum(ion);
end
I=I/1000;
ha=[0 -0.019 0 0 0 0.055 0.043 0.073 0 0];
haa=sum(ha);
cor=10^(haa*I);
H=cor.*H;


G=372.1-3.11*Tl+8.8092e-3*Tl^2-8.3457e-6*Tl^3;
mewwater=2.414e-5*10^(247.8/(Tl-140));  %wikipedia
mewamine=exp(-3.9356+(1010.8/(Tl-151.17)))/1000;
%dag papaer
mewmix=exp((xl(2)*log(mewamine))+(xl(3)*log(mewwater))+xl(2)*xl(3)*G);
r=1+0.83031*(xl(1)/xl(2))+0.35786*(xl(1)/xl(2))^2;
mewsol=1.2*mewmix*r;

mewvC02=4.35e-8*Tg+1.93e-6;
mewv02=4.84e-8*Tg+6.13e-6;
mewvN2=3.97e-8*Tg+6.03e-6;
mewvH2O=4.44e-8*Tg-4.61e-6;
mewg=exp((yg(1)*log(mewvC02))+(yg(3)*log(mewvH2O)+(yg(4)*log(mewv02))+(yg(5)*
log(mewvN2))));


for i=1:10
    mal(i)=MW(i)*Cl(i);
end

for i=1:N
    mav(i)=MW(i)*Cg(i);
end

rhol=sum(mal)*1e-3;
rhov=sum(mav)*1e-3;

Re=(ul*rhol)/(a*mewsol);
aw1=a*Ch*((ul*rhol/(a*mewsol))^0.15)*(ul^2*a/g)^0.1;
aw2=a*Ch*0.85*((ul*rhol/(a*mewsol))^0.25)*(ul^2*a/g)^0.1;

if Re<5
    aw=aw1;
else aw=aw2;
end


ht=((12*ul*(a^2)*mewsol/(rhol*g))^(1/3))*(aw/a)^(2/3);
uv=uv/(1-ht);

Dwco2=2.35e-6*exp(-2119/Tl);   %from reid page615
Dlco2=Dwco2*(mewwater/mewsol)^0.51; %modified stokes einstein  maceiras
papaer

Dvh2o=(1.20e-4*Tg^1.75)/P;  %as per reid
Dvmea=(5.32e-5*Tg^1.75)/P;  %as per reid
Dvco2=(8.65e-5*Tg^1.75)/P;

Klco2=Cll*((rhol*g/mewsol)^(1/6))*((a*Dlco2/4*epslom)^(1/2))*(ul/a)^(1/3);
```

```
Kvco2=(Cv*a*Dvco2/((4*epslom^2-
4*epslom*ht)^(1/2)))*((uv*rhov/(a*mewg))^(3/4))*(mewg/(rhov*Dvco2))^(1/3);
Kvh20=(Cv*a*Dvh2o/((4*epslom^2-
4*epslom*ht)^(1/2)))*((uv*rhov/(a*mewg))^(3/4))*(mewg/(rhov*Dvh2o))^(1/3);
Kvmea=(Cv*a*Dvmea/((4*epslom^2-
4*epslom*ht)^(1/2)))*((uv*rhov/(a*mewg))^(3/4))*(mewg/(rhov*Dvmea))^(1/3);

Kl(1)=Klco2;
Kl(2)=Kvmea;
Kl(3)=Kvh20;
Kl(4)=Klco2;
Kl(5)=Klco2;

kmea=4.4e8*exp(-5400/Tl);
koh=10^(13.65-2895/Tl)*1e-3;
kov=kmea*Cl(2)+koh*Cl(1);
E=((kov*Dlco2)^0.5)/Kl(1);

R1=H(1)/(E*Klco2);
R2=R*Tg*Z(2)/Kvco2;
KH(1)=1/(R1+R2);

Pco2=Cg(1)*R*Tg*Z(2);
PN2=Cg(4)*R*Tg*Z(2);
PO2=Cg(5)*R*Tg*Z(2);
Ph20=Cg(3)*R*Tg*Z(2);
PH2O=exp(72.55-(7206.7/Tg)-7.1385*log(Tg)+4.0460e-6*(Tg)^2);
h2o=100*(Ph20-PH2O)/PH2O;
co2fug=fhi(1,2)*P*yg(1);

td=Dlco2/(Kl(1))^2;

HDiff(1)=-(aw*KH(1)*(Pco2-(H(1)*Cl(1))));
% HDiff(4)=-(aw*Kl(1)*(PN2-(H(4)*Cl(4))))/H(4);
% HDiff(5)=-(aw*Kl(1)*(PO2-(H(5)*Cl(5))))/H(5);

[K,Z,fhi] = PEA(TP,yi,xi);
Kin=K;
Zin=Z;
fhiin=fhi;
[KB,ZB,fhib] = PEA2(TP,yg,xl);

for i=1:N;
    fv(i)=fhib(i,2)*yg(i)*P;
    fl(i)=fhib(i,1)*xl(i)*P;

    fvi(i)=fhiin(i,2)*yi(i)*P;
    fli(i)=fhiin(i,1)*xi(i)*P;

    N2(i)=-sum(Cl)*aw*Kl(i)*((fvi(i)/fhiin(i,1))-(fl(i)/fhib(i,1)))/P;
    N3(i)=aw*Kl(i)*((fli(i)/(fhiin(i,2)*Zin(2)*R*Tl))-
(fv(i)/(fhib(i,2)*Z(2)*R*Tg)));  %correct

    N1(i)=-sum(Cl)*aw*Kl(i)*(fv(i)-fl(i))/(P*fhib(i,1));
    N6(i)=aw*Kl(i)*(fl(i)-fv(i))/(R*Tg*Z(2));

    N4(i)=-sum(Cl)*aw*Kl(i)*(fv(i)-fl(i))/(P*fhib(i,1));
    N5(i)=aw*Kl(i)*(fl(i)-fv(i))/(R*Tg*fhib(i,2)*Z(2));

end
```

```
nDiff(1)=-E*Kl(1)*aw*(Cint(1)-Cl(1));
nDiff(2)= Kl(2)*aw*(Cint(2)-Cg(2));
nDiff(3)= Kl(3)*aw*(Cint(3)-Cg(3));
nDiff(4)= -Kl(4)*aw*(Cint(4)-Cl(4));
nDiff(5)= -Kl(5)*aw*(Cint(5)-Cl(5));

fuga1=[E*N4(1),N5(2),N5(3),N4(4),N4(5)];
fuga2=[E*N2(1),N3(2),N3(3),N2(4),N2(5)];
fuga3=[E*N1(1),N6(2),N6(3),N1(4),N1(5)];
nDiff;
henrydiff=nDiff;
henrydiff(1)=HDiff(1);
%henrydiff(4)=HDiff(4);
%henrydiff(5)=HDiff(5);

nd=nDiff;
nd=henrydiff;
%nd=fuga3
R1=H(1)/(Kl(1)*E);
R2=R*Tg/(Kvco2);
RR1=1/(R1+R2);
RR2=1/R1;

RR=100*(RR1-RR2)/RR1;
```

Para.m

```
wed=0;%0.276;
ded=0;%0.405;
% interaction parameters
delta=[0,0,0.065,-0.0149,-0.04838;
       0,0,-0.18,0,0;
       0.065,-0.180,0,wed,ded;
       -0.0149,0,wed,0,-0.00978;
       -0.04838,0,ded,-0.00978,0];

%critical properties
Q=[304.2,7.383e6,0.228;614.4,4.45e6,0.864;645,22.12e6,0.344;126.1,3.394e6,0.0
40;154.6,5.043e6,0.022];
q=size(Q);
N=q(1);
M=1000;

%mol weight
MW(1)=44;
MW(2)=61.08;
MW(3)=18;
MW(4)=28;
MW(5)=32;

MW(6)=62;
MW(7)=105;
MW(8)=61;
MW(9)=17;
MW(10)=19;
UA=1.5e7;

delHlv=[0 53700 40680 0 0 0 0 0 0 0 ]; % heat vapourisation
delHlvv=[0 53700 40680 0 0]';
delHr=[-65000 0 -20000 0 0 0];      % heat of reaction
```

```
Cpgi=[1.98e1 7.344e-2 -5.602e-5 1.715e-8
    9.311e0 3.009e-1 -1.818e-4 4.656e-8
    3.224e1 1.924e-3 1.055e-5 -3.596e-9
    3.115e1 -1.357e-2 2.68e-5 -1.168e-8
    2.811e1 -3.68e-6 1.746e-5 -1.065e-8];  %Cp of gas

Cpli=[-203.6060 1523.290 -3196.413 2474.455 3.855326
       520.3    -2749    5313    0        0
    -203.6060 1523.290 -3196.413 2474.455 3.855326
         0 0 0 0 0
         0 0 0 0 0
       520.3    -2749    5313    0        0
      520.3    -2749    5313    0        0
      -203.6060 1523.290 -3196.413 2474.455 3.855326
      -203.6060 1523.290 -3196.413 2474.455 3.855326
      -203.6060 1523.290 -3196.413 2474.455 3.855326];  %Cp of liquid


R=8.134;  % universal gas constant
dP=2000;  %pressure drop
eps_abs=1e-10;  % stop iteration
g=9.81;
%montz metal packing B1200
a=200;
Cll=0.971;
Cv=0.390;
Ch=0.547;
epslom=0.979;

%50mm palu plastic ring
% a=111;
% Cll=1.239;
% Cv=0.368;
% Ch=0.593;
% epslom=0.919;

DAB=16; % absorber dia
AreaAB=epslom*3.142*DAB^2/4; % absorber aera

DStripp=5.0; % strpper dia
AStripper=epslom*3.142*DStripp^2/4; % stipper dia

TlCoout=380;  % condenser oulet temp
TGRBOUT=393;    % reboiler temp
TLABin=318;     %liquid tempinto absorber
TGABin=313;        %gas ine to absorbe r temp

PrRB=200000;        % pressure reboiler
PrAB=110000;        %pressure absorber
PRichPres=20;  %rich pump pressure (m)
PleanPres=20;  %lean pump pressure  (m)

Vdot3=0.8;  %total flow
refluxrat=0.10;
RBrate=0.045;
```